Cell-based therapies for

CHRONIC KIDNEY DISEASE

Arianne van Koppen

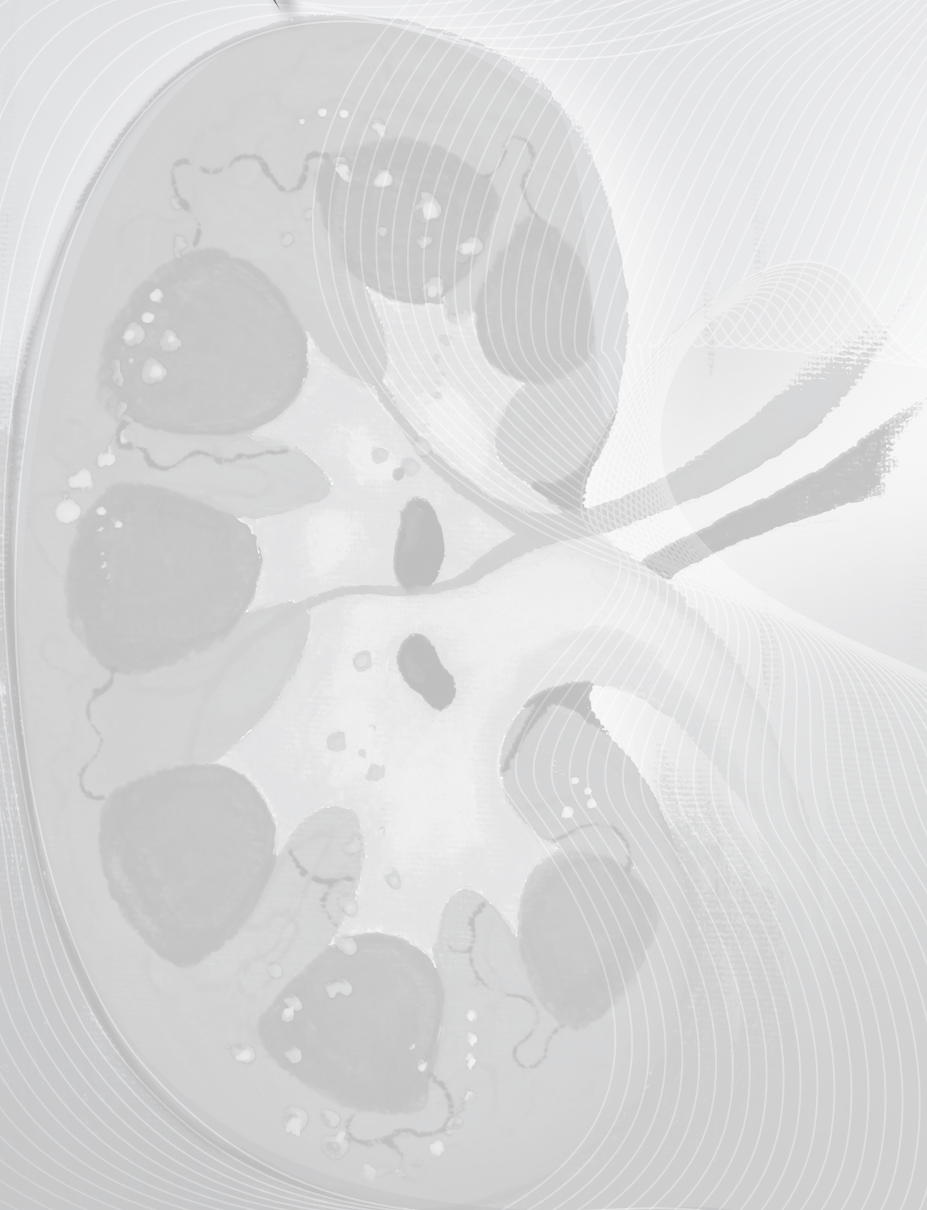

ISBN: 978-90-8891-584-0
Cover painting: Heleen Pijl- van Koppen
Design & Lay-out: www.wenziD.nl || Wendy Schoneveld
Printed by: Proefschriftmaken.nl || Uitgeverij BOXPress, ‘s-Hertogenbosch

Financial support by ChipSoft B.V. and Nierstichting Nederland.

Cell-based therapies for
CHRONIC KIDNEY DISEASE

Cel-gebaseerde therapieën voor Chronisch Nierfalen
(met een samenvatting in het Nederlands)

PROEFSCHRIFT

ter verkrijging van de graad van doctor aan de Universiteit Utrecht
op gezag van de rector magnificus, prof.dr. G.J. van der Zwaan,
ingevolge het besluit van het college voor promoties in het openbaar
te verdedigen op dinsdag 19 maart 2013 des ochtends te 10.30 uur

door

Arentje Neeltje van Koppen

geboren op 10 augustus 1984 te Dirksland

PROMOTOR

Prof. Dr. M.C. Verhaar

CO-PROMOTOR

Dr. J.A. Joles

Voor mijn ouders

CONTENTS

Chapter One

INTRODUCTION AND OUTLINE OF THIS THESIS

Past, present and future of tissue (re)generation: fact or fiction

"When no bush of the field was yet in the land and no small plant of the field had yet sprung up - for the LORD God had not caused it to rain on the land, and there was no man to work the ground, and a mist was going up from the land and was watering the whole face of the ground - *then the LORD God formed the man of dust from the ground and breathed into his nostrils the breath of life, and the man became a living creature*. And the LORD God planted a garden in Eden, in the east, and there he put the man whom he had formed. Then the LORD God said, "It is not good that the man should be alone; I will make him a helper fit for him." *So the LORD God caused a deep sleep to fall upon the man, and while he slept took one of his ribs and closed up its place with flesh. And the rib that the LORD God had taken from the man he made into a woman and brought her to the man (figure 1)*. Then the man said:"this at last is bone of my bones and flesh of my flesh; she shall be called Woman, because she was taken out of Man." Therefore a man shall leave his father and his mother and hold fast to his wife, and they shall become one flesh." Genesis 2: 5-18.

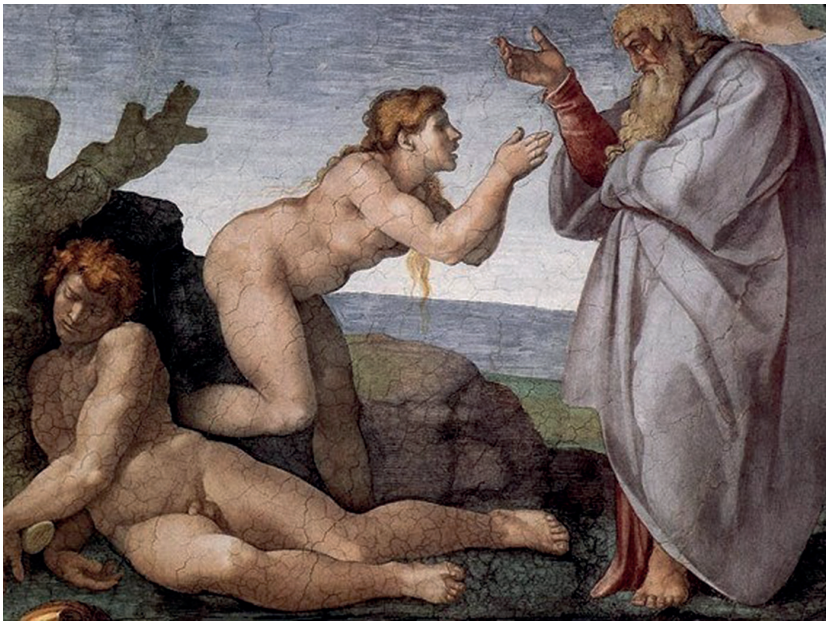

Figure 1 Creation of Eve, painting by Michelangelo.

Using body parts to form a new living being was first described in the Bible where God used a rib from the man to form a woman. Since ancient history, the possibility to regenerate body parts has been an intriguing topic. A literally lighting mythology-based example is the rise of the Phoenix, a long-lived bird that is cyclically regenerated or reborn after being burned to ash by the sun, obtaining new life by arising from the ashes of its predecessor. Another example is the myth of Prometheus. After steeling fire from the Gods, the immortal Prometheus was bound to a rock, where each day an eagle was sent to feed on his liver, only to have it grow back to be eaten again the next day (figure 2). Some think the myth indicates that the ancient Greeks knew about the liver's remarkable capacity for self-repair which is reflected by the Greek word for liver cell, i.e. hepatocyte which is derived from the verb *hēpaomai* (ἡπάομαι), meaning "mend, repair".

Not only in ancient history, also in modern literature and movies regeneration of body parts is a popular theme. Mary Shelley's popular novel 'Frankenstein' described the generation of a human being using body parts from the deceased and used "*The Modern Prometheus*" as subtitle. Regeneration is also popular in comics, think of Wolverine, The Hulk and the regeneration suit of Superman.

Regenerative Medicine is the scientific discipline that investigates how the body's natural ability to repair damaged tissues and organs can be stimulated or imitated

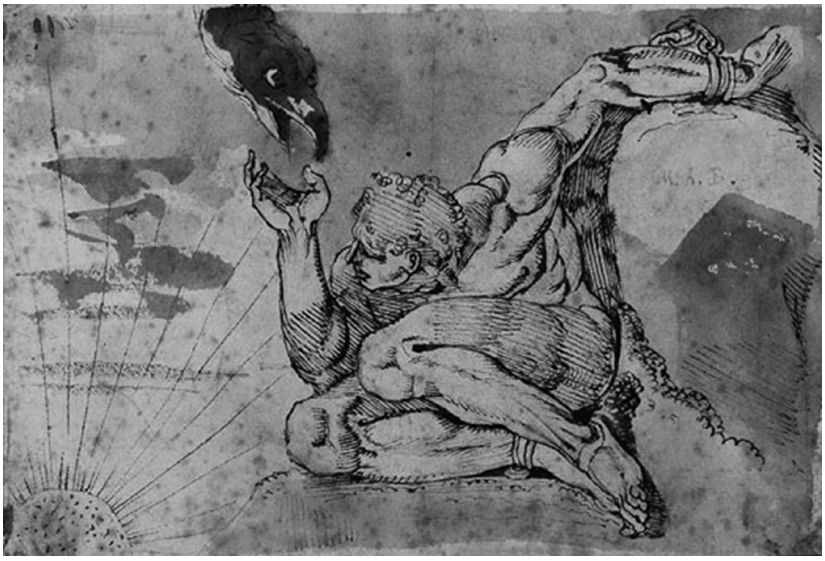

Figure 2 Punishment of Prometheus, drawing by Henri Fuseli.

so as to bring about functional recovery[1]. In the last decades, scientific research in Regenerative Medicine has made major progress. It is expected that Regenerative Medicine may provide an answer to the growing demand for medical solutions for the increasing burden of chronic diseases. Stem cells may represent a potent tool to realize these goals. Stem cells are characterized by their self-renewal capacity and their ability to give rise to differentiated cells. In the adult, stem cells have been identified in many tissues and organs, where they may act as organ specific repair systems. Adult stem cells from bone marrow were first described for the hematopoietic system. The term "stem cell" was proposed for scientific use in 1908 by a Russian histologist Maksimov and referred to the existence of hematopoietic stem cells. In 1963, the presence of self-renewing cells in the mouse bone marrow were described by McCulloch et al[2], leading to the first successful bone marrow transplant in 1968[3].

In 1981, embryonic stem cells (ES cells) were independently discovered by two groups. Martin Evans and Matthew Kaufman published a new technique for culturing the mouse embryos in the uterus to increase cell numbers which allows derivation of ES cells[4]. Gail Martin was the first to use the term "Embryonic Stem Cell"[5]. She showed that embryos could be cultured *in vitro* and that ES cells could be derived from these embryos. In 1998, a breakthrough occurred when James Thomson developed a technique to isolate and grow *human* embryonic stem cells in cell culture[6]. Because of their capacity for self-renewal and pluripotency, ES cell therapies have been proposed for regenerative medicine and tissue replacement after injury or disease. However, major challenges will have to be overcome before human ES cell therapies can be safely used for clinical application. Besides the ethical issues of the use of ES cells, there are immunological concerns as well as concerns about the potential to form tumors including teratomas[7]. These concerns have urged researchers to search for novel cell sources or strategies. The recent discovery of induced pluripotent stem cells (iPS cells) by Yamanaka et al was awarded with the Nobel prize last year. This discovery that intact mature cells can be reprogrammed to become pluripotent stem cells holds tremendous promise for regenerative therapies. iPS cells may circumvent problems associated with both ethical issues and immunological rejection[8].

Adult stem cells have been identified in many organs and tissues and contribute to tissue maintenance and repair. Adult stem cells may also be used for regenerative therapies. In this thesis we will focus on the use of bone marrow cells which have long been known to contribute to maintenance and repair of the hematopoietic system but may also contribute to regeneration of other tissues and organs[9-13].

Chronic kidney disease and regenerative therapies

Kidney disease is a major health care problem worldwide. The number of patients that are affected by chronic kidney disease (CKD) is increasing due to ageing of populations and increasing prevalence of diabetes and vascular diseases[14]. CKD is a progressive disease that may lead to end-stage renal disease (ESRD), requiring renal replacement therapy. Although kidney transplantation - despite the risk of transplant rejection and need for chronic immunosuppressive therapy – is considered the most optimal form of renal replacement therapy, many patients are still on dialysis, due to donor shortage and limited transplant availability. The burden of chronic kidney disease is not limited to its potential progression to end-stage renal failure but also contributes importantly to the global burden of death due to cardiovascular diseases. Reducing progression of chronic kidney disease is therefore a major global public health target.

Since CKD is characterised by complex derangements of homeostasis, integrative animal models are necessary to study development and progression of CKD as well as potential effects of (regenerative) therapies. The kidney consists of a broad range of different cell types that interact with each other. This complexity cannot be mimicked *in vitro*. In rats the 5/6th nephrectomy ablation model is a well-known experimental model of progressive renal disease that resembles several aspects of human CKD[15,16]. The gross reduction in renal mass causes progressive glomerular and tubulo-interstitial injury, loss of remnant nephrons and development of systemic and glomerular hypertension. It is associated with progressive intrarenal capillary loss[17], inflammation and glomerulosclerosis. The development of CKD using 5/6th nephrectomy ablation differs per strain and in certain more resistant strains requires additional interventions, such nitric oxide (NO) depletion[18-20] and a high salt diet[21]. In this thesis we use the 5/6th nephrectomy ablation model in Lewis rats in combination with NOS-inhibition and a high-salt diet to allow evaluation of the effects of regenerative strategies in established CKD.

End stage kidney disease is associated with loss of nephrons. As in adult mammals true nephrogenesis, formation of new nephrons, does not occur, strategies to enhance renal regenerative potential in a stage where most nephrons are lost are unlikely to be successful. Renal regenerative strategies have therefore mainly focused on reducing nephron loss in earlier stages of CKD. Studies in bone marrow transplant models suggest that BM-derived cells

contribute to renal repair and may therefore represent an attractive therapeutic target[13]. BM contains many cell types including mesenchymal and hematopoietic stem cells which can give rise to different cell types. Several studies demonstrated beneficial effects of the administration of BM cell subpopulations in AKI models (for recent review see Togel et al,[22]). Mechanisms to enhance renal regeneration using bone marrow cells (BMCs) were first thought to involve trans-differentiation and incorporation, however, more recent literature suggests that the ability of BMCs to differentiate into endothelial cells as well as their paracrine actions by secreting cytokines and growth factors that modulate and stimulate (diseased) host cells play a major role[23,24].

Injury to the glomerular and peritubular capillary endothelium, in combination with a defective capillary repair response plays an important role in the pathogenesis and progression of CKD[25]. The preclinical observations that enhanced renal capillary repair could prevent renal disease progression[26] suggest repair or regeneration of the renal microvascular endothelium as therapeutic target to prevent CKD progression. Endothelial regeneration and repair also involve bone marrow derived cells[27-29]. We previously showed that glomerular endothelial repair involves recruitment and homing of BM derived cells[30]. Furthermore, in a mouse model, engraftment of BMCs in peritubular capillary endothelium has been demonstrated[31]. In this thesis we studied whether bone marrow cell based therapies could decrease progression of CKD in a rat model of established CKD by enhancing renal microvascular regeneration.

Limitations of rat models for CKD are the lack of transgenic and knock-out rat models. To study the pathology and regenerative processes in cardiorenal disease, a mouse models would be valuable as it would offer the opportunity to investigate influences of specific genetic traits. Well characterized mouse models for cardiorenal disease with sufficient remaining renal tissue for analyses are sparse.

Aim and outline of the thesis

The aim of this thesis was to investigate whether cell-based therapies have the potential to reduce progression of CKD.

To investigate the potential impact of renal regenerative strategies we used the 5/6th nephrectomy model in the rat, a well-known and extensively described model for CKD. However, simply removing 5/6th of renal mass does not lead to immediate

renal failure in all rat strains. We used Lewis rats as the availability of GFP$^+$ Lewis rats[32] allows cell-tracking of administered donor cells in the recipient (non GFP$^+$) rat. The Lewis rat is relatively resistant to development of kidney injury and development of CKD is slow compared to other strains[33,34]. **Chapter 2** gives a detailed description of the rat CKD model used in **Chapter 3-5**.

In **Chapter 3** we studied the effects of BMC therapy in our rat model of established CKD. As clinical BMC therapy will involve administration of autologous BMC that have been exposed to a CKD environment we also investigated the influence of CKD on BMC therapeutic efficacy. This chapter shows that administration of healthy BMC in established CKD is effective as rescue therapy. However, administration of BMC obtained from CKD rats in the same model was not functionally effective. In **Chapter 4** we therefore aimed to improve CKD BMC function. We studied whether short term pretreatment of CKD BMC with pravastatin could enhance BMC function and improve their therapeutic efficacy.

It has been suggested that activation of BM cells in disease states such as hypertension or CKD may contribute to enhanced myocardial fibrosis. In **Chapter 5**, we studied whether BMCs that are administered to reduce CKD progression in rats with CKD and hypertension contribute to the development of cardiac fibrosis.

Over the past few years it has become increasingly clear that tissue repair by stem cells occurs in part by their paracrine actions. In **Chapter 6** we investigated whether paracrine factors secreted by human embryonic mesenchymal stromal cells could be used to slow progression of CKD.

Mouse models have large value for dissecting mechanisms and testing interventions in complex diseases such CKD or cardiorenal disease as mice provide the possibility to study the effects of defined genetic traits. However, mice are known to be very resistant to induction of renal failure requiring removal of large parts of the kidneys and leaving little renal tissue for analyses. **Chapter 7** describes the development of a 2-kidney mouse model of cardiorenal disease, using pharmacological interventions to induce renal and cardiac injury.

References

1. KNAW foresight study Well underway. 2012.
2. Till J.E., McCulloch E.A. Early repair processes in marrow cells irradiated and proliferating *in vivo*. Radiat. Res. 1963; 18:96-105.
3. Bach F.H., Albertini R.J. et al. Bone-marrow transplantation in a patient with the Wiskott-Aldrich syndrome. Lancet 1968; 2:1364-1366.
4. Evans M.J., Kaufman M.H. Establishment in culture of pluripotential cells from mouse embryos. Nature 1981; 292:154-156.
5. Martin G.R. Isolation of a pluripotent cell line from early mouse embryos cultured in medium conditioned by teratocarcinoma stem cells. Proc. Natl. Acad. Sci. U. S. A 1981; 78:7634-7638.
6. Thomson J.A., Itskovitz-Eldor J. et al. Embryonic stem cell lines derived from human blastocysts. Science 1998; 282:1145-1147.
7. Knoepfler P.S. Deconstructing stem cell tumorigenicity: a roadmap to safe regenerative medicine. Stem Cells 2009; 27:1050-1056.
8. Takahashi K., Yamanaka S. Induction of pluripotent stem cells from mouse embryonic and adult fibroblast cultures by defined factors. Cell 2006; 126:663-676.
9. Choi S.H., Jung S.Y., Kwon S.M., Baek S.H. Perspectives on stem cell therapy for cardiac regeneration. Advances and challenges. Circ. J. 2012; 76:1307-1312.
10. De Miguel M.P., Fuentes-Julian S. et al. Immunosuppressive properties of mesenchymal stem cells: advances and applications. Curr. Mol. Med. 2012; 12:574-591.
11. Takami T., Terai S., Sakaida I. Advanced therapies using autologous bone marrow cells for chronic liver disease. Discov. Med. 2012; 14:7-12.
12. Weber B., Emmert M.Y., Hoerstrup S.P. Stem cells for heart valve regeneration. Swiss. Med. Wkly. 2012; 142:w13622.
13. Yuen D.A., Gilbert R.E., Marsden P.A. Bone marrow cell therapies for endothelial repair and their relevance to kidney disease. Semin. Nephrol. 2012; 32:215-223.
14. Coresh J., Selvin E. et al. Prevalence of chronic kidney disease in the United States. JAMA 2007; 298:2038-2047.
15. Fleck C., Appenroth D. et al. Suitability of 5/6 nephrectomy (5/6NX) for the induction of interstitial renal fibrosis in rats--influence of sex, strain, and surgical procedure. Exp. Toxicol. Pathol. 2006; 57:195-205.
16. Griffin K.A., Picken M.M. et al. Functional and structural correlates of glomerulosclerosis after renal mass reduction in the rat. J. Am. Soc. Nephrol. 2000; 11:497-506.
17. Kang D.H., Kanellis J. et al. Role of the microvascular endothelium in progressive renal disease. J. Am. Soc. Nephrol. 2002; 13:806-816.
18. Bongartz L.G., Braam B. et al. Transient nitric oxide reduction induces permanent cardiac systolic dysfunction and worsens kidney damage in rats with chronic kidney disease. Am. J. Physiol Regul. Integr. Comp Physiol 2010; 298:R815-R823.
19. Fujihara C.K., De N.G., Zatz R. Chronic nitric oxide synthase inhibition aggravates glomerular injury in rats with subtotal nephrectomy. J. Am. Soc. Nephrol. 1995; 5:1498-1507.
20. Fujihara C.K., Sena C.R. et al. Short-term nitric oxide inhibition induces progressive nephropathy after regression of initial renal injury. Am. J. Physiol Renal Physiol 2006; 290:F632-F640.
21. Dikow R., Kihm L.P. et al. Increased infarct size in uremic rats: reduced ischemia tolerance? J. Am. Soc. Nephrol. 2004; 15:1530-1536.
22. Togel F.E., Westenfelder C. Kidney protection and regeneration following acute injury: progress through stem cell therapy. Am. J. Kidney Dis. 2012; 60:1012-1022.
23. Rookmaaker M.B., Tolboom H. et al. Bone-marrow-derived cells contribute to endothelial repair after thrombotic microangiopathy. Blood 2002; 99:1095.
24. Togel F., Hu Z. et al. Administered mesenchymal stem cells protect against ischemic acute renal failure through differentiation-independent mechanisms. Am. J. Physiol Renal Physiol 2005; 289:F31-F42.
25. Kang D.H., Kanellis J. et al. Role of the microvascular endothelium in progressive renal disease. J. Am. Soc. Nephrol. 2002; 13:806-816.

26. Kang D.H., Hughes J. et al. Impaired angiogenesis in the remnant kidney model: II. Vascular endothelial growth factor administration reduces renal fibrosis and stabilizes renal function. J. Am. Soc. Nephrol. 2001; 12:1448-1457.
27. Kahler C.M., Wechselberger J. et al. Peripheral infusion of rat bone marrow derived endothelial progenitor cells leads to homing in acute lung injury. Respir. Res. 2007; 8:50.
28. Kalka C., Masuda H. et al. Transplantation of *ex vivo* expanded endothelial progenitor cells for therapeutic neovascularization. Proc. Natl. Acad. Sci. U. S. A 2000; 97:3422-3427.
29. Silva G.V., Litovsky S. et al. Mesenchymal stem cells differentiate into an endothelial phenotype, enhance vascular density, and improve heart function in a canine chronic ischemia model. Circulation 2005; 111:150-156.
30. Rookmaaker M.B., Smits A.M. et al. Bone-marrow-derived cells contribute to glomerular endothelial repair in experimental glomerulonephritis. Am. J. Pathol. 2003; 163:553-562.
31. Li J., Deane J.A. et al. The contribution of bone marrow-derived cells to the development of renal interstitial fibrosis. Stem Cells 2007; 25:697-706.
32. van den Brandt J., Wang D. et al. Lentivirally generated eGFP-transgenic rats allow efficient cell tracking *in vivo*. Genesis. 2004; 39:94-99.
33. Kreutz R., Kovacevic L. et al. Effect of high NaCl diet on spontaneous hypertension in a genetic rat model with reduced nephron number. J. Hypertens. 2000; 18:777-782.
34. Szabo A.J., Muller V. et al. Nephron number determines susceptibility to renal mass reduction-induced CKD in Lewis and Fisher 344 rats: implications for development of experimentally induced chronic allograft nephropathy. Nephrol. Dial. Transplant. 2008; 23:2492-2495.

Chapter Two

5/6TH NEPHRECTOMY IN COMBINATION WITH HIGH SALT DIET AND NO SYNTHASE INHIBITION TO INDUCE CHRONIC KIDNEY DISEASE IN THE LEWIS RAT

Journal of visualized experiments; in press

Arianne van Koppen[1], Marianne C. Verhaar[1], Lennart G. Bongartz[1], Jaap A. Joles[1]

[1] *Dept. of Nephrology & Hypertension, University Medical Center Utrecht, Utrecht, the Netherlands*

Abstract

Chronic kidney disease (CKD) is a global problem. Slowing CKD progression is a major health priority. Since CKD is characterised by complex derangements of homeostasis, integrative animal models are necessary to study development and progression of CKD. To study development of CKD and novel therapeutic interventions in CKD, we use the 5/6th nephrectomy ablation model, a well known experimental model of progressive renal disease, resembling several aspects of human CKD. The gross reduction in renal mass causes progressive glomerular and tubulo-interstitial injury, loss of remnant nephrons and development of systemic and glomerular hypertension. It is also associated with progressive intrarenal capillary loss, inflammation and glomerulosclerosis. Risk factors for CKD invariably impact on endothelial function. To mimic this, we combine removal of 5/6th of renal mass with nitric oxide (NO) depletion and a high salt diet. After arrival and acclimatization, animals receive a NO synthase inhibitor (NG-nitro-L-Arginine) (L-NNA) supplemented to drinking water (20 mg/L) for a period of 4 weeks, followed by right sided uninephrectomy. One week later, a subtotal nephrectomy (SNX) is performed on the left side. After SNX, animals are allowed to recover for two days followed by LNNA in drinking water (20 mg/L) for a further period of 4 weeks. A high salt diet (6%), supplemented in ground chow (see time line figure 1), is continued throughout the experiment. Progression of renal failure is followed over time by measuring plasma urea, systolic blood pressure and proteinuria. By six weeks after SNX, renal failure has developed. Renal function is measured using 'gold standard' inulin and para-amino hippuric acid (PAH) clearance technology. This model of CKD is characterized by a reduction in glomerular filtration rate (GFR) and effective renal plasma flow (ERPF), hypertension (systolic blood pressure > 150mmHg), proteinuria (> 50 mg/24h) and mild uremia (> 10 mM). Histological features include tubulo-interstitial damage reflected by inflammation, tubular atrophy and fibrosis and focal glomerulosclerosis leading to massive reduction of healthy glomeruli within the remnant population (< 10%). Follow-up until 12 weeks after SNX shows further progression of CKD.

Introduction

Due to its progressive nature, ensuing end stage kidney disease, and associated cardiovascular morbidity and mortality, CKD is a growing public health problem[1]. Slowing CKD progression is therefore a major health priority. Since CKD is characterised by complex derangements of homeostasis, integrative animal models are necessary to study development and progression of CKD. The kidney consists of a broad range of different cell types that interact with each other. This complexity cannot be mimicked *in vitro*.

To study novel therapeutic interventions in CKD, we use the 5/6th nephrectomy ablation model, a well-known experimental model of progressive renal disease, resembling several aspects of human CKD[2,3]. The gross reduction in renal mass causes progressive glomerular and tubulo-interstitial injury, loss of remnant nephrons and development of systemic and glomerular hypertension. It is associated with progressive intrarenal capillary loss[4], inflammation and glomerulosclerosis. Risk factors for CKD invariably impact on endothelial function[5]. We used a rat strain (Lewis) that is relatively resistant to development of CKD and therefore we combined removal of 5/6th of renal mass with nitric oxide (NO) depletion[6-8] and a high salt diet[9]. After arrival and acclimatization, animals receive a NO synthase inhibitor (L-NNA) supplemented to drinking water (20 mg/L) for a period of 4 weeks, followed by right sided uninephrectomy (UNX) with continuation of L-NNA after two days. One week later, subtotal nephrectomy (SNX) i.e. removal of 2/3^{rds} of renal mass is performed on the left side. After SNX, animals are allowed to recover for 2 days followed again by 20 mg/L LNNA in drinking water for a period of 4 weeks. A high salt diet (6%), supplemented in ground chow (see time line figure 1), is continued throughout the experiment. The reason to perform the UNX on the right side and the SNX on the left side is that the renal vessels are longer on the left side which makes it easier to access the kidney without stretching the vessels too much when the kidney is exposed outside the body. In literature, models are described in which the poles of the left kidney are removed first, followed by UNX of the right kidney one week later[10-12]. In our hands this model showed a much more rapid development of renal failure, but also a much larger variation in loss of renal function. Progression of renal failure is followed over time by measuring plasma urea, systolic blood pressure and proteinuria. By six weeks after SNX, renal failure has developed, characterized by marked reduction in glomerular filtration rate (69%) and effective renal plasma flow (62%)[13], hypertension (systolic blood pressure >150mmHg), proteinuria (> 50 mg/24h) and mild uremia (>10 mM). Histological features include tubulo-interstitial damage reflected by inflammation, tubular atrophy and fibrosis and focal glomerulosclerosis leading to massive

reduction of healthy glomeruli within the remnant population (< 10 %). Follow-up until 12 weeks after SNX shows further progression of CKD, providing a window of opportunity for evaluation of therapeutic interventions.

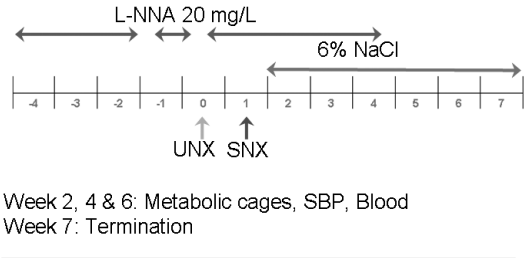

Figure 1 Time line of L-NNA, high salt diet, UNX and SNX. Longitudinal measurements to determine renal function and termination time-point are indicated. When longer follow-up is needed after SNX, 6% NaCl diet can be continued over time.

Protocol

All experiments are executed in accordance to the animal experimental ethical guide lines of the Utrecht experimental animal committee. The protocol is performed under the guidance and approval of the author's institution's animal care and use committee.

CKD is induced in male inbred Lewis rats (Charles River, Sulzfeld, Germany) at the age of 8 weeks. Rats are housed under standard conditions in a light-, temperature- and humidity-controlled environment.

1. Surgery; preparation

1.1. Sterilize surgical instruments:

- 1 student tissue forceps 1-2 teeth 12cm
- 1 student standard pattern forceps
- 2 Semken forceps
- 1 Mayo scissors
- 1 student iris scissors
- 1 Olsen-Hegar needle holder with scissors
- Blanket

1.2 Check inventory list:

- Operating table with warming pad and lamp
- O2, isoflurane
- Tissues

- Shaver
- Scales
- Sterile operating set
- Sterile gauze 5x5 and 10x10
- 70% alcohol
- 0.9% NaCl solution
- 1 ml syringe
- Needles (25G)
- Gel foam pads: spongostan
- Vicryl 4.0 and 5.0
- Buprenorphine 0.03 mg/kg (1:10 diluted in physiological salt)
- Clean cage for rats after surgery

2. Right side uninephrectomy

2.1. Disinfect the table with 70% alcohol, wash and disinfect hands and wear sterile surgical gloves. Wear a head cap and a mask.

2.2. Place rat in induction box and induce anesthesia with 4% isoflurane and 1 L flow of oxygen. Note: depending on the rat strain used, pre- and perioperative analgesia are prescribed, this needs to be discussed with the local veterinarian.

2.3. Transfer rat to table and place nose into cone. The rat and nose cone are placed on a heating pad to maintain the rat's body temperature. The rat is ventilated with a mixture of 2% isoflurane and 1 L oxygen.

2.4. Shave the flank of the rat and disinfect with alcohol. Make a 1- 1.5 cm incision parallel to the ribs using anatomical forceps and blunt scissors. Expose the kidney by blunt dissection of the back muscles.

2.5. The lower pole of the kidney is visible, carefully use the small blunt forceps to grip the perirenal fat tissue. Externalize the kidney by gently pulling on the perirenal fat with forceps. Take care to not disturb the adrenal gland during this procedure. The adrenal gland can be easily removed by placing a forceps at the medial site in the fat tissue and gently moved upwards between the adrenal gland and the kidney as depicted in figure 2.

2.6. Place kidney gently on gauze and clear of surrounding fat and connective tissue. Identify the renal artery and vein and place a ligature (4.0 vicryl) with a single knot around the vessels, but do not tie off the knot.

2.7. Move the loose knot carefully along the vessels towards the aorta by approximately 0.5 cm, to create space between the kidney and the knot. This is done to prevent the ligature from slipping off after cutting.

2.8. Tie knot with two double knots. If perfusion is halted, the color of the kidney will immediately change to brown. Do not cut the ends of the ligature.

2.9. Cut the renal vessels close to the kidney and remove the kidney. Gently pull on the long ends of the ligature to check for bleeding of the renal vessels. The ligature should stay in place on the vessel. Cut the long ends of the ligature. Note, the remnant renal vessels will retract into the abdominal cavity immediately.

2.10. Blot excised kidney dry and weigh it.

2.11. Close the skeletal muscle incision with running sutures with Vicryl 5.0. Inject 0.10 ml (0.03 mg/kg) buprenorphine i.m in the hind limb. Close the skin with Vicryl 4.0 with intracutaneous sutures. This prevents the rats from opening the wound. Note: due to respiratory depression in Lewis rats, we only give post-operative analgesia just before switching off the isoflurane.

2.12. House the rat in a clean solitary cage with easy access to food and water. Place the cage half on warming pad overnight and check the rat carefully the next day. When the wound is closed and the rat is active, which is normally between 6 and 12 hours after surgery, the rat can be placed back into group housing.

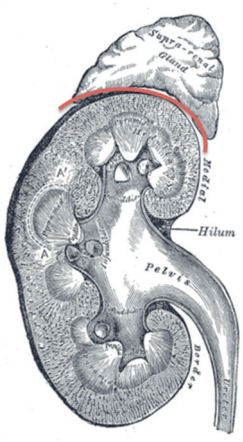

Figure 2 Adrenal gland dissection. To remove the adrenal gland without disturbing it, place forceps in the fat between the kidney and the adrenal gland and move from the vessel pole upwards to the top as indicate by the red line. Figure adapted from the 20th U.S. edition of Gray's Anatomy of the Human Body, 1918.

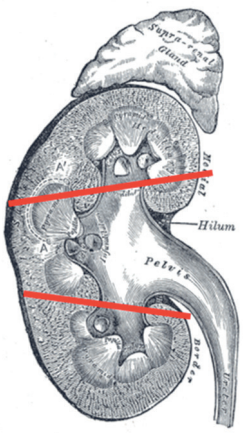

Figure 3 Subtotal nephrectomy. Red lines indicate cutting edges. Figure adapted from the 20th U.S. edition of Gray's Anatomy of the Human Body, 1918.

3). Left side subtotal nephrectomy

3.1. Seven days later, the same preparations are made on the left side as for the right side as described from 2.1 to 2.5. Before surgery, the amount of renal tissue that needs to be removed corresponding to approximately 2/3^{rds} of the weight of the right kidney is calculated. Prepare small pieces of gel foam (Spongostan®, Johnson & Johnson, New Jersey) before surgery.

3.3. Place sharp scissors around the upper pole of the left kidney and resect the upper pole in one stroke (for scissor location, see figure 3). Cover immediately with a piece of gel foam and exert mild pressure with sterile gauze.

3.4. Repeat with the lower pole of the kidney as in 3.3.

3.5. Lift kidney to prevent clotting on skin. Maintain mild pressure on both gel foam pads with sterile gauze until the bleeding stops. When bleeding persists, add another foam pad.

3.6. Place remnant kidney with adherent gel foam pads inside the abdomen. Close the muscle and skin and follow 2.9-2.12.

4). Sham surgery

4.1. Sham operated controls undergo the same procedure in order to expose the kidneys. Instead of extirpating the kidney or cutting the poles one week later, both the kidneys are decapsulated at a one week interval, taking care not to disturb the adrenal glands. Wound closure and post-operative care are identical to 2.11 and 2.12.

Representative Results

After subtotal nephrectomy, approximately 1/6th of total renal mass is left. Figure 4 shows the weight of the left kidney and the weight of the removed part of the right kidney with mean and standard deviation in our previous experiments. One should keep in mind that in the week after UNX, hypertrophy of the left kidney occurs; indicating that the weight that needs to be removed calculated based on the weight of the right kidney always results in less than 5/6th removal. However, since it is not possible to determine the weight of the left kidney during surgery; this is the most accurate way to remove approximately 5/6th of the original renal mass.

Over time, rats with CKD develop hypertension, uremia, anemia, proteinuria and a significant decrease in GFR and ERPF. After 6 weeks, established CKD has developed, a suitable time-point to test rescue interventions. Over time, strong progression of hypertension and proteinuria is observed while hematocrit and

renal function (GFR and ERPF) show mild deterioration (figure 5). Other symptoms that we do not focus on in our experiments include derangements in calcium-phosphate and lipid metabolism, and many others. Depending on the strain of rats, development of CKD can vary markedly[2,14,15]. We added the high salt diet and a NO blocker to induce hypertension and endothelial dysfunction.

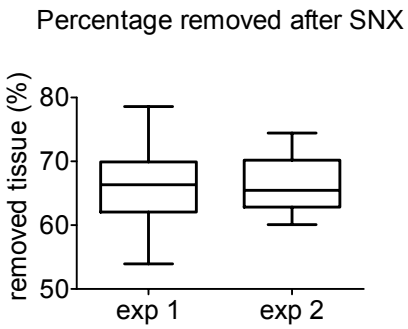

Figure 4 Percentage of removed renal tissue after sub-total nephrectomy in two different experiments. Exp 1; n=16, exp 2; n=23.

Progression of renal failure is tracked by collection of urine (for measurement of the amount of protein and creatinine), blood (plasma urea and creatinine) and systolic blood pressure. We realize that development of hypertension can be followed more precisely when using telemetry instead of tail cuff plethysmography. Creatinine clearance can be calculated but tends to underestimate the decline in GFR due to extensive tubular creatinine secretion in rats[16], underlining the importance of the gold standard method to determine renal function by inulin and PAH clearance[17,18,19]. Koeners et al. described the complete procedure[20]. Inulin and PAH clearance are calculated from their concentration in the urine sample (U), urine flow rate (V), and their plasma concentration (P). We previously showed a marked reduction of GFR and ERPF in this model using classic clearance technology, while this was less apparent from changes in plasma creatinine, plasma urea, or creatinine clearance[13].

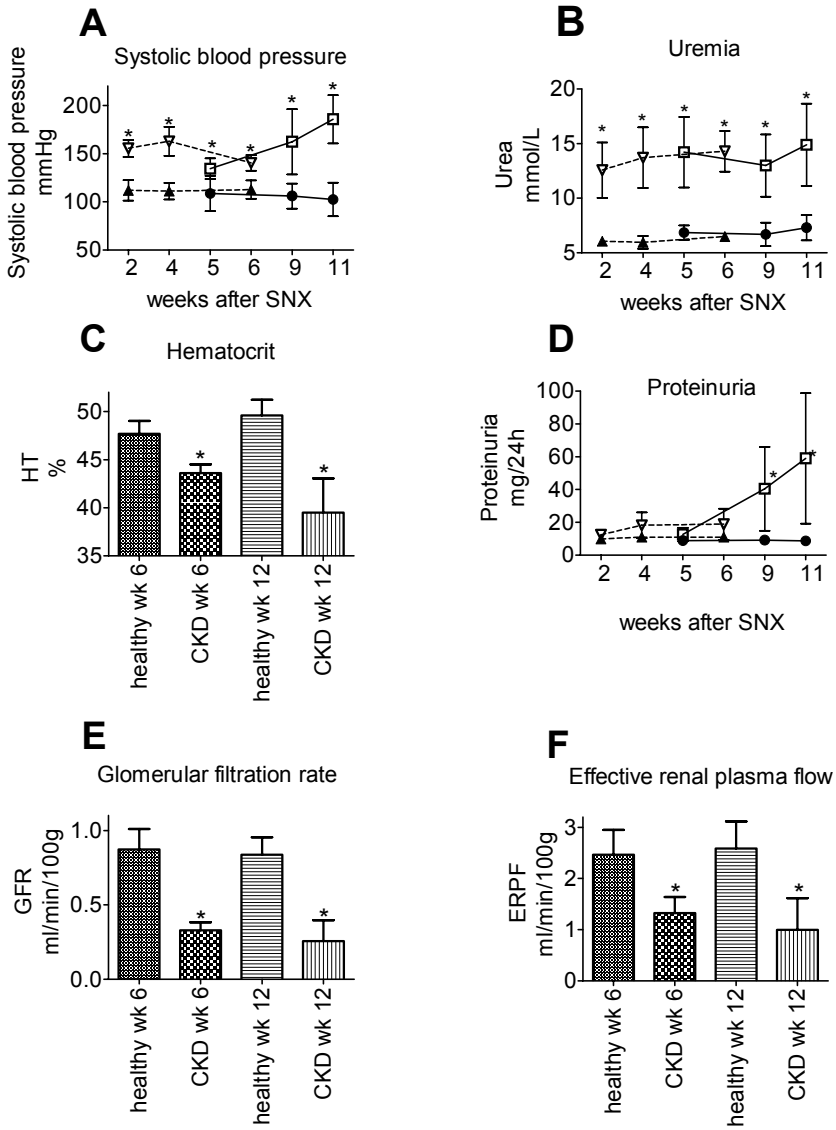

Figure 5 Development of renal failure in CKD rats terminated 6 weeks after SNX (▽dashed lines n=5) vs. healthy controls (▲dashed lines n=5) and CKD rats terminated 12 weeks after SNX (□n=8) vs. healthy controls (●n=8). CKD rats received L-NNA until week 4 and high salt diet from week 1 until termination (not shown in graphs). SNX induces hypertension (measured by tailcuff plethysmography) (A), uremia (B), anemia (C) and proteinuria (D) and marked reduction of GFR (E) and ERPF (F)[13]. *indicated $p<0.05$ vs. healthy controls for each time point tested by two-way ANOVA with Bonferroni post-test for graphs A, B and D. Graphs C, E and F are tested with a two-tailed t-test for 6 and 12 weeks time point.

Discussion

Surgical removal of 5/6th of renal mass in the Lewis rat, combined with a high-salt diet and temporary NOS inhibition leads to a model of CKD that resembles human CKD and allows study of causal mechanisms and efficacy of therapeutic interventions in CKD.

The 5/6th nephrectomy model is a well-known and extensively described model for CKD. However, simply removing 5/6th of renal mass does not lead to immediate renal failure in all rat strains. We use Lewis rats to study the effects of cell-based therapies in CKD as the availability of GFP$^+$ Lewis rats[21] allows cell-tracking of administered donor cells in the recipient (nonGFP$^+$) rat. The Lewis rat is relatively resistant to development of kidney injury and development of CKD is slow compared to other strains[15,22]. Therefore we combined removal of 5/6th of renal mass with NO depletion and a high salt diet since this resembles several aspects of human CKD like high salt intake and endothelial dysfunction. Readers should keep in mind that the need for combining 5/6th nephrectomy with high salt diet and/or NO depletion depends on the strain of rats used for the experiments.

We performed 5/6th nephrectomy in a two-step procedure instead of a one-step procedure as this is regarded as less burdensome for the animal, is associated with less surgery-related mortality and is preferred by our animal experimental committee. We preferred flank incision rather than laparatomy to reach the kidneys as laparotomy is associated with a higher risk of wound infection, loosening of stitches, subcutaneous herniation and adhesions to the intestines compared to flank incision. Furthermore, if the experimental design involves an intervention with laparotomy - as is the case in our experimental studies for the administration of bone marrow cells into the renal artery of the remnant kidney- performing laparotomies for SNX is not preferable as repeated laparotomies should be avoided.

Following surgical removal of 5/6th of renal mass, several critical problems can occur. During UNX there can be difficulties stabilizing the kidney since the surrounding fat will detach easily. Two methods can be used to get the kidney exposed. 1). Use smaller forceps to get grip on the renal vessels by gently moving down from the lower pole of the kidney towards the vasculature and carefully pull until you can stabilize the kidney. 2). Use blunt forceps to carefully pull the kidney out of the abdomen. When the kidney is exposed, gauze can be used to stop the bleeding that may occur during this procedure. To prevent bleeding, start pulling the fat at the lower pole of the kidney, where the fat is strongly attached to the kidney.

It is important to create space between the knot around renal vessel and kidney to prevent bleeding after removal of the kidney as the knot can slip off the renal vessels due to the incoming blood flow, quickly filling the abdomen with blood. A gauze can to be used to remove the blood and pressure should be applied to stop bleeding. Use forceps to grip the renal and place a new ligature. When renal vessels cannot be traced back, maintain pressure until bleeding is stopped. Add 1 ml of physiological salt to prevent dehydration due to bleeding in the abdominal cavity and wait approximately 5 minutes before closing the muscle and skin layer. Monitor rat extra carefully for the following days. When the ligature is still in place after removal of the kidney but renal vessels are bleeding, the long ends of the ligature can be used to tie off the vessels.

When after dissection of the poles, despite holding pressure on gel foam pads, bleeding persists this is likely due to injury to a large renal artery or the renal pelvis. This bleeding can be stopped by placing new gel foam pads on the wound, taking care not to move the foam pad during lifting the remnant since the larger vessels are close to the hilum, and waiting for a longer period.

Blood can be traced in the urine until 2 days post-surgery. When the renal pelvis is damaged or a large renal vessel persists to bleed, there will be a persistent trace of hematuria. Rats with persistent hematuria after surgery need to be euthanized since it is not possible to stop the bleeding. If hematuria is observed at a later time-point after surgery, which can occur up to 2 weeks after surgery, the rat should also be euthanized since blood has clotted inside the renal pelvis and will eventually clog the ureter and bladder, leading to obstruction.

When more rapid development of renal failure is required, the protocol can be reversed, i.e. first remove the poles followed by uninephrectomy a week later. This reversed model has been used in other rat strains, see for example Liu et al[23] who describes a threefold increase in serum urea and an almost fourfold decrease in serum creatinine at two weeks post-surgery. Alternatively, more renal mass can be removed. Keep in mind that removal of more renal mass will increase the risk of hemorrhages and death. Cortex can safely be removed from the top of the kidney curvature. Do not remove more medullary tissue to avoid bleeding of the large renal arteries. Variants on the SNX model are renal mass reduction by one-sided nephrectomy and either ligation of two of the three renal artery branches (infarction model) or resection or ligation of the poles of both kidneys. The differences between these models have been extensively investigated by Griffin and Bidani[24]. The infarction model is accompanied by higher renin release, a more acute and pronounced rise in blood pressure and more initial glomerular injury[3]. In both models, a state of chronic stable kidney disease develops over the course of 4 to 8 weeks. Coagulation of the renal cortex can also be used to reduce renal mass[25].

Acknowledgements

We thank Krista den Ouden for her excellent technical assistance. This technique was financially supported by the Dutch Kidney foundation, grant C06.2174. M.C.V. is supported by the Netherlands organisation for Scientific Research (NWO) Vidi-grant 016.096.359.

References

1. Go A.S., Chertow G.M. et al. Chronic kidney disease and the risks of death, cardiovascular events, and hospitalization. N. Engl. J. Med. 2004; 351:1296-1305.
2. Fleck C., Appenroth D. et al. Suitability of 5/6 nephrectomy (5/6NX) for the induction of interstitial renal fibrosis in rats--influence of sex, strain, and surgical procedure. Exp. Toxicol. Pathol. 2006; 57:195-205.
3. Griffin K.A., Picken M.M. et al. Functional and structural correlates of glomerulosclerosis after renal mass reduction in the rat. J. Am. Soc. Nephrol. 2000; 11:497-506.
4. Kang D.H., Kanellis J. et al. Role of the microvascular endothelium in progressive renal disease. J. Am. Soc. Nephrol. 2002; 13:806-816.
5. Baylis C. Nitric oxide synthase derangements and hypertension in kidney disease. Curr. Opin. Nephrol. Hypertens. 2012; 21:1-6.
6. Bongartz L.G., Braam B. et al. Transient nitric oxide reduction induces permanent cardiac systolic dysfunction and worsens kidney damage in rats with chronic kidney disease. Am. J. Physiol Regul. Integr. Comp Physiol 2010; 298:R815-R823.
7. Fujihara C.K., De N.G., Zatz R. Chronic nitric oxide synthase inhibition aggravates glomerular injury in rats with subtotal nephrectomy. J. Am. Soc. Nephrol. 1995; 5:1498-1507.
8. Fujihara C.K., Sena C.R. et al. Short-term nitric oxide inhibition induces progressive nephropathy after regression of initial renal injury. Am. J. Physiol Renal Physiol 2006; 290:F632-F640.
9. Dikow R., Kihm L.P. et al. Increased infarct size in uremic rats: reduced ischemia tolerance? J. Am. Soc. Nephrol. 2004; 15:1530-1536.
10. Elrashidy R.A., Asker M.E., Mohamed H.E. Pioglitazone attenuates cardiac fibrosis and hypertrophy in a rat model of diabetic nephropathy. J. Cardiovasc. Pharmacol. Ther. 2012; 17:324-333.
11. Haylor J., Schroeder J. et al. Skin gadolinium following use of MR contrast agents in a rat model of nephrogenic systemic fibrosis. Radiology 2012; 263:107-116.
12. Moriguchi Y., Yogo K. et al. Left ventricular hypertrophy is associated with inflammation in sodium loaded subtotal nephrectomized rats. Biomed. Res. 2011; 32:83-90.
13. van Koppen A., Joles J.A. et al. Healthy bone marrow cells reduce progression of kidney failure better than CKD bone marrow cells in rats with established chronic kidney disease. Cell Transplant. 2012.
14. Baylis C., Corman B. The aging kidney: insights from experimental studies. J. Am. Soc. Nephrol. 1998; 9:699-709.
15. Szabo A.J., Muller V. et al. Nephron number determines susceptibility to renal mass reduction-induced CKD in Lewis and Fisher 344 rats: implications for development of experimentally induced chronic allograft nephropathy. Nephrol. Dial. Transplant. 2008; 23:2492-2495.
16. Darling I.M., Morris M.E. Evaluation of "true" creatinine clearance in rats reveals extensive renal secretion. Pharm. Res. 1991; 8:1318-1322.
17. Levey A.S. Measurement of renal function in chronic renal disease. Kidney Int. 1990; 38:167-184.
18. Myers G.L., Miller W.G. et al. Recommendations for improving serum creatinine measurement: a report from the Laboratory Working Group of the National Kidney Disease Education Program. Clin. Chem. 2006; 52:5-18.
19. Hostetter T.H., Meyer T.W. The development of clearance methods for measurement of glomerular filtration and tubular reabsorption. Am. J. Physiol Renal Physiol 2004; 287:F868-F870.
20. Koeners M.P., Racasan S. et al. Nitric oxide, superoxide and renal blood flow autoregulation in SHR after perinatal L-arginine and antioxidants. Acta Physiol (Oxf) 2007; 190:329-338.
21. van den Brandt J., Wang D. et al. Lentivirally generated eGFP-transgenic rats allow efficient cell tracking *in vivo*. Genesis. 2004; 39:94-99.
22. Kreutz R., Kovacevic L. et al. Effect of high NaCl diet on spontaneous hypertension in a genetic rat model with reduced nephron number. J. Hypertens. 2000; 18:777-782.
23. Liu Z.C., Chow K.M., Chang T.M. Evaluation of two protocols of uremic rat model: partial nephrectomy and infarction. Ren Fail. 2003; 25:935-943.
24. Griffin K.A., Picken M., Bidani A.K. Method of renal mass reduction is a critical modulator of subsequent hypertension and glomerular injury. J. Am. Soc. Nephrol. 1994; 4:2023-2031.
25. Meyer F., Ioshii S.O. et al. Laparoscopic partial nephrectomy in rats. Acta Cir. Bras. 2007; 22:152-156.

Chapter Three

HEALTHY BONE MARROW CELLS REDUCE PROGRESSION OF KIDNEY FAILURE BETTER THAN CKD BONE MARROW CELLS IN RATS WITH ESTABLISHED CHRONIC KIDNEY DISEASE

Cell Transplant. 2012;21(10):2299-312

Arianne van Koppen[1], Jaap A. Joles[1], Lennart G. Bongartz[1], Jens van den Brandt[3], Holger M. Reichardt[3], Roel Goldschmeding[2], Tri Q. Nguyen[2], Marianne C. Verhaar[1]

[1] *Dept. of Nephrology and Hypertension, University Medical Center Utrecht, the Netherlands*

[2] *Dept. of Pathology, University Medical Center Utrecht, the Netherlands*

[3] *Dept. of Cellular and Molecular Immunology, University of Göttingen Medical School, Germany*

Abstract

Chronic kidney disease (CKD) is a major health care problem. New interventions to slow or prevent disease progression are urgently needed. We studied functional and structural effects of infusion of healthy and CKD bone marrow cells (BMCs) in a rat model of established CKD.

CKD was induced by 5/6 nephrectomy (SNX) in Lewis rats, and disease progression was accelerated with L-NNA and 6% NaCl diet. Six weeks after SNX, CKD rats received healthy eGFP$^+$BMCs, CKD eGFP$^+$BMCs, or vehicle by single renal artery injection. Healthy BMCs were functionally effective six weeks after administration: glomerular filtration rate (GFR; inulin clearance) (0.48 ± 0.16 vs. 0.26 ± 0.14 ml/min/100g) and effective renal plasma flow (RPF; PAH clearance) (1.6 ± 0.40 vs. 1.0 ± 0.62 ml/min/100g) were higher in healthy BMC- vs. vehicle-treated rats (both $p < 0.05$). Systolic blood pressure and proteinuria were lower five weeks after treatment with healthy BMCs vs. vehicle (SBP; 151 ± 13 vs.186 ± 25 mm Hg, proteinuria; 33 ± 20 vs. 59 ± 39 mg/d, both $p < 0.05$). Glomerular capillary density was increased and less sclerosis was detected after healthy BMC (both $p < 0.05$). Tubulo-interstitial inflammation was also decreased after healthy BMC. eGFP$^+$ cells were present in the glomeruli and peritubular capillaries of the remnant kidney in all BMC-treated rats. CKD BMCs also reduced SBP, proteinuria, glomerulosclerosis and tubular atrophy vs. vehicle in CKD rats. However, CKD BMC therapy was not functionally effective vs. vehicle: GFR: 0.28 ± 0.09 vs.0.26 ± 0.16 ml/min/100g (NS), RPF: 1.15 ± 0.36 vs. 0.78 ± 0.44 vs. ml/min/100g (NS), and failed to decrease tubulo-interstitial inflammation and fibrosis.

Single intrarenal injection of healthy BMCs in rats with established CKD slowed progression of the disease, associated with increased glomerular capillary density and less sclerosis, whereas injection of CKD BMCs was less effective.

Introduction

Chronic kidney disease (CKD) due to its progressive nature, ensuing end stage kidney disease, and associated cardiovascular morbidity and mortality, is a growing public health problem worldwide[18]. Slowing CKD progression is therefore a major health priority.

Injury to the glomerular and peritubular capillary endothelium, in combination with a defective capillary repair response plays an important role in the pathogenesis and progression of CKD[25]. Endothelial regeneration and repair not only relies on resident endothelial cells but also involves bone marrow (BM) derived endothelial progenitor cells (EPC)[23,24,44]. We were the first to show that glomerular endothelial repair involves recruitment and homing of BM derived cells[41]. Furthermore, in a mouse model, engraftment of BMCs in peritubular capillary endothelium has been demonstrated[34]. These data indicate that BM-derived progenitor cells may function as an 'in-house' regenerating system of the renal microcirculation. Recent studies demonstrated beneficial effects of healthy BMC administration in acute renal injury models[33,46]. Although few animal studies showed a positive effect of BMC treatment on the loss of renal function in the early stage of CKD[1,7-10,42,50], to our knowledge none have studied the effect of BMCs on progression of established CKD.

We previously showed that in CKD patients both number and function of EPC are reduced[22]. Whether such CKD progenitor cell dysfunction affects therapeutic efficacy of BMCs administration in kidney disease has not yet been established.

We hypothesized that healthy BMCs support endothelial repair and hence renal function, thus reducing progression of established CKD, whereas CKD BMCs are less effective. Therefore, in the setting of established CKD induced by subtotal nephrectomy, we studied effects of intra-arterial delivery of healthy and CKD BMCs in the remnant kidney on renal hemodynamics and injury as well as renal incorporation of administered BMCs.

Methods

Animal model

Male inbred Lewis rats (Charles River, Sulzfeld, Germany) and enhanced green fluorescent protein positive (eGFP$^+$) Lewis males[47] were housed under standard conditions in a light-, temperature- and humidity-controlled environment. The protocol was approved by the Utrecht University committee of Animal Experiments. CKD was induced in 8-week-old inbred male Lewis rats by two-stage subtotal

nephrectomy (SNX) (uninephrectomy of left kidney (UNX) followed 7 days later by 2/3 removal of right kidney), accelerated with L-N^G-Nitroarginine (L-NNA), a nitric oxide (NO)-synthase inhibitor (L-NNA) and 6% NaCl diet (t = 0), as described[45]. BMCs were harvested from femur and tibia of $eGFP^+$ age-matched Lewis males, in Dulbecco's modified Eagles medium (DMEM). The cell suspension was filtered (100 µm sieve), the total number of cells was counted (CellDyne 5000) and a suspension based on white blood cellcount was prepared for injection ($50*10^6$ cells/0.5 ml DMEM). The $eGFP^+$ signal of BM and blood cells obtained from donor rats was confirmed by flow cytometry (95% and 88% $eGFP^+$ respectively).

Experimental design

Effects of administration of healthy BMCs in CKD rats

At wk 5, CKD was confirmed (plasma urea > 9 mmol/L), and rats were stratified based on plasma urea and SBP (table 1) as follows: CKD-healthy BMC (n = 8), rats with CKD, intrarenal injection of 50*106 healthy BMCs in wk 6; CKD-vehicle (n = 8), rats with CKD, intrarenal injection of 0.5 ml DMEM (vehicle) in wk 6; 2-kidney controls (2K) (n = 8), animals that were not submitted to either SNX or treatment. Cells were injected directly into the remnant kidney via the renal artery to prevent sequestration of cells in the lungs, which is observed after intravenous injection[30]. We used SBP to follow progression of renal failure and based on these data determined the moment of termination (when SBP > 170 mmHg). At wk 12 terminal kidney function was measured under barbiturate anesthesia (see below). Directly thereafter, rats were sacrificed and tissues were collected and either frozen or fixed in 4% paraformaldehyde (PFA) for embedding in paraffin. For detailed time line, see figure 1.

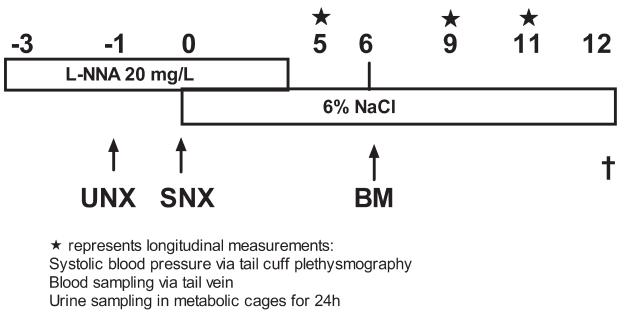

Figure 1 Representation of experimental set up. UNX= uninephrectomy; SNX= subtotal nephrectomy; BM= bone marrow administration; L-NNA= L-N^G-Nitroarginine. Stars indicate longitudinal measurements.

Table 1 Systolic blood pressure, plasma urea and plasma creatinine. Week 5 represents one week before BMC injection. Mean±SD. * p<0.05 compared 2K controls, †p<0.05 compared to CKD vehicle. BMCs were injected in week 6 after SNX.

	2K controls (n=8)	CKD vehicle (n=8)	CKD healthy BMC (n=8)
Systolic blood pressure (mm Hg)			
Week 5	108±18	134±11*	131±22
Plasma urea (mmol/L)			
Week 5	6.9±0.8	14.2±3.2*	12.4±4.0
Week 9	6.8±1.2	13.0±2.8*	10.7±4.7
Week 11	7.3±1.2	14.9±3.2*	10.6±1.9†
Plasma creatinine (µmol/L)			
Week 5	21.0±3.4	73.4±26.9*	59.4±27.8
Week 9	19.8±3.9	66.2±17.7*	54.3±22.7
Week 11	23.9±5.4	74.6±25.8*	50.4±7.2†

To evaluate healthy BMC effect and distribution over time a separate time series experiment was performed. CKD was induced and rats were treated as above. Rats were terminated at different time points as follows D1 (n = 5), 1 day after injection; D7 (n = 5), 7 days after injection; and D21 (n = 5), 21 days after injection, see figure 2. Terminal kidney function was measured, rats were sacrificed and tissues were collected and frozen or fixed in 4% PFA for embedding in paraffin.

Effects of administration of CKD BMCs in CKD rats

The experimental set-up used for the healthy BMC experiment was also used to study the efficacy of CKD BMC infusion. To obtain CKD BMCs, CKD was induced in BMC donor rats as described above. Rats were sacrificed 6 weeks after induction of CKD and BMCs were harvested. Recipient rats were stratified based on plasma urea and SBP (table 2) in three groups: CKD-vehicle (n = 9), rats with CKD, intrarenal injection of 0.5 ml DMEM (vehicle) in wk 6; CKD-healthy BMC (n = 7), rats with CKD, intrarenal injection of $50*10^6$ healthy BMCs in wk 6; CKD-CKD BMC (n = 7), rats with CKD, intrarenal injection of $50*10^6$ CKD BMCs in wk 6. In this group of rats progression of CKD was slower compared to the previous experiment. We used SBP to follow progression of renal failure as in the previous experiment and determined the moment of termination based on SBP > 170. At wk 20 terminal kidney function was measured under barbiturate anesthesia (see below).

Longitudinal chronic kidney disease evaluation

Rats were weighed weekly and in wk 5, 9 and 11, 24h urine, blood samples were collected and systolic blood pressure (SBP) was measured by tail cuff

sphygmomanometry. To collect 24h urine, rats were placed in metabolism cages without food for 24h, but with free access to water with 2% glucose. Urine was collected on antibiotic/antimycotic solution (Sigma, St. Louis, MO; A5955) and stored at –80°C. Blood samples were collected from the tail vein.

Urine protein was measured with Coomassie blue. Sodium and potassium were determined by flame photometry. Plasma urea and plasma and urinary creatinine were determined by DiaSys Urea CT FS (DiaSys Diagnostic Systems, Holzheim, Germany). Creatinine clearance was calculated by standard formula.

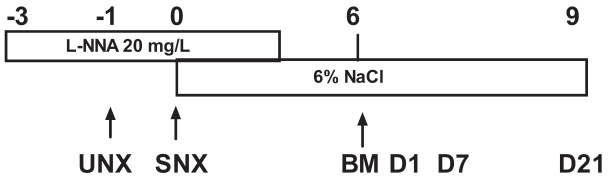

Figure 2 Representation of time experiments. UNX= uninephrectomy; SNX= subtotal nephrectomy; BM= bone marrow administration; L-NNA= L-N^G-Nitroarginine; D1-21 indicates time points of sacrifice.

Table 2 Longitudinal plasma variables CKD BMC experiment. BMCs were injected in week 6 after SNX. Week 5 represents one week before BMC injection. Mean±SD.

	CKD vehicle (n=9)	CKD healthy BMC (n=7)	CKD CKD BMC (n=7)
Plasma urea (mmol/L)			
Week 5	13.7±1.6	12.1±1.3	13.0±2.3
Week 9	9.8±2.1	8.6±1.5	8.7±1.1
Week 11	9.9±2.7	8.8±0.6	8.7±1.4
Week 13	11.1±4.0	8.6±1.4	9.0±2.2
Week 15	11.7±4.1	8.7±1.1	9.1±1.6
Week 17	12.4±7.4	8.0±1.5	9.1±1.8
Week 19	13.0±9.6	8.1±0.9	9.5±1.9
Plasma creatinine (µmol/L)			
Week 5	56.9±11.7	51.9±7.7	49.2±4.8
Week 9	43.0±11.5	38.4±2.5	40.0±4.1
Week 11	46.5±10.9	41.1±4.9	44.2±5.6
Week 13	50.8±19.6	42.2±2.3	47.0±6.4
Week 15	57.4±19.4	45.2±6.3	52.7±8.9
Week 17	58.9±41.0	37.5±3.1	45.4±8.5
Week 19	61.3±47.6	45.1±2.5	48.9±14.5

Terminal kidney function

Kidney function was assessed by inulin clearance to determine glomerular filtration rate (GFR) and PAH clearance to determine the effective renal plasma flow (ERPF) as described previously[29].

Renal Morphology

Glomerulosclerosis and tubulo-interstitial damage were scored on PAS-stained paraffin-embedded slides[28]. Monocytes/macrophages (ED-1 stain) and proliferating cells (ki67-stain) were counted in glomeruli and tubulo-interstitum[2]. Apoptotic cells were counted as the extent of active caspase-3 staining (BD Pharmingen 559565) in the images of 6 randomly selected fields (x200 magnification) per section that were captured and digitized using a digital camera[49]. The number of positively stained nuclei per field was then quantified using Image J Software (Rasband, W.S., ImageJ, U.S. National Institutes of Health, Bethesda, MD). Glomerular area and mean intensity of rat endothelial cell antigen (RECA)$^+$ cells were also determined using ImageJ Software.

Detection and characterization of eGFP$^+$ cells

Indirect immunofluorescence was performed on 5 µm snap-frozen sections, followed by fixation with 4% paraformaldehyde for 10 min, incubated for 30 min with 2% BSA/PBS and incubated for 60 min at room temperature with the primary antibody (polyclonal RbαeGFP 1:200 in PBS/2%BSA; Abcam 6556). Each of these steps was followed by washing with PBS. Subsequently, slides were washed three times with PBS/T 0.05% and incubated for 30 min with the secondary antibody αRb-AlexaFluor488 1:200 in PBS/2%BSA, then incubated for 5 min with DAPI (1:750 in PBS), and finally washed twice with distilled water for 5 min due to the water-solubility of eGFP and covered with mowiol and a cover-slip. As antibody control, blank and isotype staining was used. For conventional immunofluorescence we used a fluorescent microscope (TRR5500 Leica GmbH, Wetzlar, Germany) and for more detailed analysis confocal microscopy was performed (LSM510 Leica). The eGFP$^+$ signal of spleen-, BM-derived and blood cells was measured by flow cytometry.

To further characterize the eGFP$^+$ cells, immunofluorescent double staining was performed on 5-µm snap-frozen sections. The following primary antibodies were used in combination with anti-GFP: rat endothelial cell antigen, a murine IgG_1 mAb against a surface antigen presented on all rat endothelial cells (RECA) (Serotec Ltd., Oxford, England, MCA970R); monocyte/ macrophage marker ED-1, a murine IgG_1 mAb to a cytoplasmic antigen present in monocytes and macrophages (mouse-α -ED-1, kindly provided by Ed Dub, Dept. of Cell Biology, Free University, Amsterdam, the Netherlands); α-smooth muscle actin (α- SMA), a murine IgG2a

mAb against N-terminal synthetic decapeptide of α-smooth muscle actin (Sigma C6198). Slices were defrosted and fixed with 65 ml MetOH + 100 µl H_2O_2 (-20°C), blocked for 30 min with 0.5 ml 1 % Sap + 0.5 ml 20 % NGS + 4 ml PBS, incubated for 60 min with RECA 1:100 in PBS/1 % BSA / ED-1 1:100 in PBS or α-SMA-cy3 1:500 in PBS/2 % BSA, washed and incubated with GtαMo-TRITC 1:100 in PBS/1 % BSA for 30 min, washed and incubated with RbαGFP 1:250 in PBS/2 % BSA at RT for 60 min, washed and incubated with αRb-AlexaFluor488 1:200 in PBS for 30 min. and finally washed twice with distilled water and covered with mowiol and a cover-slip.

Echocardiography

Trans-thoracic echocardiography was performed with a digital ultrasound machine (Philips Sonos 5500, Eindhoven, NL) and a 15-MHz linear array transducer (Hewlett Packard Company, Palo Alto, USA), as described[5].

Gene expression in heart tissue

To determine fluid overload in the heart cDNA was isolated from frozen left ventricles and expression of atrial natriuretic peptide (ANP) and brain natriuretic peptide (BNP) was determined using quantitative real-time RT-PCR (ABi PRiSM 790Sequence Detection SYStem, applied Biosystems, Foster City, CA). The following TaqMan® Gene Expression Assays (Applied Biosystems) were used: (ANP: Rn00561661_m1), (BNP: Rn00580641_m1), (ß-actin: Rn00667869_m1) and (calnexin: Rn00596877_m1). Reactions were carried out in duplicate. Cycle time (Ct) values for ANP were normalized for mean Ct-values of Calnexin and ß-actin, which we previously determined to be the two most stable housekeeping genes across all groups using the geNorm-program (http://medgen.ugent.be/~jvdesomp/genorm/), and expressed relative to a calibrator (the sample with the lowest expression: the 2K controls), using the ΔΔCt-method. Hence, steady state mRNA levels were expressed as n-fold difference relative to the calibrator.

Cytokine array

A rat cytokine array (R&D systems) was performed on bone marrow cell lysate according to manufacturer's instructions. Samples from four healthy and four CKD animals were analyzed separately and equal amounts of protein were loaded on the blots. Each spot on the blot is represented in duplicate and averages of these two pixel densities were used to calculate the average density with Image J software. Background staining and spot size were analysed as recommended by the manufacturer. Briefly, pictures were converted to 8-bit inverted jpeg files and spots were circled. Per blot, equal spot sizes were analysed.

Statistical analyses

Data are presented as mean ± SD and analyzed by analysis of variance One-way ANOVA with a Dunnet post-test, Two-way RM ANOVA with a Bonferroni post-test, and Student's T-test or Mann Whitney test with Graphpad (Prism Software, La Jolla, Calif.) $p < 0.05$ was considered significant. Animals that did not complete the experiment were excluded from analysis.

Results

Healthy BMC treatment reduces CKD progression

At wk 5, CKD was confirmed by increased systolic blood pressure, plasma urea and plasma creatinine in both healthy- and CKD BMC administration experiments (table 1 and 2). As compared with 2K control rats, vehicle-treated CKD rats showed a 69% reduction in GFR as determined by inulin clearance and a 62% reduction in ERPF as determined by PAH clearance at wk 12 (figure 3A/B). All healthy BMC-treated CKD rats had significantly higher GFR and ERPF as well as calculated renal blood flow (RBF) compared to vehicle-treated CKD rats (43 vs. 69%; 38 vs. 62% and 45 vs. 65% reduction of GFR, ERPF and RBF respectively). Terminal mean arterial pressure and renal vascular resistance, filtration fraction and fractional excretions of sodium and potassium were not significantly different between healthy BMC-treated CKD rats vs. vehicle-treated CKD rats (table 3).

As compared with 2K controls, CKD rats terminated at day 1 (D1) showed a 55% reduction in GFR and a 49% reduction in ERPF. At the end of the experiment, as compared to animals from group D1, vehicle-treated CKD rats showed a further reduction in GFR and ERPF while in healthy BMC-treated CKD rats this further reduction in GFR and ERPF was halted.

Healthy BMC infusion reduces the increase of systolic blood pressure, plasma urea and creatinine and proteinuria, and reduces development of anemia.

Systolic blood pressure showed a significant increase over time in vehicle-treated CKD rats, however, no significant increase was observed over time in healthy BMC-treated CKD rats (figure 4A). Systolic blood pressure was significantly lower in healthy BMC-treated CKD rats compared to vehicle-treated CKD rats by wk 9 (137 ± 13 vs. 162 ± 34 mm Hg; $p < 0.05$ and this difference persisted until wk 11 (151 ± 13 vs. 186 ± 25 mm Hg; $p < 0.01$). In vehicle-treated CKD rats diuresis was significantly higher compared to 2K controls, whereas in healthy BMC-treated CKD rats it was not different from 2K controls at wk 11 (data not shown).

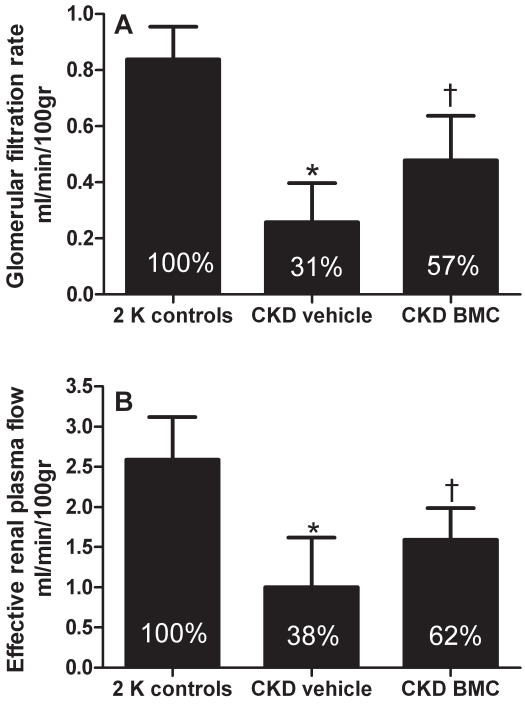

Figure 3 Healthy BMC administration improves terminal kidney function. A: Glomerular filtration rate; B: Effective renal plasma flow. Percentages are relative to healthy controls. 2K control (n=8); CKD vehicle (n=8); CKD healthy BMC (n=8). Mean±SD. * p<0.05 compared to 2K controls, †p<0.05 compared to CKD vehicle.

Table 3 Terminal kidney function measurements. Mean±SD. * p<0.05 compared to 2K controls, †p<0.05 compared to CKD vehicle.

	2K controls (n=8)	CKD vehicle (n=8)	CKD healthy BMC (n=8)
Body weight (g)	421±36	339±30*	368±32
Filtration fraction (%)	0.34±0.048	0.27±0.068	0.30±0.07
FE potassium (%)	13±3.9	61±29*	46±40
FE sodium (%)	0.49±0.33	3.8±7.9*	3.6±8.2
RBF (ml/min/100g)	4.9±0.8	1.7±1.1*	2.7±0.65†
MAP (mm Hg)	99±12	110±21 (n=7)	120±23
RVR (mmHg/ml/min)	4.9±1.0	25±23*	14±5.1

FE= fractional excretion; RBF= renal blood flow; MAP= mean arterial pressure; RVR= renal vascular resistance

Over time, an increase in proteinuria was observed in vehicle-treated CKD rats, but not in healthy BMC-treated CKD rats (figure 4B). Proteinuria was significantly lower by wk 11 in healthy BMC-treated rats compared to vehicle- treated CKD rats (figure 4B). Sodium, potassium and NO metabolite excretion were not significantly different between healthy BMC- and vehicle treatment (data not shown). Plasma creatinine and urea were lower at wk 11 in healthy BMC-treated CKD rats compared to vehicle-treated CKD rats (table 1), but no significant differences in creatinine clearance were found between these groups.

CKD animals developed mild anemia, however hematocrit was significantly higher in healthy BMC-treated CKD rats as compared to vehicle-treated CKD rats (44 ± 4 vs. $40 \pm 3\%$). Haemoglobin levels were also significantly higher in healthy BMC-treated CKD rats vs. vehicle-treated CKD rats (10.0 ± 0.5 vs. 8.7 ± 0.3 mmol/l, $p < 0.05$).

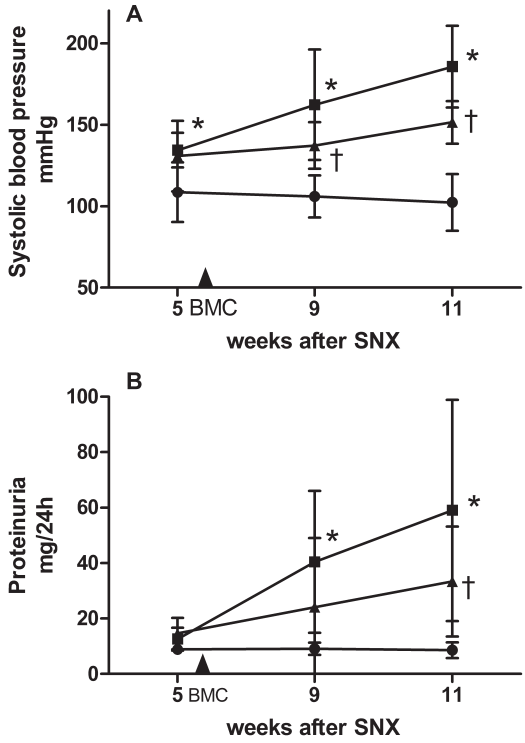

Figure 4 Healthy BMC administration reduces the increase in systolic blood pressure and proteinuria. A: Systolic blood pressure; B: Proteinuria ● = 2K control (n=8); ■ = CKD vehicle (n=8); ▲= CKD healthy BMC (n=8). Mean±SD. * p<0.05 compared to 2K controls, †p<0.05 compared to CKD vehicle.

Healthy BMC treatment increases the number of glomerular endothelial cells and reduces glomerulosclerosis, inflammation and apoptosis

Both vehicle- and healthy BMC-treated CKD rats show marked glomerulosclerosis as compared with 2K-controls with only 10 and 14% normal, non-sclerotic glomeruli as compared to 73% normal glomeruli in 2K-controls (figure 5A). Comparing the number of glomeruli with segmental and global sclerosis between CKD groups reveals a favourable shift with significantly more glomeruli with segmental sclerosis and less glomeruli with global sclerosis in healthy BMC-treated CKD rats compared to vehicle-treated CKD rats (figure 5A).

Significantly more global glomerulosclerosis was observed after vehicle treatment compared with rats terminated on day 1 (D1 rats) (60 ± 24 vs. 14 ± 14%), while there was no significant difference between healthy BMC-treatment after 6 weeks vs. D1 (35 ± 18 %).

Both vehicle-treated and healthy BMC-treated CKD groups had more tubulo-interstitial damage than 2K controls (figure 5B). Tubulo-interstitial inflammation

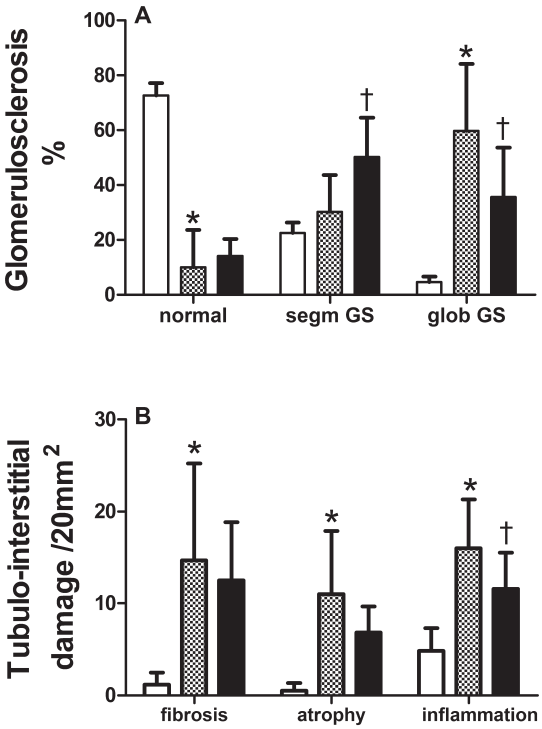

Figure 5 Renal damage is reduced after healthy BMC administration. A: Segmental (segm) and global (glob) glomerulosclerosis (GS); B: Tubulo-interstitial damage. White bars = 2K control (n=6); dotted bars = CKD vehicle (n=8); black bars = CKD healthy BMC (n=8). Mean±SD.* $p<0.05$ compared to 2K controls †$p<0.05$ compared to CKD vehicle.

Table 4 Glomerular morphology.

	2K controls (n=6)	CKD vehicle (n=8)	CKD healthy BMC (n=8)
ED-1$^+$ cells/glomerulus	1.29±0.64	5.54±1.72*	3.84±0.93†
Caspase 3$^+$ cells/glomerulus	0.6±0.3	0.8±0.4	0.6±0.3
Caspase 3$^+$ cells/200xfield	34±29	144±91*	98.5±56
Ki67$^+$ cells/glomerulus	2.76±1.24	6.38±2.31*	8.11±1.34

Mean±SD. *p<0.05 compared to 2K controls, †p<0.05 compared to CKD vehicle.

Table 5 Cytokine production in healthy (n=4) and CKD (n=4) bone marrow cell lysate. Equal amounts of protein were loaded in duplicate. Mean±SD.

Cytokine expression as average pixel density	Healthy BMC (n=4)	CKD BMC (n=4)	p-value
CINC-1	59010±8434	56190±13010	0.6857
IL1α	15120±14450	1227±2453	0.1241
LIX	30900±20890	28820±23480	1.000
L-selectin	63620±4427	67710±7489	0.3429
MIP1α	16530±14300	1319±2639	0.0571
sICAM-1	59310±9683	51790±36090	1.000
Thymus chemokine	48510±8877	39550±31330	0.6857
VEGF	12680±3122	2645±3140	0.0285

CINC-1= Cytokine-Induced Neutrophil Chemoattractant-1. IL1α= Interleukin 1alpha. LIX= Lipopolysaccharide-induced CXC Chemokine. L-selectin= Leucocyte cell-adhesion molecule. Mip1α= Macrophage Inflammatory Protein-1 alpha. sICAM= soluble Inter-Cellular Adhesion Molecule. VEGF= Vascular Endothelial Growth Factor

was less abundant after healthy BMC treatment than in vehicle-treated CKD rats. Interstitial fibrosis and tubular atrophy were not different between CKD groups. Macrophage influx was lower in glomeruli of healthy BMC- vs. vehicle-treated CKD rats (table 4), but tubular macrophage influx was not different. The number of both glomerular and tubular apoptotic cells was higher in vehicle-treated CKD rats compared to 2K-controls, and apoptosis tended to decrease after healthy BMC treatment in CKD rats (not significant; table 4). The number of glomerular proliferating cells was higher in vehicle-treated CKD rats compared to 2K-controls and this tended to be even higher after healthy BMC treatment, although this was not significant (table 4). The glomerular size, assessed by measuring the circumference of the glomeruli, did not differ significantly between CKD groups (figure 6A). However, counts of RECA-positive pixels in glomeruli indicate higher numbers of endothelial cells in the glomeruli of healthy BMC treated CKD rats vs. vehicle treatment (figure 6B).

CKD BMC treatment is less effective in reducing CKD progression

As compared with vehicle- treated CKD rats, healthy BMC-treated rats still showed a higher GFR as determined by inulin clearance (0.26 ± 16 vs. 0.43 ± 0.09 ml/min/100g) and higher ERPF as determined by PAH clearance (0.78 ± 0.44 vs. 1.31 ± 0.41 ml/min/100g) 14 weeks after administration. CKD-BMC-treated CKD rats did not show higher GFR (0.28 ± 0.09 ml/min/100g) or ERPF (1.15 ± 0.36 ml/min/100g) vs. vehicle- treated CKD rats (figure 7A + B). As compared to vehicle-treated CKD rats, calculated renal blood flow was higher in healthy BMC-treated CKD rats (1.32 ± 0.65 vs. 2.26 ± 0.68 $P < 0.05$), while RBF after CKD BMC (1.93 ± 0.62) was not significantly different vs. vehicle

CKD BMC infusion reduces the increase in systolic blood pressure, plasma urea and creatinine, and proteinuria.

Systolic blood pressure was lower in both healthy- and CKD-BMC recipients compared to vehicle-treated CKD rats by wk 11 (134 ± 16 and 126 ± 23 vs. 140 ± 24 mm Hg); and this difference persisted until wk 19 (136 ± 19 and 140 ± 27 vs. 160 ± 31 mm Hg) (figure 8A). Proteinuria was significantly lower by wk 19 in both

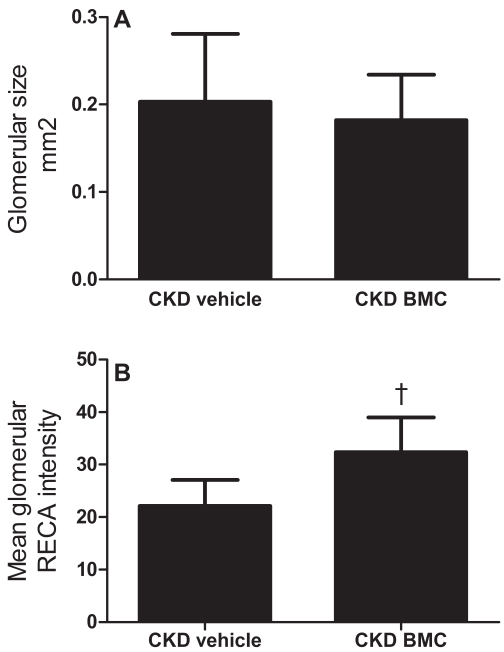

Figure 6 Healthy BMC therapy induces no differences in glomerular expansion while RECA intensity is increased. A: Glomerular expansion; B: Mean glomerular RECA intensity. Mean±SD. †p<0.05 compared to CKD vehicle.

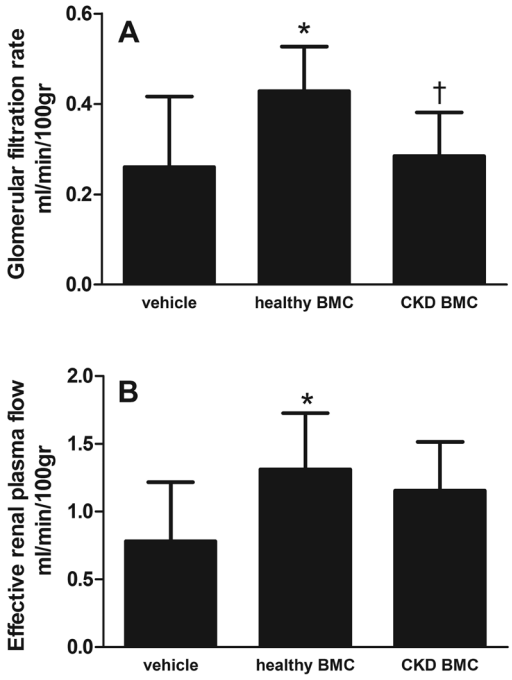

Figure 7 Healthy BMCs effectively increased terminal kidney function, while CKD BMCs did not. A: Glomerular filtration rate; B: Effective renal plasma flow. Vehicle (n=9); healthy BMC (n=7); CKD BMC (n=7). Mean±SD. * p<0.05 compared to vehicle, †p<0.05 compared to healthy BMC.

healthy- and CKD BMC-treated CKD rats compared to vehicle-treated CKD rats (figure 8B). Plasma creatinine and urea were lower by wk 19 in both healthy- and CKD BMC-treated CKD rats compared to vehicle-treated CKD rats (table 2).

BMC treatment reduces renal damage independent of kidney function in the cell donor

Both CKD and healthy BMC-treated CKD rats show significantly more healthy glomeruli compared to vehicle-treated CKD rats (40 ± 11 vs. 21 ± 10 %), indicating less glomerulosclerosis (figure 9A). Vehicle-treated CKD rats demonstrate enhanced tubulo-interstitial damage compared to BMC-treatment. Tubular interstitial inflammation was less after BMC vs. vehicle-treatment in CKD, particularly after healthy BMC treatment. Interstitial fibrosis was decreased after healthy BMC-treatment, however, no effect of CKD BMC-treatment was observed. Tubular atrophy was decreased after BMC treatment vs. vehicle, independent of the disease status of the cell donor (figure 9B). The number of glomerular proliferating cells was increased after both healthy- and CKD BMC treatment compared to vehicle treatment (9.5 ± 2.2 and 9.7 ± 3.3 vs. 7.5 ± 2.3/glomerulus).

Detection and characterization of eGFP$^+$ cells

In frozen slices of the remnant kidney, we were able to visualize eGFP$^+$ cells at 6 and 14 weeks after administration of healthy and CKD BMCs, respectively, both in glomeruli and interstitium, while tubular eGFP$^+$ cells were rare (figure 10A). However, we did not observe incorporated eGFP$^+$ glomerular or interstitial cells, rather cells seem to be attached to the luminal site of the endothelial lining as observed by confocal microscopy (figure 10B/C). No differences were found in the number of eGFP$^+$ cells in remnant kidneys of healthy or CKD BMC recipients (1.53 ± 0.36/glomerulus vs. 1.44 ± 0.73/glomerulus). Double-staining with eGFP and RECA showed no transdifferentiation of BMCs towards endothelial cells i.e. no eGFP/RECA double-positive cells were observed. Double-staining with eGFP and ED-1 showed no transdifferentiation of BMCs towards monocytes/macrophages and eGFP/αSMA double-positive cells were also not observed. In the time series experiments, we observed increasing numbers of eGFP$^+$-cells in the remnant glomeruli at D1 (0.06 ± 0.04); D7 (0.49 ± 0.85); D21 (3.81 ± 1.89) and D42

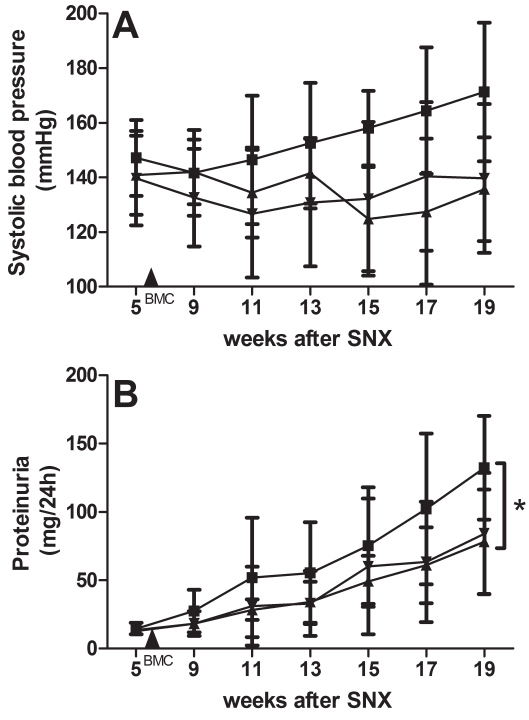

Figure 8 BMC treatment effectively decreased systolic blood pressure and proteinuria. A: Systolic blood pressure (SBP); B: Proteinuria. ■ = vehicle (n=9); ▲= healthy BMC (n=7); ▼= CKD BMC (n=7). Mean±SD. * $p<0.05$ compared to vehicle.

(4.56 ± 1.44; ANOVA, $p = 0.0027$). However, no eGFP/RECA1 double-positive cells were found. In bone marrow and spleen, a few (1-4 %) eGFP$^+$ cells were consistently detected by FACS analyses.

Heart function

Echocardiography revealed no significant effect of intrarenal healthy BMC administration on ejection fraction compared to vehicle treatment (0.60 ± 0.13 vs. 0.66 ± 0.07) and other cardiac parameters (data not shown). No differences were found after healthy BMC treatment compared to vehicle on cardiac gene expression of ANP (5.13 ± 0.85 vs. 5.79 ± 0.73 ΔΔCT) and BNP (1.85 ± 0.78 vs. 2.09 ± 0.85 ΔΔCT).

Rat cytokine array

A rat cytokine array of BMC lysates only showed a significant reduction in VEGF in CKD versus healthy BMCs (table 5). Only data of detectable cytokines are shown.

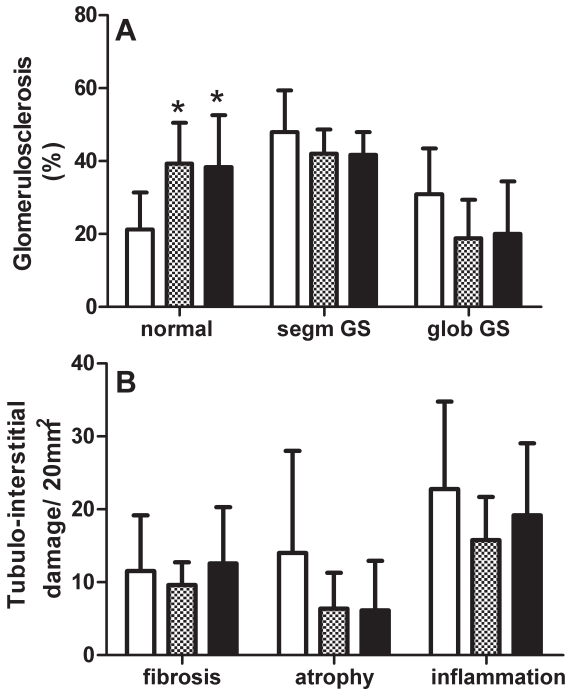

Figure 9 Renal damage was reduced after BMC administration. A: Segmental (segm) and global (glob) glomerulosclerosis (GS); B: Tubulo-interstitial damage. White bars = vehicle (n=9); dotted bars = healthy BMC (n=7); black bars = CKD BMC (n=7). Mean±SD. * p<0.05 compared to vehicle.

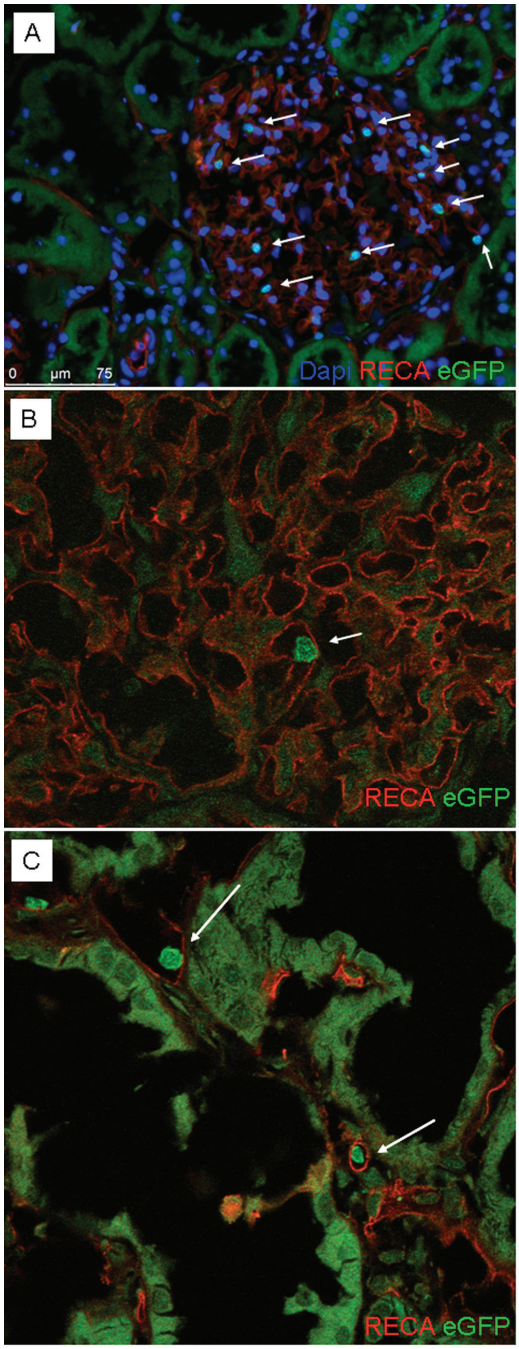

Figure 10 eGFP⁺ cells are detected in the remnant kidney after eGFP⁺ BMC administration via the renal artery. (A) Arrows indicate double positive cells (dapi and eGFP). eGFP⁺ cells are found in close proximity to the glomerular (B) and pericapillary (C) microvasculature. Arrows indicated eGFP⁺ cells in tubulo-interstitial space (C) and glomerular space (B).

Discussion

The main finding of our study is that administration of healthy BMCs into the renal artery of rats with established, progressive CKD markedly reduces the progression of kidney failure. At 6 weeks after single intra-arterial healthy BMC injection, we observed almost two-fold better kidney function as determined by GFR and ERPF, and significantly less glomerulosclerosis, tubulo-interstitial inflammation and apoptosis as compared to vehicle treated CKD rats. Our observation that glomerular capillary density is increased in BMC treated CKD rats suggests endothelial repair or regeneration. CKD BMC injection did not effectively increase GFR and ERPF, but decreased glomerulosclerosis and tubular inflammation and atrophy. Both intrarenal healthy and CKD BMC administration attenuated the increase in systolic blood pressure and proteinuria over time. The relatively low number of $eGFP^+$ BMCs in all recipients, and their close proximity to the microvasculature is consistent with paracrine mechanisms.

Our study is the first to demonstrate that healthy BMC administration as a 'rescue intervention'– i.e. 6 weeks after CKD induction - can markedly attenuate the reduction of both GFR and ERPF as assessed by classical "gold standard" inulin and PAH clearance methodology. Previous studies have demonstrated that BMC administration can accelerate recovery of experimental acute kidney failure (reviewed in[35]) and that synthetic stimulation can enhance the recovery induction ability of BMCs[31]. Following a different paradigm, cell-based therapy of rat renal progenitor-like cell line derived from the S3 segment of renal proximal tubules increased renal function and decreased renal damage after acute renal failure[27]. In CKD, the use of an enriched epithelial cell subpopulation of unfractioned cultures from all major compartments of the kidney, effectively decreased progression of renal failure[26]. A few studies have reported that administration of BMCs or subpopulations of BMCs may attenuate development of CKD if administered when glomerulosclerosis is not yet manifest[1,7,10,33,42] thus indicating preventive effects in early stages of kidney injury rather than therapeutic 'rescue' in established CKD. Only one study by Yuen *et al*. reported on BMC therapy at a later time point, i.e. 4 weeks after SNX, although the severity of CKD at the time of injection is not known[50]. They showed that administration of culture-modified cells, i.e. BM cells that were cultured for 7-10 days on fibronectin-coated plates, resulted in ~28% lower plasma creatinine levels and less proteinuria as well as decreased sclerosis and fibrosis as compared to intravenous saline injection at four weeks after infusion.

Strength of our study is that we evaluated the functional effect of our therapy by using clearance studies. Our study showed a similar and relatively mild reduction of plasma creatinine (~32%) levels at 6 weeks after BMC administration as

compared to vehicle, comparable to the data reported by Yuen *et al*. However, using inulin clearance we show a striking, almost twofold higher GFR after 6 weeks in CKD rats treated with healthy BMCs as compared to vehicle-treated CKD rats, which was reproduced in the second experiment where we also investigated the role of CKD BMC administration. Indeed, in rodents with CKD, creatinine clearance tends to underestimate the degree of renal failure[12,32,37]. The discrepancies between clinical markers of renal function and classic clearance technology underline the importance of bona fide measurements of renal function in models of CKD.

Our findings may have relevance for treatment of CKD in humans. We used the 5/6th nephrectomy ablation model, a well known experimental model of progressive renal disease, resembling human CKD[16,20]. The severe reduction in renal mass causes progressive glomerular injury, loss of remnant nephrons and development of systemic and glomerular hypertension. It has been associated with capillary loss[25] and is characterized by renal inflammation and gradual development of glomerulosclerosis[5]. We injected BMCs via the renal artery at 6 weeks after induction of CKD, a time point at which we and others[5] have shown that kidney failure is established, accompanied by proteinuria and anemia. Besides an almost twofold higher GFR at six weeks after a single healthy BMC injection in our animals with established CKD on kidney function, we also observed beneficial effects in our longitudinal CKD evaluation studies. We found that CKD rats with BMC treatment had significantly lower systolic blood pressure at three and five weeks after BMC injection compared to CKD-vehicle rats, with a difference of up to 35 mmHg between the groups, as well as less proteinuria. CKD-BMC treated rats also had higher terminal hematocrit than vehicle treated CKD rats.

A limitation of our study is that we do not have data on GFR and ERPF at time point of BMC or vehicle injection, i.e. six weeks after induction of CKD. However, if we compare GFR and ERPF at 6 wks after BMC or vehicle injection with GFR and ERPF at one day after BMC-injection - assuming that BMCs will not have a major effect on kidney function within a single day - our data show no further deterioration of GFR and ERPF in CKD rats after BMC therapy, while in CKD vehicle rats, both GFR and ERPF declined. This is consistent with halting of progression of kidney disease.

Our observation of similar increases in GFR and ERPF, and hence no change in filtration fraction, and our finding that there was no difference in glomerular area between BMC or vehicle treated groups, indicate that compensatory hyperfiltration or hyperperfusion in the remnant kidney cannot explain the beneficial effect of BMC administration on kidney function[51]. Rather, our data points at a beneficial effect of BMCs on glomerular structure. We found a favorable shift in glomerulosclerosis after BMC treatment. The beneficial effect of BMCs on glomerulosclerosis development may be explained by an effect on endothelial

regeneration. Several studies have shown that impaired glomerular endothelial repair is associated with progressive glomerulosclerosis[38,43] and that enhancing glomerular endothelial repair may lead to regression of glomerulosclerosis[17]. Indeed, we found a significantly higher glomerular capillary density in kidney sections of CKD-healthy BMC compared to CKD-vehicle rats. The lack of difference in filtration fraction between BMC and vehicle treated CKD rats also points at preglomerular and intraglomerular cells as primary targets of BMC administration. This is in line with a recent study in a porcine model of chronic renovascular disease[9] where BMC administration appeared to mainly enhance ramification of the preglomerular arteriolar tree.

A possible mechanism underlying the preservation or repair of glomerular microvasculature could be engraftment and integration of the injected BMCs into the glomerular endothelium. We have previously demonstrated in chimeric rats that endogenous BMCs may home to injured glomerular endothelium, differentiate into endothelial cells and participate in regeneration of the glomerular microvasculature[41]. We detected BMCs in glomeruli and at luminal endothelial sites of the remnant kidney, however, we observed no incorporation of cells in the glomeruli or glomerular microvasculature, nor did we observe any trans-differentiation of BMCs towards endothelial cells. We performed a time series to study whether incorporation or transdifferentiation of BMCs might have occurred at earlier time points after BMC injection. These data show no higher presence of eGFP$^+$ cells in the remnant kidney directly after injection and also no incorporation or transdifferentiation.

Previous studies have questioned the role of incorporation of BM-derived EPC to adult neovascularization in several experimental models[39,53]. Recent studies in renal disease models also document that the number of cells in the kidney after injection are low[1,50]. The role of BMC incorporation into the endothelium seems dependent on the nature of the vascular injury. In addition, BMCs have been suggested to have a supporting function, by the secretion of growth factors and cytokines[53]. Grunewald et al. showed that BMCs can be recruited to sites of neovascularization and retained close to blood vessels where they act in a paracrine fashion to stimulate neovascularization[21]. Consistently, in hind limb ischemia models accumulations of eGFP$^+$ cells were observed around growing vessels[14,53]. This seems in agreement with our findings of eGFP$^+$ BMCs in close proximity of the endothelium. However, our study does not allow conclusions on the exact paracrine mechanisms. Possible effects could be through protection against apoptosis or by enhancing proliferation. In acute renal failure, decreased apoptosis after BMC treatment has been documented[4,36]. Indeed, in our CKD model the number of apoptotic cells was lower after BMC as compared to vehicle administration. Furthermore, we found more proliferating cells after BMC treatment.

Interestingly, the number of eGFP$^+$ cells in the remnant kidney showed an increase between one and three weeks after injection and did not decrease over the following weeks. This may be related to our finding that injected eGFP$^+$ BMCs were present in both bone marrow and spleen of the recipients. BMCs can home and proliferate in the bone marrow, but also in the spleen which can function as a stem cell niche[15]. This BMC availability from other niches may in part explain the long term effect of BMCs on kidney function. These observations suggest that other administration routes such as intravenous injections may be also be effective. Indeed, Yuen *et al*[50] compared IV injection versus intra-arterial injection of cultured modified cells (CMCs) in a rat model of 5/6 SNX and found that these administration routes were equally effective on functional parameters (urinary protein, plasma creatinine and systolic blood pressure).

When considering clinical application, autologous BMC therapy has the major advantage of avoiding immunologic reactions. However, BMC availability and function are dependent on age and disease state[3]. In our study, a potential disadvantage of autologous BMC therapy for CKD is that the presence of CKD has been shown to negatively influence BMC function, differentiation and proliferation[13,19,22,48]. In a rat CKD model, Drewa et al showed that BM progenitors from CKD rats lacked *in vitro* proliferative capacity[13]. A functional impairment of BMCs may limit the therapeutic potential of autologous BM cell therapy. Indeed, our data show that administration of CKD BMCs in a CKD recipient is less effective in restoring GFR and ERPF compared to healthy BMCs, although we did observe a beneficial effect on blood pressure and proteinuria. No differences were found in number of eGFP$^+$ cells in the remnant kidney between CKD and healthy BMC recipients, suggesting that the attenuated functional effect of CKD BMCs may due to impaired paracrine actions of these cells. Indeed, in CKD BMC lysate expression of VEGF was significantly decreased compared to healthy BMC lysate indicating a shift to a low-angiogenic phenotype.

In certain circumstances, BMCs may give rise to myofibroblasts and contribute to kidney fibrosis[6]. In diseased states differentiation of BMCs may shift towards a more inflammatory phenotype[40]. Furthermore, it has been reported that diseased BM progenitor cells can deliver a disease phenotype to a healthy kidney[11,52]. At six weeks after healthy BMC treatment we did not observe a difference between groups in interstitial fibrosis and even document a favourable shift towards less globally sclerotic glomeruli. In addition, tubulo-interstitial inflammation and glomerular macrophage number were significantly lower in the BMC treated group as compared to the vehicle treated group. Treatment with CKD BMCs also did not induce formation of sclerosis, nor did we observe a significant increase in tubulo-interstitial inflammation, fibrosis or atrophy. We did not observe adverse effects related to the injection of $50*10^6$ BMCs into the renal artery. In kidney sections

obtained 1 and 7 days after BMC injection we detected no morphological effects, no signs of embolism and no differences in tubular necrosis as compared to time controls.

In conclusion, our study demonstrated a marked renoprotective effect of renal artery injection of healthy BMCs in a rat model with established CKD, as shown by a twofold higher GFR and considerably less glomerular damage after a single BMC injection. CKD BMC therapy was less effective, indicating the need for further research to restore this dysfunction. Neither healthy nor CKD BMC injection caused adverse effects. Our findings may provide a basis for further research towards potential clinical application of BMC-based therapies in human CKD.

Acknowledgements

We thank Krista den Ouden, Nel Willekes, Chantal Tilburgs and Paula Martens for their expert technical assistance.

This study was financially supported by the Dutch Kidney foundation, grant C06.2174 M.C.V. is supported by the Netherlands organisation for Scientific Research (NWO) Vidi-grant 016.096.359.

References

1. Alexandre, C. S.; Volpini, R. A.; Shimizu, M. H.; Sanches, T. R.; Semedo, P.; Di Jura, V. L.; Camara, N. O.; Seguro, A. C.; Andrade, L. Lineage-negative bone marrow cells protect against chronic renal failure. Stem Cells 27:682-692; 2009.
2. Attia, D. M.; Verhagen, A. M.; Stroes, E. S.; van Faassen, E. E.; Grone, H. J.; De Kimpe, S. J.; Koomans, H. A.; Braam, B.; Joles, J. A. Vitamin E alleviates renal injury, but not hypertension, during chronic nitric oxide synthase inhibition in rats. J. Am. Soc. Nephrol. 12:2585-2593; 2001.
3. Ayala-Lugo, A.; Tavares, A. M.; Paz, A. H.; Alegretti, A.; Miquelito, L.; Bock, H.; Giugliani, R.; Clausell, N.; Cirne-Lima, E.; Rohde, L. E. Age-dependent availability and functionality of bone marrow stem cells in an experimental model of acute and chronic myocardial infarction. Cell Transplant. 20:407-419; 2011.
4. Barreira, A. L.; Takiya, C. M.; Castiglione, R. C.; Maron-Gutierrez, T.; Barbosa, C. M.; Ornellas, D. S.; Verdoorn, K. S.; Pascarelli, B. M.; Borojevic, R.; Einicker-Lamas, M.; Leite, M., Jr.; Morales, M. M.; Vieyra, A. Bone marrow mononuclear cells attenuate interstitial fibrosis and stimulate the repair of tubular epithelial cells after unilateral ureteral obstruction. Cell. Physiol. Biochem. 24:585-594; 2009.
5. Bongartz, L. G.; Braam, B.; Verhaar, M. C.; Cramer, M. J.; Goldschmeding, R.; Gaillard, C. A.; Doevendans, P. A.; Joles, J. A. Transient nitric oxide reduction induces permanent cardiac systolic dysfunction and worsens kidney damage in rats with chronic kidney disease. Am. J. Physiol. Regul. Integr. Comp. Physiol. 298:R815-R823; 2010.
6. Broekema, M.; Harmsen, M. C.; van Luyn, M. J.; Koerts, J. A.; Petersen, A. H.; van Kooten, T. G.; van Goor, H.; Navis, G.; Popa, E. R. Bone marrow-derived myofibroblasts contribute to the renal interstitial myofibroblast population and produce procollagen I after ischemia/reperfusion in rats. J. Am. Soc. Nephrol. 18:165-175; 2007.
7. Caldas, H. C.; Fernandes, I. M.; Gerbi, F.; Souza, A. C.; Baptista, M. A.; Ramalho, H. J.; Kawasaki-Oyama, R. S.; Goloni-Bertollo, E. M.; Pavarino-Bertelli, E. C.; Braile, D. M.; bbud-Filho, M. Effect of whole bone marrow cell infusion in the progression of experimental chronic renal failure. Transplant. Proc. 40:853-855; 2008.
8. Cavaglieri, R. C.; Martini, D.; Sogayar, M. C.; Noronha, I. L. Mesenchymal stem cells delivered at the subcapsule of the kidney ameliorate renal disease in the rat remnant kidney model. Transplant. Proc. 41:947-951; 2009.
9. Chade, A. R.; Zhu, X.; Lavi, R.; Krier, J. D.; Pislaru, S.; Simari, R. D.; Napoli, C.; Lerman, A.; Lerman, L. O. Endothelial progenitor cells restore renal function in chronic experimental renovascular disease. Circulation 119:547-557; 2009.
10. Choi, S.; Park, M.; Kim, J.; Hwang, S.; Park, S.; Lee, Y. The role of mesenchymal stem cells in the functional improvement of chronic renal failure. Stem Cells Dev. 18:521-529; 2009.
11. Cornacchia, F.; Fornoni, A.; Plati, A. R.; Thomas, A.; Wang, Y.; Inverardi, L.; Striker, L. J.; Striker, G. E. Glomerulosclerosis is transmitted by bone marrow-derived mesangial cell progenitors. J. Clin. Invest. 108:1649-1656; 2001.
12. Doi, K.; Leelahavanichkul, A.; Yuen, P. S.; Star, R. A. Animal models of sepsis and sepsis-induced kidney injury. J. Clin. Invest. 119:2868-2878; 2009.
13. Drewa, T.; Joachimiak, R.; Kaznica, A.; Flisinski, M.; Brymora, A.; Manitius, J. Bone marrow progenitors from animals with chronic renal failure lack capacity of *in vitro* proliferation. Transplant. Proc. 40:1668-1673; 2008.
14. Fadini, G. P.; Albiero, M.; Boscaro, E.; Agostini, C.; Avogaro, A. Endothelial progenitor cells as resident accessory cells for post-ischemic angiogenesis. Atherosclerosis 204:20-22; 2009.
15. Fang, T. C.; Otto, W. R.; Jeffery, R.; Hunt, T.; Alison, M. R.; Cook, H. T.; Wright, N. A.; Poulsom, R. Exogenous bone marrow cells do not rescue non-irradiated mice from acute renal tubular damage caused by HgCl2, despite establishment of chimaerism and cell proliferation in bone marrow and spleen. Cell Prolif. 41:592-606; 2008.
16. Fleck, C.; Appenroth, D.; Jonas, P.; Koch, M.; Kundt, G.; Nizze, H.; Stein, G. Suitability of 5/6 nephrectomy (5/6NX) for the induction of interstitial renal fibrosis in rats--influence of sex, strain, and surgical procedure. Exp. Toxicol. Pathol. 57:195-205; 2006.

17. Fogo, A. B. Progression versus regression of chronic kidney disease. Nephrol. Dial. Transplant. 21:281-284; 2006.
18. Go, A. S.; Chertow, G. M.; Fan, D.; McCulloch, C. E.; Hsu, C. Y. Chronic kidney disease and the risks of death, cardiovascular events, and hospitalization. N. Engl. J. Med. 351:1296-1305; 2004.
19. Goligorsky, M. S.; Yasuda, K.; Ratliff, B. Dysfunctional endothelial progenitor cells in chronic kidney disease. J. Am. Soc. Nephrol. 21:911-919; 2010.
20. Griffin, K. A.; Picken, M. M.; Churchill, M.; Churchill, P.; Bidani, A. K. Functional and structural correlates of glomerulosclerosis after renal mass reduction in the rat. J. Am. Soc. Nephrol. 11:497-506; 2000.
21. Grunewald, M.; Avraham, I.; Dor, Y.; Bachar-Lustig, E.; Itin, A.; Jung, S.; Chimenti, S.; Landsman, L.; Abramovitch, R.; Keshet, E. VEGF-induced adult neovascularization: recruitment, retention, and role of accessory cells. Cell 124:175-189; 2006.
22. Jie, K. E.; Zaikova, M. A.; Bergevoet, M. W.; Westerweel, P. E.; Rastmanesh, M.; Blankestijn, P. J.; Boer, W. H.; Braam, B.; Verhaar, M. C. Progenitor cells and vascular function are impaired in patients with chronic kidney disease. Nephrol. Dial. Transplant. 25:1875-1882; 2010.
23. Kahler, C. M.; Wechselberger, J.; Hilbe, W.; Gschwendtner, A.; Colleselli, D.; Niederegger, H.; Boneberg, E. M.; Spizzo, G.; Wendel, A.; Gunsilius, E.; Patsch, J. R.; Hamacher, J. Peripheral infusion of rat bone marrow derived endothelial progenitor cells leads to homing in acute lung injury. Respir. Res. 8:50; 2007.
24. Kalka, C.; Masuda, H.; Takahashi, T.; Kalka-Moll, W. M.; Silver, M.; Kearney, M.; Li, T.; Isner, J. M.; Asahara, T. Transplantation of *ex vivo* expanded endothelial progenitor cells for therapeutic neovascularization. Proc. Natl. Acad. Sci. USA. 97:3422-3427; 2000.
25. Kang, D. H.; Kanellis, J.; Hugo, C.; Truong, L.; Anderson, S.; Kerjaschki, D.; Schreiner, G. F.; Johnson, R. J. Role of the microvascular endothelium in progressive renal disease. J. Am. Soc. Nephrol. 13:806-816; 2002.
26. Kelley, R.; Werdin, E. S.; Bruce, A. T.; Choudhury, S.; Wallace, S. M.; Ilagan, R. M.; Cox, B. R.; Tatsumi-Ficht, P.; Rivera, E. A.; Spencer, T.; Rapoport, H. S.; Wagner, B. J.; Guthrie, K.; Jayo, M. J.; Bertram, T. A.; Presnell, S. C. Tubular cell-enriched subpopulation of primary renal cells improves survival and augments kidney function in rodent model of chronic kidney disease. Am. J. Physiol. Renal Physiol. 299:F1026-1039; 2010.
27. Kinomura, M.; Kitamura, S.; Tanabe, K.; Ichinose, K.; Hirokoshi, K.; Takazawa, Y.; Kitayama, H.; Nasu, T.; Sugiyama, H.; Yamasaki, Y.; Sugaya, T.; Maeshima, Y.; Makino, H. Amelioration of cisplatin-induced acute renal injury by renal progenitor-like cells derived from the adult rat kidney. Cell Transplant. 17:143-158; 2008.
28. Koeners, M. P.; Braam, B.; van der Giezen, D. M.; Goldschmeding, R.; Joles, J. A. A perinatal nitric oxide donor increases renal vascular resistance and ameliorates hypertension and glomerular injury in adult fawn-hooded hypertensive rats. Am. J. Physiol. Regul. Integr. Comp. Physiol. 294:R1847-R1855; 2008.
29. Koeners, M. P.; Racasan, S.; Koomans, H. A.; Joles, J. A.; Braam, B. Nitric oxide, superoxide and renal blood flow autoregulation in SHR after perinatal L-arginine and antioxidants. Acta Physiol. 190:329-338; 2007.
30. Kraitchman, D. L.; Tatsumi, M.; Gilson, W. D.; Ishimori, T.; Kedziorek, D.; Walczak, P.; Segars, W. P.; Chen, H. H.; Fritzges, D.; Izbudak, I.; Young, R. G.; Marcelino, M.; Pittenger, M. F.; Solaiyappan, M.; Boston, R. C.; Tsui, B. M.; Wahl, R. L.; Bulte, J. W. Dynamic imaging of allogeneic mesenchymal stem cells trafficking to myocardial infarction. Circulation 112:1451-1461; 2005.
31. La Manna G.; Bianchi, F.; Cappuccilli, M.; Cenacchi, G.; Tarantino, L.; Pasquinelli, G.; Valente, S.; Della, B. E.; Cantoni, S.; Claudia, C.; Neri, F.; Tsivian, M.; Nardo, B.; Ventura, C.; Stefoni, S. Mesenchymal stem cells in renal function recovery after acute kidney injury. Use of a differentiating agent in a rat model. Cell Transplant. 2010.
32. Levey, A. S. Measurement of renal function in chronic renal disease. Kidney Int. 38:167-184; 1990.
33. Li, B.; Morioka, T.; Uchiyama, M.; Oite, T. Bone marrow cell infusion ameliorates progressive glomerulosclerosis in an experimental rat model. Kidney Int. 69:323-330; 2006.
34. Li, J.; Deane, J. A.; Campanale, N. V.; Bertram, J. F.; Ricardo, S. D. The contribution of bone marrow-derived cells to the development of renal interstitial fibrosis. Stem Cells 25:697-706; 2007.
35. Little, M. H.; Rae, F. K. Review article: Potential cellular therapies for renal disease: can we translate results from animal studies to the human condition? Nephrology 14:544-553; 2009.

36. Morigi, M.; Introna, M.; Imberti, B.; Corna, D.; Abbate, M.; Rota, C.; Rottoli, D.; Benigni, A.; Perico, N.; Zoja, C.; Rambaldi, A.; Remuzzi, A.; Remuzzi, G. Human bone marrow mesenchymal stem cells accelerate recovery of acute renal injury and prolong survival in mice. Stem Cells 26:2075-2082; 2008.
37. Myers, G. L.; Miller, W. G.; Coresh, J.; Fleming, J.; Greenberg, N.; Greene, T.; Hostetter, T.; Levey, A. S.; Panteghini, M.; Welch, M.; Eckfeldt, J. H. Recommendations for improving serum creatinine measurement: a report from the Laboratory Working Group of the National Kidney Disease Education Program. Clin. Chem. 52:5-18; 2006.
38. Ostendorf, T.; Kunter, U.; Eitner, F.; Loos, A.; Regele, H.; Kerjaschki, D.; Henninger, D. D.; Janjic, N.; Floege, J. VEGF(165) mediates glomerular endothelial repair. J. Clin. Invest. 104:913-923; 1999.
39. Peters, B. A.; Diaz, L. A.; Polyak, K.; Meszler, L.; Romans, K.; Guinan, E. C.; Antin, J. H.; Myerson, D.; Hamilton, S. R.; Vogelstein, B.; Kinzler, K. W.; Lengauer, C. Contribution of bone marrow-derived endothelial cells to human tumor vasculature. Nat. Med. 11:261-262; 2005.
40. Rabelink, T. J.; de Boer, H. C.; de Koning, E. J.; van Zonneveld, A. J. Endothelial progenitor cells: more than an inflammatory response? Arterioscler. Thromb. Vasc. Biol. 24:834-838; 2004.
41. Rookmaaker, M. B.; Smits, A. M.; Tolboom, H.; Van 't Woud, K.; Martens, A. C.; Goldschmeding, R.; Joles, J. A.; van Zonneveld, A. J.; Grone, H. J.; Rabelink, T. J.; Verhaar, M. C. Bone-marrow-derived cells contribute to glomerular endothelial repair in experimental glomerulonephritis. Am. J. Pathol. 163:553-562; 2003.
42. Sangidorj, O.; Yang, S. H.; Jang, H. R.; Lee, J. P.; Cha, R. H.; Kim, S. M.; Lim, C. S.; Kim, Y. S. Bone marrow-derived endothelial progenitor cells confer renal protection in a murine chronic renal failure model. Am. J. Physiol. Renal Physiol. 299:F325-F335; 2010.
43. Shimizu, A.; Kitamura, H.; Masuda, Y.; Ishizaki, M.; Sugisaki, Y.; Yamanaka, N. Rare glomerular capillary regeneration and subsequent capillary regression with endothelial cell apoptosis in progressive glomerulonephritis. Am. J. Pathol. 151:1231-1239; 1997.
44. Silva, G. V.; Litovsky, S.; Assad, J. A.; Sousa, A. L.; Martin, B. J.; Vela, D.; Coulter, S. C.; Lin, J.; Ober, J.; Vaughn, W. K.; Branco, R. V.; Oliveira, E. M.; He, R.; Geng, Y. J.; Willerson, J. T.; Perin, E. C. Mesenchymal stem cells differentiate into an endothelial phenotype, enhance vascular density, and improve heart function in a canine chronic ischemia model. Circulation 111:150-156; 2005.
45. Tornig, J.; Amann, K.; Ritz, E.; Nichols, C.; Zeier, M.; Mall, G. Arteriolar wall thickening, capillary rarefaction and interstitial fibrosis in the heart of rats with renal failure:the effects of ramipril, nifedipine and moxonidine. J. Am. Soc. Nephrol. 7:667-675; 1996.
46. Uchimura, H.; Marumo, T.; Takase, O.; Kawachi, H.; Shimizu, F.; Hayashi, M.; Saruta, T.; Hishikawa, K.; Fujita, T. Intrarenal injection of bone marrow-derived angiogenic cells reduces endothelial injury and mesangial cell activation in experimental glomerulonephritis. J. Am. Soc. Nephrol. 16:997-1004; 2005.
47. van den Brandt, J.; Wang, D.; Kwon, S. H.; Heinkelein, M.; Reichardt, H. M. Lentivirally generated eGFP-transgenic rats allow efficient cell tracking *in vivo*. Genesis 39:94-99; 2004.
48. Westerweel, P. E.; Hoefer, I. E.; Blankestijn, P. J.; de Bree, P.; Groeneveld, D.; van Oostrom O.; Braam, B.; Koomans, H. A.; Verhaar, M. C. End-stage renal disease causes an imbalance between endothelial and smooth muscle progenitor cells. Am. J. Physiol. Renal Physiol. 292:F1132-F1140; 2007.
49. Yang, B.; El Nahas, A. M.; Thomas, G. L.; Haylor, J. L.; Watson, P. F.; Wagner, B.; Johnson, T. S. Caspase-3 and apoptosis in experimental chronic renal scarring. Kidney Int. 60:1765-1776; 2001.
50. Yuen, D. A.; Connelly, K. A.; Advani, A.; Liao, C.; Kuliszewski, M. A.; Trogadis, J.; Thai, K.; Advani, S. L.; Zhang, Y.; Kelly, D. J.; Leong-Poi, H.; Keating, A.; Marsden, P. A.; Stewart, D. J.; Gilbert, R. E. Culture-modified bone marrow cells attenuate cardiac and renal injury in a chronic kidney disease rat model via a novel antifibrotic mechanism. PLoS One 5:e9543; 2010.
51. Zatz, R. Haemodynamically mediated glomerular injury: the end of a 15-year-old controversy? Curr. Opin. Nephrol. Hypertens. 5:468-475; 1996.
52. Zheng, F.; Cornacchia, F.; Schulman, I.; Banerjee, A.; Cheng, Q. L.; Potier, M.; Plati, A. R.; Berho, M.; Elliot, S. J.; Li, J.; Fornoni, A.; Zang, Y. J.; Zisman, A.; Striker, L. J.; Striker, G. E. Development of albuminuria and glomerular lesions in normoglycemic B6 recipients of db/db mice bone marrow: the role of mesangial cell progenitors. Diabetes 53:2420-2427; 2004.
53. Ziegelhoeffer, T.; Fernandez, B.; Kostin, S.; Heil, M.; Voswinckel, R.; Helisch, A.; Schaper, W. Bone marrow-derived cells do not incorporate into the adult growing vasculature. Circ. Res. 94:230-238; 2004.

Chapter Four

EXPOSING CKD RAT BONE MARROW CELLS TO PRAVASTATIN *EX VIVO* IMPROVES THEIR *IN VIVO* THERAPEUTIC EFFICACY IN RATS WITH ESTABLISHED CKD

Submitted

Arianne van Koppen[1], Diana Papazova[1], Nynke Oosterhuis[1], Hendrik Gremmels[1], Joost Fledderus[1], Jaap A. Joles[1], Marianne C. Verhaar[1]

[1] *Dept. of Nephrology and Hypertension, University Medical Center Utrecht, the Netherlands*

Abstract

We previously showed that healthy donor bone marrow cell (BMC) infusion was more effective in supporting glomerular filtration and limiting renal injury in rats with chronic kidney disease (CKD) than CKD donor BMC infusion. Thus, CKD BMC dysfunction would limit therapeutic efficacy of autologous BMC therapy in CKD. Statins have been shown to increase the number and functional activities of BM-derived endothelial progenitor cells and improve endothelial repair mechanisms. We have studied whether exposing CKD rat BMC to pravastatin *ex vivo* improves their subsequent *in vivo* therapeutic efficacy in rats with established CKD and compared these findings to systemic *in vivo* treatment of CKD rats with pravastatin.

CKD was induced by 5/6 nephrectomy (SNX), L-NNA and 6% NaCl diet in Lewis rats. Six weeks after CKD induction, healthy BMCs (HBM), healthy BMCs exposed to 1mM pravastatin for 2h (HBMP), CKD BMCs (CBM) or CKD BMCs exposed to pravastatin *ex vivo* (1mM for 2h; CBMP) were injected into the renal artery (all at a dose of $50*10^6$cells). In addition, the effects of two weeks of oral pravastatin treatment (50 mg/kg/day) vs. no treatment on renal function and injury was studied in CKD rats. Urea was measured at regular intervals. Six weeks after BMC injection (wk12), hematocrit, MAP, glomerular filtration rat (GFR; inulin) and effective renal plasma flow (RPF; PAH) were determined. Renal injury was scored. Direct effects of pravastatin on BMC function were evaluated *in vitro*.

Progression of CKD was slower in CBMP vs. CBM (plasma urea wk 11: 13 ± 3 vs. 16 ± 8 mM; $p < 0.05$). At wk 12 MAP, GFR, RPF, filtration fraction and hematocrit were not significantly different in CBMP vs. HBM or HBMP, whereas all were decreased in CBM. Glomerulosclerosis (GS) and tubulo-interstitial injury were decreased in CBMP vs. CBM. In contrast, 2 weeks of systemic *in vivo* pravastatin treatment of rats with established CKD had no beneficial effects on renal function and injury. *In vitro* results showed improved migration towards the chemo-attractant SDF1α as well as decreased apoptosis in pravastatin-pretreated CKD BMC. The secretome of pravastatin-pretreated CKD BMC contained less pro-inflammatory cytokine CXCL5, whereas CXCL7, which is involved in cell migration and progenitor cell attraction, was increased.

Our data shows that short *ex vivo* exposure of CKD BMC to pravastatin improves BMC function and their subsequent therapeutic efficacy in a clinical CKD setting, whereas systemic pravastatin treatment in CKD rats did not provide renal protection.

Introduction

The rapidly rising number of patients with chronic kidney disease (CKD) worldwide urgently calls for new interventions. Bone marrow (BM)-derived stem and progenitor cell-based therapies have been proposed as promising approach for the treatment of acute and chronic kidney disease. We recently demonstrated that administration of healthy donor BM cells (BMCs) in a rat model of established CKD reduced progression of CKD[1]. For clinical application of BMC therapy in CKD, the use of autologous BMCs would be preferred. However, we also showed that impairment of BMC function in CKD limits the therapeutic efficacy of such therapy in our model of established CKD[1]. Therefore, to develop optimized autologous BM-derived cell therapy for the treatment of CKD, we need to counteract the functional impairment of CKD BMCs.

Several investigators have reported strategies to enhance autologous BM-derived endothelial progenitor cell (EPC) function by systemic treatment or *ex vivo* conditioning with various classes of pharmaceuticals[2-5]. Lipid-lowering 3-hydroxy-3-methyl-glutaryl Coenzyme A reductase (HMG-CoA) inhibitors (statins) have been shown to augment EPC function in *in vitro* assays as well as in preclinical models[6-11], possibly by pleiotropic effects such as increased nitric oxide (NO) bioavailability, and anti-inflammatory and anti-oxidant effects. In addition, statins prevented EPC senescence via regulation of cell cycle proteins[7]. *Ex vivo* statin exposure increased proliferation, migration, angiogenesis and decreased apoptosis of homocysteine-induced dysfunctional EPCs[12] and attenuated survival and function of oxLDL-damaged EPCs[13]. HMG-CoA inhibition was shown to promote BM-dependent re-endothelialization and to diminish vascular lesion development[14].

We hypothesized that exposing CKD rat BMCs to pravastatin *ex vivo* improves their subsequent *in vivo* therapeutic efficacy within the uremic environment, hence decreasing the progression of renal failure in a rat model of established CKD. Therefore, in the setting of established CKD[1], we studied long-term (up to 12 weeks) effects of intra-arterial delivery of pravastatin-pretreated CKD BMCs in the renal artery of the remnant kidney on renal hemodynamics and injury. We compared this to systemic *in vivo* treatment with pravastatin in the same model.

Methods

In vivo experiments

Animal model

CKD was induced in 8-week-old inbred male Lewis rats (recipients) and eGFP$^+$ Lewis rats (donors) by two-stage subtotal nephrectomy (SNX) as described (t = 0)[1,15]. At wk 5, CKD was confirmed (plasma urea > 9 mmol/L) in all CKD rats. BMCs were harvested from femur and tibia of healthy and CKD age-matched Lewis or eGFP$^+$ Lewis male donors, in Dulbecco's modified Eagle medium (DMEM), six weeks after induction of CKD (for donor characteristics, see supplemental table 1). The cell suspension was filtered (100 µm sieve) and BMCs were counted (Abbott Cell-Dyn 1800). Isolated BMCs were incubated with or without 1mM pravastatin in DMEM for 2 hours at 5% CO_2 in a humidified incubator at 37˚C. Cells were washed to remove pravastatin and resuspended in DMEM in a concentration of $100*10^6$ cells /ml.

Experimental design

Effects of ex vivo pravastatin-pretreated BMCs in established CKD

At wk 5 after CKD induction recipient rats (n = 29) were stratified based on plasma urea and systolic blood pressure (SBP; supplemental table 1). $50*10^6$ BMCs, isolated from healthy and CKD eGFP$^+$ donors and incubated with or without 1mM pravastatin, were used as follows: healthy BMC (HBM) recipients (n = 5), injected with healthy eGFP$^+$ BMC exposed to DMEM; healthy + pravastatin BMC (HPBM) recipients (n = 5), injected with healthy eGFP$^+$ BMC exposed to pravastatin; CKD BMC (CBM) recipients (n = 10), injected with CKD eGFP$^+$ BMC exposed to DMEM; CKD + pravastatin (CBMP) recipients (n = 9), injected with CKD eGFP$^+$ BMC exposed to pravastatin. Cells were injected directly into the remnant kidney via the renal artery to prevent sequestration of cells in the lungs, which has been reported after intravenous injection[16]. Longitudinal measurements were performed and at wk 12 terminal kidney function was measured (see below). Directly thereafter, rats were sacrificed and tissues were collected and either frozen or fixed in 4% paraformaldehyde (PFA) for renal morphology measurements.

Effects of systemic in vivo pravastatin treatment in established CKD

At wk 5 after CKD induction, CKD rats were divided into two groups as follows: CKD (n = 5), no supplement in drinking water; CKD + pravastatin (n = 6), 50 mg/kg/day pravastatin added to drinking water. Healthy rats (n = 6) that received no supplement in drinking water were used as controls. Longitudinal measurements were performed and at wk 7 terminal kidney function was measured (see below).

Directly thereafter, rats were sacrificed and tissues were collected and either frozen or fixed in 4% paraformaldehyde (PFA) for renal morphology measurements.

Longitudinal chronic kidney disease evaluation

Rats were weighed weekly and at regular intervals 24h urine and blood samples were collected and systolic blood pressure (SBP) was measured by tail cuff sphygmomanometry (week 5, 9 and 11 for the *ex vivo* pravastatin pretreatment experiments and wk 2, 4 and 6 for the systemic *in vivo* pravastatin treatment studies). To collect 24h urine, rats were placed in metabolism cages without food for 24h, but with free access to water with 2% glucose. Urine was collected on antibiotic/antimycotic solution (Sigma, St. Louis, MO; A5955) and stored at –80°C. Blood samples were collected from the tail vein. Urinary protein levels were measured with Coomassie blue. Sodium and potassium levels were determined by flame photometry. Nitric oxide metabolites were measured with a nitric oxide metabolites detection kit (Cayman Chemical). Plasma urea and plasma and urinary creatinine levels were determined by DiaSys Urea CT FS (DiaSys Diagnostic Systems, Holzheim, Germany). Creatinine clearance was calculated by standard formula.

Terminal kidney function

Kidney function was assessed by inulin clearance to determine glomerular filtration rate (GFR) and PAH clearance to determine the effective renal plasma flow (ERPF) as described[17].

Renal Morphology

Glomerulosclerosis and tubular interstitial damage were scored on PAS-stained paraffin-embedded tissue. Glomerular influx of donor BMCs (GFP^+) and presence of lymphocytes ($CD3^+$), monocytes/macrophages ($ED\text{-}1^+$), proliferating cells ($Ki67^+$), apoptotic cells ($TUNEL^+$), cells undergoing DNA damage repair ($\gamma H2AX^+$), and endothelial cells ($JG12^+$) was counted in 50 glomeruli[18]. Tubular amount of lymphocytes ($CD3^+$), apoptotic cells ($TUNEL^+$), collagen I and III (Picro Sirius red), cells undergoing DNA damage repair ($\gamma H2AX^+$) and influx of donor BMCs (GFP^+) was determined in 20 tubular fields as described before[1,15].

In vitro experiments

BMCs harvested from $eGFP^+$ CKD Lewis rats (for characteristics, see supplemental table 1) were incubated with or without 1mM pravastatin in DMEM for 2 hours at 37 degrees Celsius. Directly after incubation, cells were centrifuged and conditioned medium was stored for further analysis (cytokine array). Cells were washed,

resuspended in 1 ml DMEM and used for assessment of *in vitro* migration and apoptosis. $1x10^6$ cells were stored in Trizol (Invitrogen) for RNA extraction.

Migration assay

Migration of pretreated CKD BMCs was determined using a modified Boyden chamber assay. 300.000 living cells were loaded on top of the 5 µm polycarbonate membrane (Transwell permeable support system, Corning, USA) and bottom wells contained 200 ng/ml SDF1α, 0 ng/ml SDF1α was used as negative control. After 180 minutes, transwells were removed horizontally and 1 ml of 2mM PBS-EDTA was added to each well and incubated for 15 minutes on ice. Cell suspensions were collected and counted by Flow Cytometry. Percentage of migrated DMEM-treated BMCs towards 200 ng/ml SDF1α was set at 100% and compared to migration of pravastatin-treated cells.

Apoptosis

50 ul of cell suspension was used to create a cell smear, air dryed, fixed with formalin and stored at -20° Celsius. TUNEL-staining (Apoptag Plus in situ Peroxidase kit, Millipore, Temecula, CA, USA) was performed according to manufacturer guidelines. The number of apoptotic cells was determined as the number of TUNEL-positive cells in the images of 20 randomly selected fields (x200 magnification).

qPCR

To determine the effects of pretreatment of CKD BMC with pravastatin on the mRNA expression of endothelial nitric oxide synthase (eNOS), protein kinase B (PKB), monocyte chemotactic protein 1 (MCP-1) and tumor necrosis factor α (TNFα), RNA was isolated from BMCs, reverse transcribed to cDNA and quantified using quantitative real-time PCR (ABi PRiSM 790Sequence Detection SYStem, applied Biosystems, Foster City, CA). The following TaqMan® Gene Expression Assays (Applied Biosystems) were used: (eNOS: Rn02132634_s1), (PKB: Rn00583646_m1), (MCP-1: Rn00580555_m1), (TNFa: Rn99999017_m1 (ß-actin: Rn00667869_m1) and (calnexin: Rn00596877_m1). Reactions were carried out in duplicate. Cycle time (Ct) values for genes of interest were normalized for mean Ct-values of Calnexin and β-actin, which we previously determined to be the two most stable housekeeping genes across all groups using the geNorm-program (http://medgen.ugent.be/~jvdesomp/genorm/), and expressed relative to a calibrator (the DMEM sample), using the ΔΔCt-method. Hence, steady state mRNA levels were expressed as n-fold difference relative to the calibrator.

Cytokine array

A rat cytokine array (R&D Systems) of 27 cytokines was performed according to manufacturer's instructions on conditioned medium of BMC samples obtained from six CKD rats pretreated in DMEM with or without 1mM pravastatin. Equal amounts of protein were loaded on the blots. Each spot on the blot is represented in duplicate and averages of the two pixel densities were used to calculate the average pixel density with Image J software. Background staining and spot size were analysed as recommended by the manufacturer. In brief, pictures were converted to 8-bit inverted TIF files and spots were circled. Per blot, equal spot sizes were analysed.

Statistical analyses

Data are presented as mean ± SD and analyzed by analysis of variance (One-way ANOVA with a Student-Newman-Keuls post-test, Two-way ANOVA with a Bonferroni post-test, and Student's T-test) with Graphpad Prism Software, La Jolla, Calif.) $P < 0.05$ was considered significant.

Results

In vivo experiments

Ex vivo pravastatin pre-treatment of CKD BMC improved their in vivo therapeutic efficacy

As compared to HBM rats, CBM rats had a 38% lower GFR and 45% lower ERPF as determined by inulin and PAH clearance at wk 12. However, in CBMP rats GFR and ERPF were not significantly different as compared to HBM rats (figure 1). Terminal mean arterial pressure (MAP) was 20 mm Hg lower in CBMP rats compared to CBM and not different from either HBM or HBMP (table 1). Hematocrit was lower in CBM vs. HBM but higher in CBMP vs. CBM (table 1). Filtration fraction was higher in CBM vs. HBM whereas CBMP was not significantly different vs. HBM (table 1).
At wk 11, plasma urea was higher in CBM compared to HBM (16.1 ± 7.9 vs. 10.7 ± 1.7 mM $p < 0.05$) whereas CBMP (12.9 ± 3.2mM) was not significantly different from HBM (10.7 ± 1.7 mM). Diuresis, proteinuria, creatinine clearance and excretion of NO metabolites were not significantly different between groups (table 2).
In all CKD groups, only approximately 10% of all glomeruli were completely normal, confirming severe kidney injury in this model. The number of totally sclerotic glomeruli was higher in CBM vs. HBM ($P < 0.05$). Comparing the number of partly and totally sclerotic glomeruli between CBM and CBMP revealed a

favourable shift with more glomeruli being partly sclerotic and less glomeruli totally sclerotic in CBMP ($P < 0.05$; figure 2a). Tubular interstitial inflammation, interstitial fibrosis and tubular atrophy were all reduced in CBMP vs. CBM treated rats (figure 2b).

Glomerular macrophage and leukocyte influx as well as the number of proliferating glomerular cells, glomerular JG12$^+$ cells and apoptotic cells were not significantly different between groups (supplemental table 2). No significant difference was found in the number of tubular macrophages, nor in the amount of collagen I and III deposition, apoptotic cells and the amount of γH2AX positive cells between groups (supplemental table 2). The number of GFP$^+$ cells in the remnant kidney was not significantly different between groups. As shown previously, no integration of these cells was observed, and most were attached to the endothelial lining of small vessels[1].

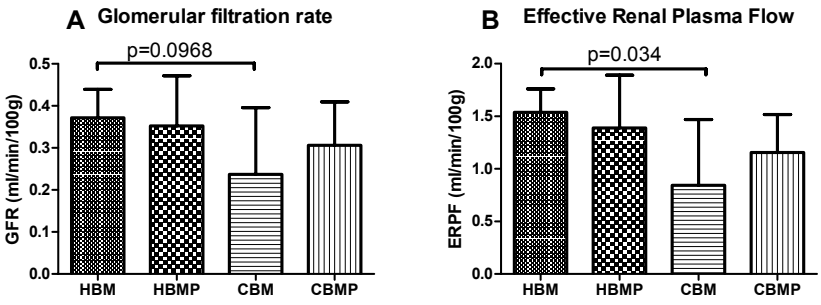

Figure 1 Effect of *in vitro* exposure of healthy and CKD BMC to pravastatin on terminal kidney function in CKD BMC recipients *in vivo*. a: Glomerular filtration rate; b: Effective renal plasma flow. HBM (n=5); HBMP (n=5); CBM (n=10); CBMP (n=9).

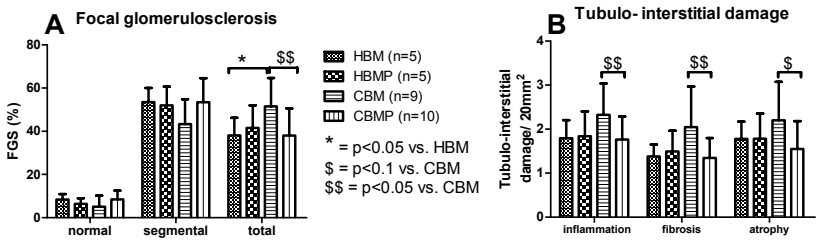

Figure 2 Effect of *in vitro* exposure of healthy and CKD BMC to pravastatin on renal morphology in CKD BMC recipients *in vivo*. a: Focal glomerulosclerosis; b: Tubulo-interstitial damage. *p<0.1; **p<0.05 vs. HBM, $p<0.1; $$p<0.05 vs. CBM.

Systemic *in vivo* treatment of CKD rats did not reduce CKD progression

CKD rats developed hypertension, mild uremia and anemia and proteinuria (supplemental table 3) and had lower body weight, mean arterial pressure, GFR, ERPF, filtration fraction and hematocrit as compared to healthy controls (table 3). Systemic 2-weeks *in vivo* pravastatin treatment did not influence any of these variables. NO metabolite excretion was not significantly different between CKD and CKD + prava rats. In CKD rats, the number of normal glomeruli was reduced compared to healthy rats (supplemental table 3).

Table 1 Terminal kidney function measurements of *ex vivo* pravastatin-pretreated BMC recipients. Mean±SD. * p<0.1; ** p<0.05 compared to HBM, $ p<0.1; $$ p<0.05 compared to CBM.

Wk 12	HBM (n=5)	HBMP (n=5)	CBM (n=10)	CBMP (n=9)
MAP (mmHg)	149 ± 28	146 ± 35	173 ± 21*	153 ± 21$
Hematocrit (%)	45.4 ± 0.9	44.2 ± 0.8	42.5 ± 3.2*	45.8 ± 1.9$$
FF (%)	24.1 ± 2.4	26.2 ± 4.7	29.9 ± 4.5**	26.4 ± 3.7

MAP= mean arterial pressure. FF= filtration fraction

Table 2 Longitudinal plasma and urinary variables of *ex vivo* pravastatin-pretreated BMC. Week 5 represents one week before BMC injection. Mean±SD. * p<0.05 compared to HBM.

	HBM (n=5)	HBMP (n=5)	CBM (n=10)	CBMP (n=9)
Plasma urea (mmol/L)				
Wk 5	10±9	10±1	12±3	11±2
Wk 7	11±1	11±2	12±4	11±2
Wk 9	11±1	11±3	14±6	12±2
Wk 11	11±2	12±2	16±8*	13±3
Diuresis (ml/24h)				
Wk 5	35±6	31±11	32±11	37±7
Wk 7	30±10	25±10	30±11	31±12
Wk 9	29±13	29±10	34±10	39±8
Wk 11	36±6	30±17	34±8	35±5
Creatinine clearance (ml/min)				
Wk 5	21.6±5.6	21.9±6.8	23.7±17.3	22.7±8.4
Wk 7	23.7±7.7	16.6±5.7	21.7±12.4	25.2±8.9
Wk 9	44.4±22.3	47.4±26.5	52.1±31.7	61.7±27
Wk 11	69.8±28.7	65.7±25.2	75.7±25.1	80.5±18.3
NO metabolites (µmol/24h)				
Wk 5	3.13±0.49	3.27±0.89	4.01±1.67	3.30±0.61
Wk 7	3.17±0.17	3.78±0.77	3.83±1.00	3.85±0.82
Wk 9	2.44±0.72	3.46±1.00	3.09±0.89	2.98±0.77
Wk 11	2.86±0.66	2.62±0.55	2.79±1.38	2.86±0.62

In vitro experiments

In vitro pravastatin pre-treatment of BMCs improves BMC function

Pravastatin pretreated CKD BMC showed increased migration towards 200 ng/ml SDF1α as compared to untreated CKD BMC. Increased migration after pravastatin pretreatment was observed in BMCs from 8 out of 10 rats ($p = 0.0137$; figure 3). The number of apoptotic cells was lower in pravastatin pretreated CKD BMCs as compared to DMEM-treated BMC in 8 out of 10 rats ($p = 0.16$). Pravastatin pretreatment of CKD BMC did not alter mRNA expression of TNFα, eNOS, PKB or MCP-1 (supplemental table 4). Out of 27 cytokines on the cytokine array, we detected expression of 4 cytokines. Pravastatin pretreatment of CKD BMC decreased the secretion of pro-inflammatory cytokine CXCL5 and increased chemokine CXCL7, whereas secretion of L-Selectin and soluble ICAM was not different between DMEM- and pravastatin-treated CKD BMC (figure 4).

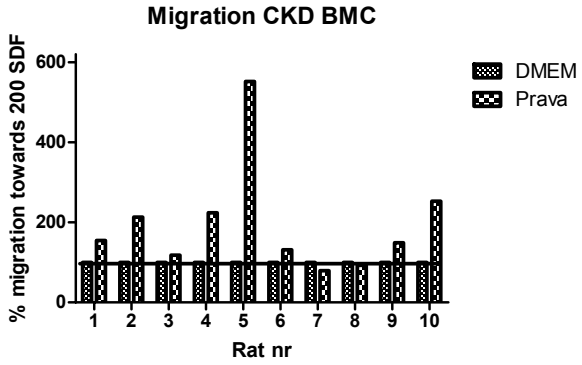

Figure 3 Effect of *in vitro* pravastatin treatment on migration capacity of BMC. DMEM (n=10); PRAVA (n=10).

Table 3. Terminal kidney function measurements after systemic *in vivo* pravastatin treatment. Mean±SD. * $p<0.05$ compared to Healthy 2-kidney.

Wk 7	**Healthy 2-kidney (n=5)**	**CKD (n=5)**	**CKD+ prava** (n=6)
Body weight (g)	377±14	323±23*	312±21*
MAP (mmHg)	107±8	109±7	117±18
GFR (ml/min/100g)	0.87±0.14	0.33±0.05*	0.30±0.05*
ERPF (ml/min/100g)	2.47±0.49	1.33±0.32*	1.11±0.21*
Hematocrit (%)	51±2	44±1*	43±3*
FF (%)	36±3	25±3*	27±5*

MAP= mean arterial pressure. GFR= glomerular filtration rate. ERPF= effective renal plasma flow. FF= filtration fraction.

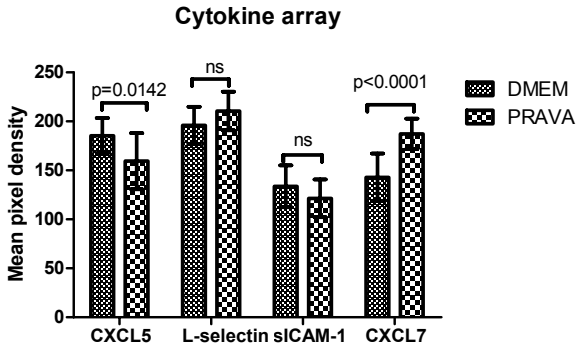

Figure 4 Cytokine expression in CKD BMC was decreased after pravastatin stimulation *in vitro*. DMEM (n=6); PRAVA (n=6).

Discussion

The present study demonstrates for the first time that BMC dysfunction in CKD can be reversed by short-term (2 hours) pretreatment with pravastatin outside the CKD environment and that this effect persists when the cells are returned to the CKD environment, providing augmented therapeutic efficacy *in vivo*.

Our recent studies have shown that single injection of healthy BMCs in rats with established CKD slowed progression of the disease, characterized by increased glomerular capillary density and less sclerosis, whereas injection of CKD BMC was less effective[1]. Thus, CKD induces alterations in BMC function that reduce endothelial regenerative capacity and efficacy of CKD BMC therapy in rats. Previously, statins have been reported to exert beneficial effects on endothelial as well as on BM-derived endothelial progenitor cell function both after *in vitro* incubation as after systemic *in vivo* treatment[6,9,19,20]. Here we show that short term *ex vivo* pretreatment with pravastatin reverses dysfunction in BMCs obtained from rats with established CKD. CKD rats injected with pravastatin-pretreated CKD BMCs showed similar GFR and ERPF as CKD rats receiving BMCs from healthy donors, whereas rats receiving DMEM-pretreated CKD BMCs had markedly lower GFR and ERPF. DMEM-pretreated healthy BMC and pravastatin-pretreated CKD BMC recipients also had a lower filtration fraction than DMEM-pretreated CKD BMC recipients, indicating better preserved glomerular structure. Mean arterial pressure in rats that received pravastatin-pretreated CKD BMCs or healthy BMCs was 20 mm Hg lower compared to recipients that received CKD BMC without pravastatin pre-treatment. Consistently, we observed significantly less glomerulosclerosis, tubular inflammation, atrophy and fibrosis in remnant kidneys of rats

that received pravastatin-pretreated CKD BMCs compared to DMEM-pretreated CKD BMC recipients. *Ex vivo* pravastatin pretreatment did not further improve renal function or structure in HBMP treated rats compared to HBM treated rats, whereas CBMP was significantly more effective than CBM, indicating that pravastatin specifically corrected CKD BMC function.

Interestingly, 2 weeks of systemic *in vivo* treatment with pravastatin did not influence CKD progression in our model of established CKD. Although lipid-lowering effects of statins do not occur in rodents, pleiotropic effects have been reported[21-23] such as reduced inflammation and oxidative stress, enhanced endothelial function and increased mobilization and function of endothelial progenitor cells. Some studies showed beneficial effects of statins on CKD progression in experimental CKD, whereas others reported harmful effects such as induction of renal fibrosis[24]. Clinical studies also reported conflicting results on the effect of statins on CKD progression[25]. The lack of effect of statin treatment in our *in vivo* study cannot be explained by insufficient dosing of pravastatin. Similar statin doses have previously been shown to increase eNOS in rat kidneys[26] and EPC mobilization in mice[8].

Statins have previously been reported to exert beneficial actions on EPC migration, survival and differentiation[6]. We observed augmented migratory capacity of CKD BMC after 2 hours pravastatin pretreatment *in vitro*. Recently, the role of transdifferentiation and incorporation of BMCs in enhancing tissue regeneration has been questioned[27-29]. BMCs appear to have a supportive function, secreting growth factors and cytokines, thereby stimulating resident cells to engage in regeneration[30-32]. Our observations that few eGFP$^+$ BMCs were found in kidney sections of all recipients and that those found were in close proximity to the microvasculature, are consistent with paracrine actions of BMCs. Using a cytokine array we showed that short-term pravastatin pretreatment influences paracrine factor secretion by BMCs. Pravastatin pretreatment of CKD BMCs significantly decreased expression of the pro-inflammatory chemokine CXCL5, which was shown to be involved in the inflammatory cascade and in stimulation of local production of cytokines that have pro-apoptotic effects[33]. The most prominent change in expression on the array was a significant increase in chemokine CXCL7 after *in vitro* pravastatin stimulation. CXCL7 has been shown to stimulate migration of human BMC *in vitro*[34], which could explain the increased migration capacity of CKD BMC after stimulation with pravastatin *in vitro*. Interestingly, Hristov et al demonstrated that of CXC chemokine receptor 2 (CXCR2), the receptor for CXCL7, is important for homing of circulating EPCs to sites of arterial injury[35]. In our model CXCL7 upregulation by pravastatin in CKD BMCs could have augmented the capacity of the injected BMCs to recruit CXCR2-expressing progenitor cells to the kidney and stimulate renal regeneration.

Our observation of impaired BMC function in CKD rats is consistent with clinical studies reporting impaired function of BM-derived EPC obtained from CKD patients[36,37]. We previously showed that culturing healthy BM mononuclear cells in uremic serum caused reduced outgrowth of EPC, suggesting that uremic serum contains either impairing toxins or lacks essential stimulants to support EPC function[37]. Indeed, better *in vivo* removal of uremic toxins in CKD patients has been shown to improve EPC function[38,39]. However, culturing of BM cells in non-uremic conditions *in vitro* could not reverse BMC function. Importantly, our experiments show that 2h incubation with pravastatin reverses rat CKD-BMC dysfunction, which may have important clinical consequences if confirmed in human CKD. Our data do not allow exact elucidation of the molecular mechanisms underlying the beneficial effects of pravastatin on CKD BMCs. The rapid induction of improvement in CKD BMC function is remarkable but seems consistent with previous reports showing that short term statin incubation (< 10 minutes) induces a rapid elevation of NO production in endothelial cells[40] and rapid (< 30 minutes) induction of Akt-mediated phosphorylation of endothelial nitric oxide synthase (eNOS) leading to NO production[41].

In conclusion, short-term pretreatment of CKD BMCs with pravastatin reversed CKD BMC dysfunction and improved their therapeutic efficacy *in vivo*, possibly by enhancing the migratory capacity of CKD BMCs as well as improving their paracrine profile. In contrast, systemic *in vivo* pravastatin treatment did not improve the progressive course of CKD. Our findings have relevance for potential clinical application of BMC therapy in patients with CKD as clinical application would involve autologous - and thus CKD - BMCs to avoid immunological reactions. If confirmed for human CKD BMC our findings will provide a solid basis for development of clinical trials and application of autologous BMC-based therapies in human CKD.

Acknowledgements

We thank Krista den Ouden, Adele Dijk, Nel Willekes, Maaike Meerlo and Paula Martens for their expert technical assistance.

References

1. van Koppen A., Joles J.A. et al. Healthy Bone Marrow Cells Reduce Progression of Kidney Failure Better Than CKD Bone Marrow Cells in Rats With Established Chronic Kidney Disease. Cell Transplant. 2012; 21:2299-2312.
2. Patschan D., Patschan S. et al. Epac-1 activator 8-O-cAMP augments renoprotective effects of syngeneic [corrected] murine EPCs in acute ischemic kidney injury. Am. J. Physiol Renal Physiol 2010; 298:F78-F85.
3. Vaughan E.E., Liew A. et al. Pretreatment of endothelial progenitor cells with osteopontin enhances cell therapy for peripheral vascular disease. Cell Transplant. 2012; 21:1095-1107.
4. Zemani F., Silvestre J.S. et al. *Ex vivo* priming of endothelial progenitor cells with SDF-1 before transplantation could increase their proangiogenic potential. Arterioscler. Thromb. Vasc. Biol. 2008; 28:644-650.
5. Patschan D., Krupincza K. et al. Dynamics of mobilization and homing of endothelial progenitor cells after acute renal ischemia: modulation by ischemic preconditioning. Am. J. Physiol Renal Physiol 2006; 291:F176-F185.
6. Liu Y., Wei J., Hu S., Hu L. Beneficial effects of statins on endothelial progenitor cells. Am. J. Med. Sci. 2012; 344:220-226.
7. Assmus B., Urbich C. et al. HMG-CoA reductase inhibitors reduce senescence and increase proliferation of endothelial progenitor cells via regulation of cell cycle regulatory genes. Circ. Res. 2003; 92:1049-1055.
8. Dimmeler S., Aicher A. et al. HMG-CoA reductase inhibitors (statins) increase endothelial progenitor cells via the PI 3-kinase/Akt pathway. J. Clin. Invest 2001; 108:391-397.
9. Lavi R., Zhu X.Y. et al. Simvastatin decreases endothelial progenitor cell apoptosis in the kidney of hypertensive hypercholesterolemic pigs. Arterioscler. Thromb. Vasc. Biol. 2010; 30:976-983.
10. Llevadot J., Murasawa S. et al. HMG-CoA reductase inhibitor mobilizes bone marrow--derived endothelial progenitor cells. J. Clin. Invest 2001; 108:399-405.
11. Walter D.H., Rittig K. et al. Statin therapy accelerates reendothelialization: a novel effect involving mobilization and incorporation of bone marrow-derived endothelial progenitor cells. Circulation 2002; 105:3017-3024.
12. Bao X.M., Wu C.F., Lu G.P. Atorvastatin inhibits homocysteine-induced dysfunction and apoptosis in endothelial progenitor cells. Acta Pharmacol. Sin. 2010; 31:476-484.
13. Ma F.X., Chen F., Ren Q., Han Z.C. Lovastatin restores the function of endothelial progenitor cells damaged by oxLDL. Acta Pharmacol. Sin. 2009; 30:545-552.
14. Werner N., Priller J. et al. Bone marrow-derived progenitor cells modulate vascular reendothelialization and neointimal formation: effect of 3-hydroxy-3-methylglutaryl coenzyme a reductase inhibition. Arterioscler. Thromb. Vasc. Biol. 2002; 22:1567-1572.
15. van Koppen A., Joles J.A. et al. Human embryonic mesenchymal stem cell-derived conditioned medium rescues kidney function in rats with established chronic kidney disease. PLoS. One. 2012; 7:e38746.
16. Kraitchman D.L., Tatsumi M. et al. Dynamic imaging of allogeneic mesenchymal stem cells trafficking to myocardial infarction. Circulation 2005; 112:1451-1461.
17. Koeners M.P., Racasan S. et al. Nitric oxide, superoxide and renal blood flow autoregulation in SHR after perinatal L-arginine and antioxidants. Acta Physiol (Oxf) 2007; 190:329-338.
18. Attia D.M., Verhagen A.M. et al. Vitamin E alleviates renal injury, but not hypertension, during chronic nitric oxide synthase inhibition in rats. J. Am. Soc. Nephrol. 2001; 12:2585-2593.
19. Baran C., Durdu S. et al. Effects of preoperative short term use of atorvastatin on endothelial progenitor cells after coronary surgery: a randomized, controlled trial. Stem Cell Rev. 2012; 8:963-971.
20. Schmidt-Lucke C., Fichtlscherer S. et al. Improvement of endothelial damage and regeneration indexes in patients with coronary artery disease after 4 weeks of statin therapy. Atherosclerosis 2010; 211:249-254.
21. Nam H.K., Lee S.J. et al. Rosuvastatin Attenuates Inflammation, Apoptosis and Fibrosis in a Rat Model of Cyclosporine-Induced Nephropathy. Am. J. Nephrol. 2012; 37:7-15.

22. Rajtik T., Carnicka S. et al. Pleiotropic effects of simvastatin are associated with mitigation of apoptotic component of cell death upon lethal myocardial reperfusion-induced injury. Physiol Res. 2012; 61 Suppl 2:S33-S41.
23. Zeichner S., Mihos C.G., Santana O. The pleiotropic effects and therapeutic potential of the hydroxymethyl-glutaryl-CoA reductase inhibitors in malignancies: a comprehensive review. J. Cancer Res. Ther. 2012; 8:176-183.
24. Kassimatis T.I., Konstantinopoulos P.A. The role of statins in chronic kidney disease (CKD): friend or foe? Pharmacol. Ther. 2009; 122:312-323.
25. Kalaitzidis R.G., Elisaf M.S. The role of statins in chronic kidney disease. Am. J. Nephrol. 2011; 34:195-202.
26. Ito D., Ito O. et al. Atorvastatin upregulates nitric oxide synthases with Rho-kinase inhibition and Akt activation in the kidney of spontaneously hypertensive rats. J. Hypertens. 2010; 28:2278-2288.
27. Perry T.E., Song M. et al. Bone marrow-derived cells do not repair endothelium in a mouse model of chronic endothelial cell dysfunction. Cardiovasc. Res. 2009; 84:317-325.
28. Shantsila E., Watson T., Lip G.Y. Endothelial progenitor cells in cardiovascular disorders. J. Am. Coll. Cardiol. 2007; 49:741-752.
29. Urbich C., Dimmeler S. Endothelial progenitor cells: characterization and role in vascular biology. Circ. Res. 2004; 95:343-353.
30. Doorn J., Moll G. et al. Therapeutic applications of mesenchymal stromal cells: paracrine effects and potential improvements. Tissue Eng Part B Rev. 2012; 18:101-115.
31. Mezey E. The therapeutic potential of bone marrow-derived stromal cells. J. Cell Biochem. 2011; 112:2683-2687.
32. Togel F., Westenfelder C. The role of multipotent marrow stromal cells (MSCs) in tissue regeneration. Organogenesis. 2011; 7:96-100.
33. Chandrasekar B., Melby P.C. et al. Chemokine-cytokine cross-talk. The ELR + CXC chemokine LIX (CXCL5) amplifies a proinflammatory cytokine response via a phosphatidylinositol 3-kinase-NF-kappa B pathway. J. Biol. Chem. 2003; 278:4675-4686.
34. Kalwitz G., Endres M. et al. Gene expression profile of adult human bone marrow-derived mesenchymal stem cells stimulated by the chemokine CXCL7. Int. J. Biochem. Cell Biol. 2009; 41:649-658.
35. Hristov M., Zernecke A. et al. Importance of CXC chemokine receptor 2 in the homing of human peripheral blood endothelial progenitor cells to sites of arterial injury. Circ. Res. 2007; 100:590-597.
36. Jie K.E., Zaikova M.A. et al. Progenitor cells and vascular function are impaired in patients with chronic kidney disease. Nephrol. Dial. Transplant. 2010; 25:1875-1882.
37. Westerweel P.E., Hoefer I.E. et al. End-stage renal disease causes an imbalance between endothelial and smooth muscle progenitor cells. Am. J. Physiol Renal Physiol 2007; 292:F1132-F1140.
38. Chan C.T., Li S.H., Verma S. Nocturnal hemodialysis is associated with restoration of impaired endothelial progenitor cell biology in end-stage renal disease. Am. J. Physiol Renal Physiol 2005; 289:F679-F684.
39. de Groot K., Bahlmann F.H. et al. Uremia causes endothelial progenitor cell deficiency. Kidney Int. 2004; 66:641-646.
40. Kaesemeyer W.H., Caldwell R.B., Huang J., Caldwell R.W. Pravastatin sodium activates endothelial nitric oxide synthase independent of its cholesterol-lowering actions. J. Am. Coll. Cardiol. 1999; 33:234-241.
41. Kureishi Y., Luo Z. et al. The HMG-CoA reductase inhibitor simvastatin activates the protein kinase Akt and promotes angiogenesis in normocholesterolemic animals. Nat. Med. 2000; 6:1004-1010.

Supplemental material

Supplemental table 1 Donor characteristics and stratification of donor and recipient rats. At 1 wk before BMC or in vivo pravastatin administration (wk 5 for ex vivo experiment, wk 4 for in vivo experiment) rats were stratified based on plasma urea and systolic blood pressure. Mean±SD.

Donor rats	**HBM (n=2)**	**HBMP (n=2)**	**CBM (n=4)**	**CBMP (n=5)**
SNX (%)	-	-		
Wk 5 SBP (mmHg)	-	-	148±34	152±8
Wk 5 Urea (mmol/L)	4.6±0.01	4.1±0.9	15.0±4.4	15.9±6.9
Wk 5 Proteinuria (mg/24h)	1.4±0.4	1.8±0.7	24±8	49±46
Recipient rats	**HBM (n=5)**	**HBMP (n=5)**	**CBM (n=10)**	**CBMP (n=9)**
SNX (%)	66.3±1.6	66.7±6.4	66.5±3.5	67.6±7.1
Wk 5 SBP (mmHg)	156±15	155±16	159±25	155±19
Wk 5 Urea (mmol/L)	10.1±0.9	10.3±1.5	12.1±3.2	10.6±2.3
Wk 5 Proteinuria (mg/24h)	21.6±5.6	21.9±6.8	23.7±17.3	22.7±8.4

Systemic *in vivo* pravastatin treatment

Recipient rats	**Healthy 2-kidney (n=5)**	**CKD (n=5)**	**CKD+ prava (n=6)**
SNX (%)		77±6	75±9
Wk 4 SBP (mmHg)	111±9	163±15	165±15
Wk 4 Urea (mmol/L)	5.9±0.6	13.7±2.8	14.7±2.6
Wk 4 Proteinuria (mg/24h)	11.0±0.8	18.2±7.9	17.3±8.9

***In vitro* pravastatin treatment**	**CKD (n=10)**
SNX (%)	66±2
Wk 5 SBP (mmHg)	169±28
Wk 5 Urea (mmol/L)	11±2
Wk 5 Proteinuria (mg/24h)	18±28

Supplemental table 2 Glomerular and tubular histological characteristics after ex vivo pravastatin pre-treatment. Mean±SD per 50 glomeruli or 20 tubular fields.

	HBM (n=5)	HBMP (n=5)	CBM (n=10)	CBMP (n=9)
Glomerular				
CD3	0.68±0.34	0.72±0.33	0.76±0.19	0.67±0.27
ED-1	7.4±1.0	5.0±2.9	10.5±5.5	7.9±1.9
Ki67	8.0±0.76	6.4±1.7	7.8±1.8	7.8±2.3
TUNEL	2.6±1.3	2.1±1.3	7.0±4.6	4.4±3.7
γH2AX	1.5±1.6	0.6±0.4	1.2±0.8	1.4±0.8
GFP^+	7.0±6.6	2.5±0.7	2.3±1.9	5.2±2.9
JG12	42.5±10	44.4±9.9	42.8±12.5	48.1±9.0
Tubular				
CD3	81±11	96±45	122±59	98±27
TUNEL	35±24	65±59	147±116	95±79
Collagen I and III	4.5±3.1	3.1±1.9	5.6±4.2	4.8±2.6
γH2AX	5.0±1.6	4.3±2.0	6.1±2.8	5.3±1.5
GFP^+	83±82	31±24	23±20	50±38

Supplemental table 3 Longitudinal, terminal and histological measurements after *in vivo* pravastatin treatment. * p<0.05 vs. healthy 2-kidney controls, $ p<0.05 vs. CKD. Mean ± SD.

	Healthy 2-kidney controls (n=5)	CKD (n=5)	CKD+prava (n=6)
SBP (mmHg)			
Wk 2	111±11	155±9*	163±11*
Wk 4	111±9	163±15*	165±15*
Wk 6	113±10	140±8*	147±9*
Plasma urea (mmol/L)			
Wk 2	6.1±0.4	12.6±2.5*	12.3±1.6*
Wk 4	6.0±0.6	13.7±2.8*	14.7±2.6*
Wk 6	6.5±0.3	14.3±1.9*	12.8±1.8*
Hematocrit (%)			
Wk 2	50±1	49±3	50±1
Wk 4	48±2	45±1*	45±1*
Wk 6	48±1	44±1*	45±1*
Proteinuria (mg/24h)			
Wk 2	9.8±0.9	12.4±2.4	10.8±2.2
Wk 4	11.0±0.8	18.2±7.8*	17.3±8.9*
Wk 6	11.0±0.8	18.8±9.5*	18.3±6.9*
NO metabolites (µmol/24h)			
Wk 2	4.3±0.8	1.4±0.3*	2.0±1.1*
Wk 4	6.2±0.9	2.2±0.6*	2.1±0.4*
Wk 6	5.1±0.9	3.7±0.4*	3.6±0.6*
FGS (%)			
Normal	98.8±2	32±8*	18±9*$
Partial	0.8±1	52±8*	56±9*
Total	0.4±1	16±5*	26±8*

Supplemental table 4 Gene expression in CKD BMCs is not changed after *in vitro* treatment with pravastatin. Mean ± SD.

Foldchange	DMEM (n=10)	Prava (n=10)	p-value
TNFα	1.000±1.290	0.868±0.969	0.7504
eNOS	1.000±4.609	2.161±2.874	0.5422
PKB	1.000±0.889	0.905±0.5512	0.6906
MCP-1	1.000±1.254	1.191±0.6933	0.6101

Chapter Five

EFFECTS OF CELL THERAPY IN CKD ON DEVELOPMENT OF CARDIAC FIBROSIS

Journal of Hypertension, in press

This is a non-final version of an article published in final form in Journal of Hypertension, volume 31, 2013. http://journals.lww.com/jhypertension/pages/default.aspx

Arianne van Koppen[1], Jaap A. Joles[1], Marianne C. Verhaar[1]

[1]*Dept. of Nephrology & Hypertension, University Medical Center Utrecht, Utrecht, 3584 CX, Netherlands*

Recently, Keeley and colleagues reported[1] that the amount of bone marrow (BM)-derived circulating fibrocytes is increased and associated with left ventricular hypertrophy in patients with hypertensive heart disease (HHD). The results of this study raise the important question whether activation of BM cells contributes to the enhanced myocardial fibrosis in HHD. If so, the BM may be a new therapeutic target in HHD[2]. On the other hand, this may have major consequences for the clinical translation of BM cell-based therapies for cardiovascular disease in hypertensive patients. Many clinical trials are currently investigating BM cell therapy for cardiovascular disease. However, if hypertension enhances the number of circulating fibrocytes and promotes their activation, thus driving the myocardial fibrotic process and contributing to the pathogenesis of HHD, such therapies may – in the presence of hypertension - lead to unwanted effects on BM cells and myocardial fibrosis. We investigated whether BM cells that were administered in a hypertensive, chronic kidney disease (CKD) rat model, contributed to the development of cardiac fibrosis and dysfunction.

We have recently reported that administration of GFP^+ BM cells in a hypertensive CKD rat model had beneficial effects on renal function[3]. As this model is also characterized by cardiac fibrosis and dysfunction[4], this study allowed us to investigate the contribution of administered BM cells to myocardial fibrosis. A single dose ($50*10^6$ cells) of GFP^+ BM cells – obtained from either healthy or hypertensive CKD enhanced green fluorescent protein positive ($eGFP^+$) Lewis male donor rats[5] - was injected via the renal artery in male inbred Lewis rats (Charles River, Sulzfeld, Germany) when hypertension had developed (SBP > 150 mmHg). Follow-up lasted 6 weeks. Rats were euthanized and organs were perfused and snap-frozen in liquid nitrogen. In each group (vehicle treated rats, $n = 5$; healthy BM cell recipients, $n = 5$; hypertensive BM cell recipients, $n = 5$), 5 µm sections were scored for the presence of administered $eGFP^+$ BM cells. Cardiac fibrosis was quantified using Picro Sirius red staining for collagen type I and III and the number of GFP^+/collagen I double positive cells was assessed.

We confirmed development of cardiac fibrosis in our hypertensive CKD rat model (figure 1). The extent of cardiac fibrosis was not different between vehicle and healthy BM cell recipients (16 ± 4 vs. $17 \pm 6\%$) whereas there was a trend towards increased cardiac fibrosis in rats that had received BM cells from hypertensive CKD donors ($23 \pm 4\%$; $p = 0.056$ vs. vehicle). Influx of GFP^+ cells in the heart was low, both in rats that received healthy BM cells as well as in rats that received BM cells from hypertensive donors. Disease status of the administered cells did not influence cardiac engraftment (healthy: 2.0 ± 2.3 GFP^+ cells/slide vs. hypertensive: 1.4 ± 1.1 GFP^+ cells /slide). Although large patches of fibrosis were detected, we observed no GFP^+ cells in fibrotic areas. No GFP^+/collagen I double positive cells were detected (figure 2a). Most GFP + cells were found in interstitial spaces (figure 2b).

In conclusion, in our hypertensive CKD model, BM cells administered as therapy for treatment of progressive renal disease – either obtained from healthy or hypertensive donors – did not contribute to cardiac fibrosis by transdifferentiation and durable incorporation of these cells. However, we observed a trend towards more cardiac fibrosis in rats that received hypertensive BM cells as compared to rats that received vehicle or healthy BM cells. This may be due to differences in paracrine effects between hypertensive and healthy BM cells, with activated hypertensive BM cells releasing cytokines and growth factors that favor profibrotic processes in resident cells. In line, we previously showed that hypertensive CKD-derived BM cells expressed a different, pro-inflammatory cytokine expression pattern compared to healthy BM cells, which may also explain the reduced efficacy of hypertensive CKD BM cell administration in this hypertensive CKD model[3]. Our data suggest that autologous BM cell therapy in hypertension/CKD may not only be less effective in reducing renal disease progression but may induce unwanted side effects by enhancing cardiac fibrosis.

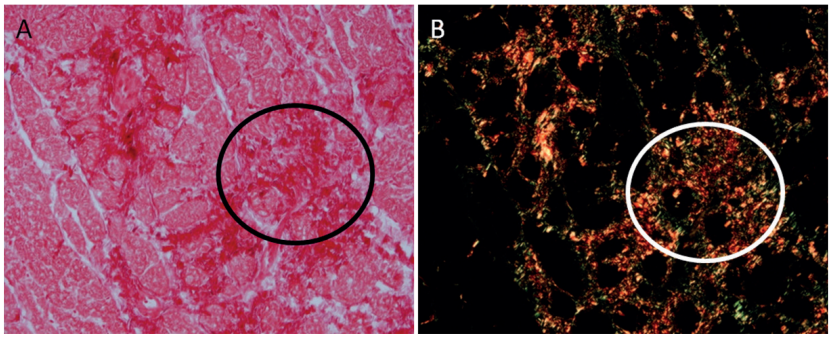

Figure 1 Picro Sirius red staining on cardiac tissue. Collagen is depicted in red in unpolarized (A) and yellow (B) in polarized images.

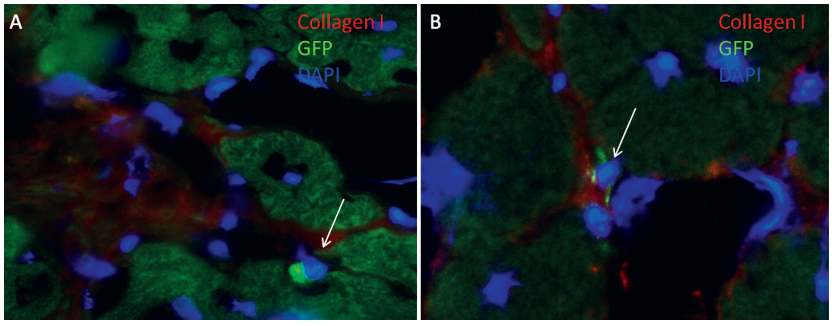

Figure 2 GFP$^+$ cells were rarely detected in cardiac tissue. No GFP/collagen I double staining was observed (A). Most GFP$^+$ cells were found in interstitial spaces (B).

References

1. Keeley E.C., Mehrad B. et al. Elevated circulating fibrocyte levels in patients with hypertensive heart disease. J. Hypertens. 2012; 30:1856-1861.
2. Simko F., Paulis L. Hypertensive heart disease: bone marrow as a significant player in pathologic remodelling? J. Hypertens. 2012; 30:1702-1705.
3. van Koppen A., Joles J.A. et al. Healthy Bone Marrow Cells Reduce Progression of Kidney Failure Better Than CKD Bone Marrow Cells in Rats With Established Chronic Kidney Disease. Cell Transplant. 2012; 21:2299-2312.
4. Bongartz L.G., Braam B. et al. Target organ cross talk in cardiorenal syndrome: animal models. Am. J. Physiol Renal Physiol 2012; 303:F1253-F1263.
5. van den Brandt J., Wang D. et al. Lentivirally generated eGFP-transgenic rats allow efficient cell tracking in vivo. Genesis. 2004; 39:94-99.

Chapter Six

HUMAN EMBRYONIC MESENCHYMAL STEM CELL-DERIVED CONDITIONED MEDIUM RESCUES KIDNEY FUNCTION IN RATS WITH ESTABLISHED CHRONIC KIDNEY DISEASE

PLoS One. 2012;7(6):e38746

Arianne van Koppen[1], Jaap A. Joles[1], Bas W.M. van Balkom[1], Sai Kiang Lim[2], Dominique de Kleijn[3], Rachel H. Giles[1], Marianne C. Verhaar[1]

[1]Dept. of Nephrology and Hypertension, University Medical Center Utrecht, Utrecht, The Netherlands
[2]Institute of Medical Biology, Singapore
[3]Dept of Experimental Cardiology, University Medical Center Utrecht, Utrecht, The Netherlands

Abstract

Chronic kidney disease (CKD) is a major health care problem, affecting more than 35% of the elderly population worldwide. New interventions to slow or prevent disease progression are urgently needed. Beneficial effects of mesenchymal stem cells (MSC) have been described, however it is unclear whether the MSCs themselves or their secretome is required. We hypothesized that MSC-derived conditioned medium (CM) reduces progression of CKD and studied functional and structural effects in a rat model of established CKD.

CKD was induced by 5/6 nephrectomy (SNX) combined with L-NNA and 6% NaCl diet in Lewis rats. Six weeks after SNX, CKD rats received either 50 µg CM or 50 µg non-CM (NCM) twice daily intravenously for four consecutive days. Six weeks after treatment CM administration was functionally effective: glomerular filtration rate (inulin clearance) and effective renal plasma flow (PAH clearance) were significantly higher in CM vs. NCM-treatment. Systolic blood pressure was lower in CM compared to NCM. Proteinuria tended to be lower after CM. Tubular and glomerular damage were reduced and more glomerular endothelial cells were found after CM. DNA damage repair was increased after CM. MSC-CM derived exosomes, tested in the same experimental setting, showed no protective effect on the kidney.

In a rat model of established CKD, we demonstrated that administration of MSC-CM has a long-lasting therapeutic rescue function shown by decreased progression of CKD and reduced hypertension and glomerular injury.

Introduction

The number of patients with chronic kidney disease (CKD) is rising to epidemic proportions[1]. In 2008, the median prevalence of CKD was 7% in persons aged 30 years or older. In persons aged 64 years or older prevalence of CKD varied from 23% to 36% and is still increasing[2]. The ensuing end-stage kidney disease, as well as the associated increase in cardiovascular risk, has significant socio-economic and major public health implications[3]. Nowadays, renal replacement therapy consists of either dialysis or, preferably, kidney transplantation, which is severely limited due to donor shortage. Both renal replacement strategies are associated with increased morbidity and mortality[4]. Consequently, new interventions to slow or prevent CKD progression are being actively pursued. Mesenchymal stem cell (MSC)-based therapies have been proposed as potential new treatment modality. Administration of MSCs has been shown to offer protection in several models of acute kidney injury[5]. Some data demonstrate a positive effect of MSC treatment on the loss of renal function in early stage CKD models as well[6]. In these studies, however, incorporation and trans-differentiation of injected MSCs were rare events, suggesting that MSCs primarily have a supportive function, probably by secreting growth factors and cytokines[7]. Such a paracrine mode of action has the therapeutic potential for cell-free treatment strategies using MSC-secreted factors. Importantly, if administration of MSC-derived secreted factors can reduce CKD progression, this may have major clinical relevance as such therapy could overcome problems associated with (allogenic) MSC administration such as immune incompatibility, MSC maldifferentiation[8,9] and tumorgenicity[10,11]. Thus far, the *in vivo* effects of MSC-secreted factors have only been studied in acute kidney disease. Bi et al. demonstrated that administration of conditioned medium (CM) from bone marrow-derived MSCs in a model of acute kidney injury (AKI) increased survival and limited renal injury, assessed as decreased blood urea nitrogen (BUN) concentrations[12]. Geishara et al., however, could not confirm such beneficial effects of MSC-CM in experimental AKI[13]. The relevance of these observations in AKI to CKD is unclear. To our knowledge, the effect of MSC secreted factors has not been investigated in a model of established CKD.

The paracrine factors secreted by MSC that are responsible for the (reno)protective effects have not been fully elucidated. Next to immunomodulatory and anti-inflammatory properties of MSC, important roles were suggested for proangiogenic factors like vascular endothelial growth factor (VEGF), hepatocyte growth factor (HGF) and insulin-like growth factor (IGF)[14–17]. Recent reports support a central role for microvesicles[18,19] or exosomes[20] in MSC-mediated tissue repair. In experimental myocardial infarction the cardio-protective effects of human embryonic MSC-CM were attributed to exosomes[21,22].

We hypothesized that MSC-secreted factors have a therapeutic rescue function by supporting renal repair and hence renal function and thus reduce progression of established CKD. Therefore, in the setting of established CKD induced by subtotal nephrectomy, the effects of repeated intravenous delivery of human embryonic MSC-derived CM on renal hemodynamics and injury were studied.

Results

CM treatment reduces CKD progression

Six weeks after SNX, CKD was established and rats received treatment with CM or NCM. At 6 weeks after treatment (12 weeks after SNX), treatment with CM resulted in significantly higher GFR and ERPF compared to treatment with NCM (both $p < 0.05$) at $t = 12$ weeks (figure 1). No differences were observed in hematocrit, mean arterial pressure (MAP), renal vascular resistance (RVR), filtration fraction (FF) and fractional excretion of sodium and potassium between CM and NCM (table 1). We observed no significant differences in GFR and ERPF in healthy controls between CM and NCM treatment. Exosome treatment had no effect on CKD progression (supplemental table 1).

CM treatment reduces the increase of systolic blood pressure (SBP) in CKD rats

CKD animals showed significant hypertension compared to healthy controls (figure 2a). SBP was significantly lower in CKD-CM treated rats compared to CKD-NCM treated rats at week 11 (146 ± 17 vs. 163 ± 21 mm Hg; $p < 0.05$, figure 2a). CKD rats showed more proteinuria compared to healthy controls. Protein excretion tended to be lower in CKD-CM-treated compared to CKD-NCM-treated rats (figure 2b;

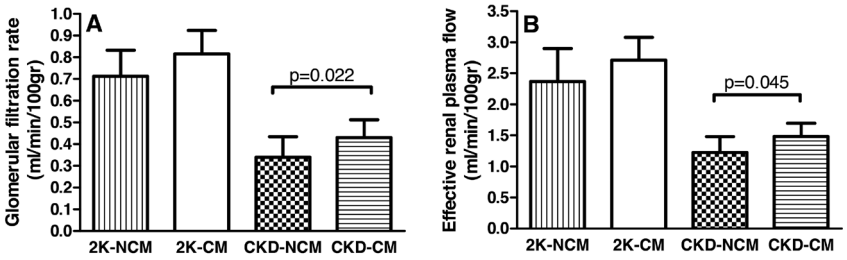

Figure 1 CM treatment increases kidney function. CM treatment increased glomerular filtration rate (GFR) and effective renal plasma flow (ERPF) in CKD. A: Glomerular filtration rate; B: Effective renal plasma flow. 2K-NCM (n=6); 2K-CM (n=6); CKD-CM (n=13); CKD-NCM (n=13). Post-hoc test p-value is shown.

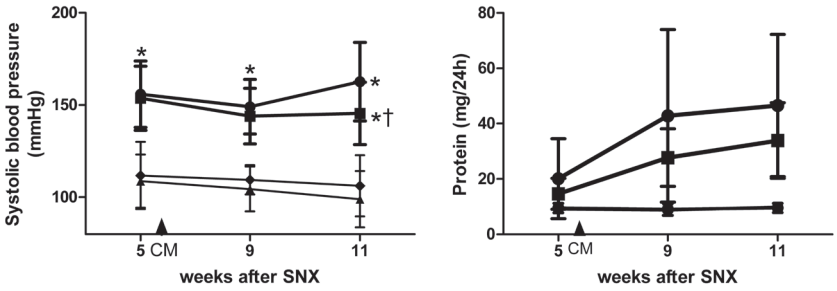

Figure 2 CM treatment decreased systolic blood pressure (A) and proteinuria (B) in CKD. ▼2K-NCM (n=6); ♦ 2K-CM (n=6); ■ CKD-CM (n=13); ● CKD-NCM (n=13). * P<0.05: CKD vs. 2K, † P<0.05: CKD-CM vs. CKD-NCM.

Table 1 Terminal kidney function measurements. Mean±SD *P<0.05: 2K vs. CKD.

	2K-NCM	**2K-CM**	**CKD-NCM**	**CKD-CM**
	n=6	**n=6**	**n=13**	**n=13**
Body weight (g)	442±43	432±23	364±22*	355±16*
MAP (mm Hg)	99±9	93±13	122±22*	135±19*
RBF (ml/min/100g)	4.64±1.37	5.22±0.66	2.10±0.49*	2.56±0.43*
RVR (mm Hg/ml/min)	4.9±1.1	4.1±0.6	17±9*	15±4*
Hematocrit	50±1	49±2	45±2*	46±2*
FF	0.32±0.03	0.30±0.05	0.28±0.05	0.29±0.05
FeNa (%)	0.44±0.24	0.38±0.24	1.59±1.79*	1.55±0.77*
FeK (%)	13±6	14±6	38±11*	45±13*

MAP=mean arterial pressure. RBF=renal blood flow. RVR=renal vascular resistance. FF=filtration fraction. FeNa=fractional excretion of sodium. FeK=fractional excretion of potassium.

$p = 0.071$). No differences were observed in urea and creatinine clearance between CKD-CM and CKD-NCM rats at wk 11 (table 2). Plasma creatinine was increased in CKD-NCM compared to CKD-CM ($p = 0.05$). Importantly, CM or NCM administration did not influence SBP, proteinuria or creatinine clearance in healthy control rats. Exosome treatment had no effect of SBP (supplemental table 2).

CM increases the number of glomerular endothelial cells and reduces glomerulosclerosis and tubular damage in CKD rats

The percentage of glomerular endothelial cells, (JG12 positive), was significantly higher in CKD-CM compared to CKD-NCM- treated rats ($p < 0.05$, Figure 3). Both CKD-CM and CKD-NCM-treated rats showed marked glomerulosclerosis as compared to healthy rats with respectively 31% and 26% normal, non-sclerotic

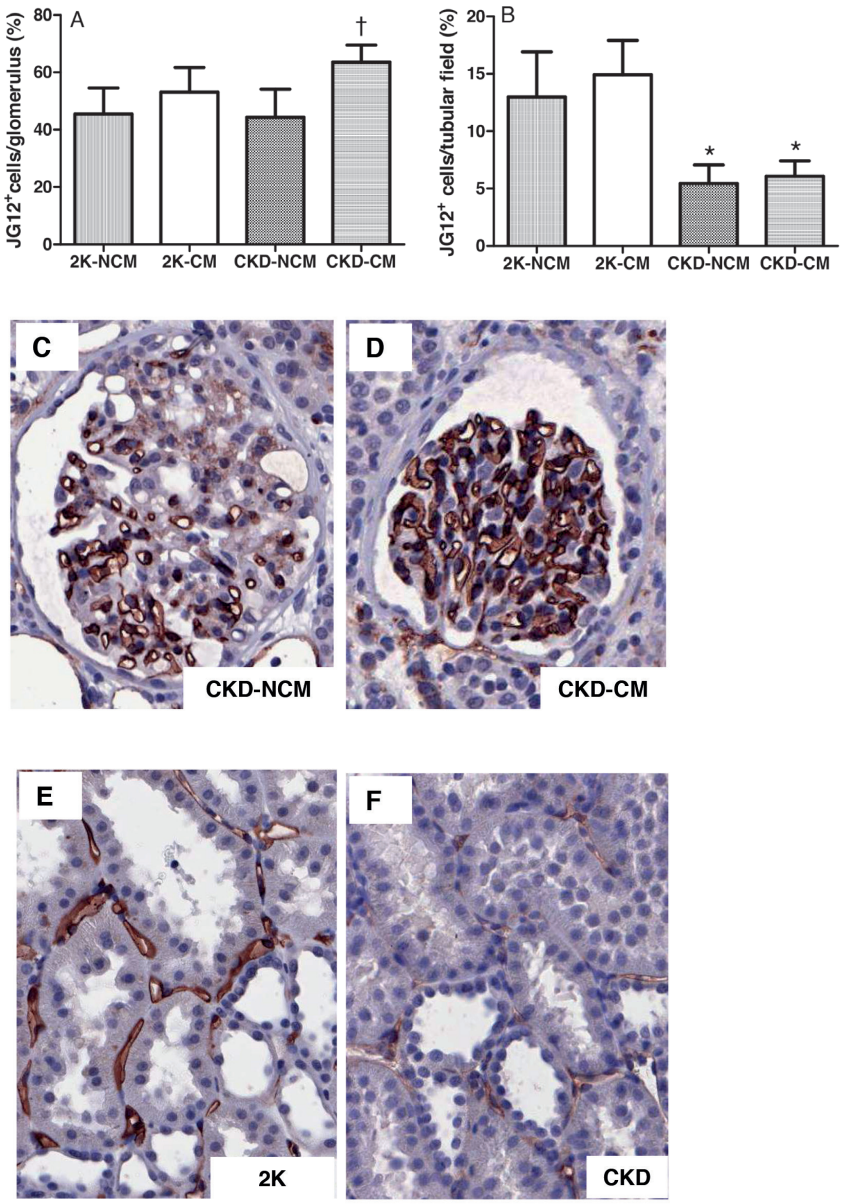

Figure 3 CM treatment increased the number of glomerular endothelial cells (A, C-D), but did not increase tubular endothelial cell number (B, E-F) shown by a JG12 staining. 2K-NCM (n=6); 2K-CM (n=6); CKD-NCM (n=13); CKD-CM (n=13). * P<0.05: CKD vs. 2K, †P<0.05: CKD-CM vs. CKD-NCM.

glomeruli as compared to more than 85% normal glomeruli in healthy controls. Comparing the number of partly and totally sclerotic glomeruli between the CKD groups reveals a favourable shift with significantly more partly sclerotic glomeruli and less totally sclerotic glomeruli in CKD-CM compared to CKD-NCM-treated rats (Figure 4). DNA damage and repair was measured by induction of cellular γ-H2AX; γ-H2AX expression has been established as a sensitive indicator of clonogenic survival after tissue damage and induction of DNA damage repair[23,24]. We noted with interest that CM significantly increased glomerular γ-H2AX induction in CKD rats compared to healthy rats whereas CKD-NCM rats were not different compared to healthy rats (Figure 5). The numbers of glomerular proliferating cells as determined by Ki67 and glomerular inflammatory $CD3^+$ and $ED\text{-}1^+$ cells were not different between the CKD-CM and CKD-NCM -treated rats (table 3).
Compared to healthy rats, both CKD-NCM and CKD-CM-treated rats demonstrated enhanced tubulo-interstitial damage. However, tubular atrophy and interstitial fibrosis were significantly lower after CM treatment in CKD rats (figure 6).
Tubular deposition of collagen I and III was decreased in CKD-CM rats compared to CKD-NCM rats (figure 7). The number of endothelial cells per tubular field was not different between CKD-NCM and CKD-CM treatment, neither were the numbers of tubular $ED\text{-}1^+$ and $CD3^+$ cells. The number of apoptotic cells was not different in glomeruli and tubulo-interstitium of CM and NCM as determined by TUNEL staining (table 3).

Table 2 Longitudinal measurements after CM treatment at week 6 after SNX. Week numbers indicate the week after SNX. Week 5 represents the week before treatment.

	2K-NCM n=6	2K-CM n=6	CKD-NCM n=13	CKD-CM n=13	P (CKD-CM vs. CKD-NCM)
Urea (mmol/L)					
wk 5	5.7±0.9	6.2±1.0	10.3±2.4*	10.2±2.5*	0.854
wk 9	5.9±0.5	5.9±1.1	10.8±2.2*	12.2±1.9*	0.058
wk 11	6.5±0.8	6.9±1.5	9.7±1.9*	9.9±1.8*	0.701
Plasma creatinine (µmol/L)					
wk 5	20.1±3.3	20.8±1.1	49.7±8.8*	48.6±9.9*	0.948
wk9	21.8±6.6	25.6±4.5	44.9±11.4*	42.9±6.6*	0.558
wk11	28.9±7.5	22.7±3.1	51.0±14.2*	42.8±6.9*	0.050
Creatinine clearance (ml/min)					
wk 5	4.18±0.52	4.13±1.31	1.18±0.22*	1.13±0.25*	0.795
wk 9	3.84±1.27	3.00±0.44*	1.48±0.36*	1.43±0.21*	0.801
wk 11	2.84±0.74	3.27±0.93	1.32±0.35*	1.50±0.28*	0.386

*P<0.05 vs. respective 2K controls. Posthoc p-value is shown.

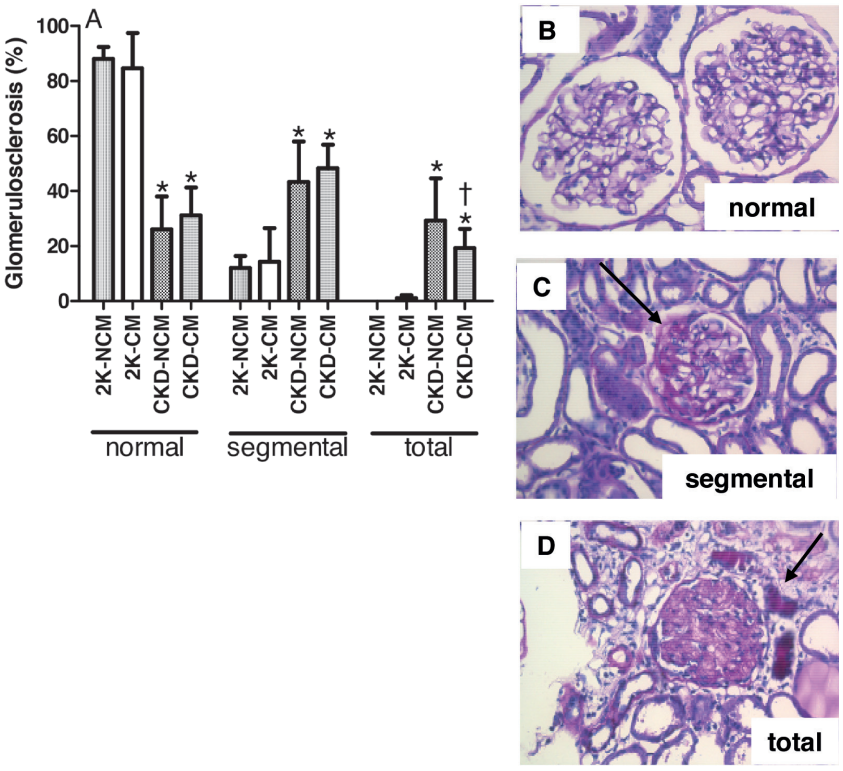

Figure 4 Glomerulosclerosis on PAS-stained sections was reduced after CM treatment (A). Normal (B), segmental (C) and totally sclerotic are shown (D). Black arrows indicate sclerotic areas. 2K-NCM (n=6); 2K-CM (n=6); CKD-NCM (n=13); CKD-CM (n=13). * P<0.05: CKD vs. 2K, †P<0.05: CKD-CM vs. CKD-NCM.

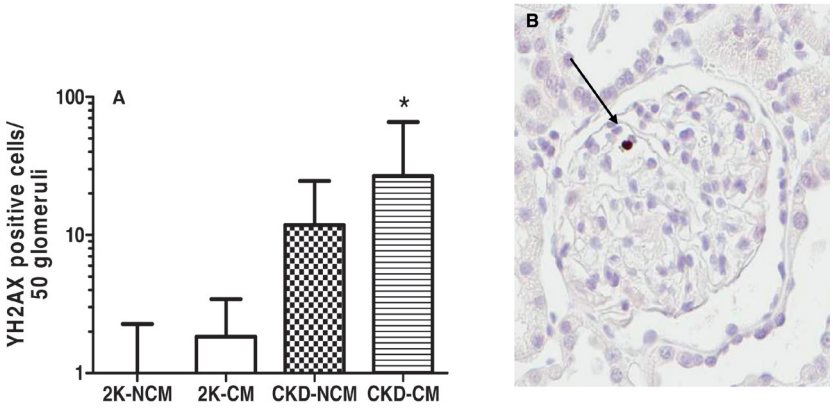

Figure 5 CM treatment increased DNA damage repair shown by γ-H2AX after logarithmic transformation, indicating glomerular nuclei undergoing DNA damage repair. Black arrow indicates positive nucleus. 2K-NCM (n=6); 2K-CM (n=6); CKD-NCM (n=13); CKD-CM (n=13). * P<0.05: CKD vs. 2K

Cytokine profile in remnant kidney is altered after CM treatment

To screen whether CM affected local production of inflammatory cytokines by kidney cells in healthy and CKD kidneys, a cytokine array was performed on kidney homogenates (figure 8a). Seven inflammatory cytokines, Monokine Induced by Gamma-Interferon (MIG); Macrophage Inflammatory Protein-1 alpha (MIP1α); Macrophage Inflammatory Protein-3 alpha (MIP3α); thymus chemokine, Tissue Inhibitor of Metalloproteinase-1 (TIMP-1); VEGF and Interleukin 1 Receptor Antagonist (IL1-RA) were only detected in CKD and not in healthy kidneys.
Fractalkine and Regulated upon Activation, Normal T-cell Expressed, and Secreted (RANTES) were lower in CKD kidneys, whereas L-selectin was higher in CKD kidneys compared to healthy kidneys. In healthy kidneys CM had no significant effects on cytokines, whereas in CKD kidneys CM increased the expression of both Fractalkine and IL-1Ra. Gene expression of Fractalkine was decreased in CKD compared to healthy controls and increased by CM in CKD (figure 8b).

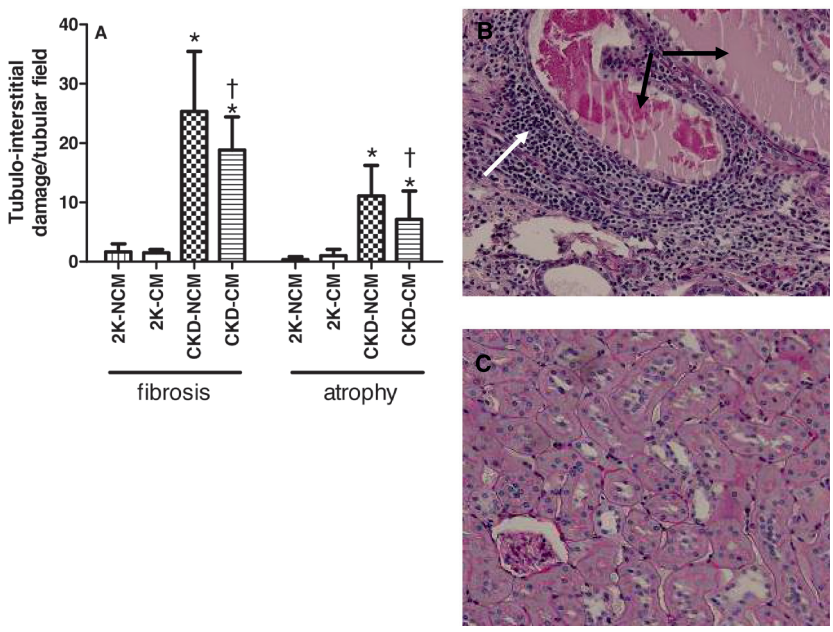

Figure 6 Tubulo-interstitial damage on PAS-stained sections was reduced after CM treatment in CKD rats, illustrated by decreased tubular fibrosis and atrophy (A). Differences between CKD (B) and healthy (C) tubular kidney tissue are shown. White arrow indicates infitration, black arrows showing proteincasts. 2K-NCM (n=6); 2K-CM (n=6); CKD-NCM (n=13); CKD-CM (n=13). * P<0.05: CKD vs. 2K, †P<0.05: CKD-CM vs. CKD-NCM

CM effectively induces angiogenesis and wound closure

To evaluate the effectiveness of CM *in vitro*, an angiogenesis assay and wound closure assay were performed. CM was able to significantly induce angiogenesis compared to NCM (figure 9a). We also analysed the effect of CM on wound closure in an *in vitro* scratch wound assay. As PBS induces cell death in the scratch wound assay, PBS could not be used as vehicle or control. We therefore used CM and NCM diluted in DMEM. CM-treated HMECs showed increased wound closure compared to NCM treatment (figure 9b).

Table 3 Renal morphology.

	2K-NCM n=6	2K-CM n=6	CKD-NCM n=13	CKD-CM n=13
Glomerular measurements				
Ki 67$^+$ cells/glomerulus	3.85±1.01	4.17±1.38	5.11±1.52	5.99±1.60*
ED1$^+$ cells/glomerulus	1.33±0.51	1.33±0.51	2.70±1.34*	2.59±0.84*
CD3$^+$ cells/glomerulus	0.14±0.08	0.09±0.07	0.46±0.36*	0.34±0.13
Tubular measurements				
ED1$^+$ cells/tubular field	12.7±0.8	13.5±3.5	32.9±10.2*	34.3±3.9*
CD3$^+$ cells/20 tubular fields	2.2±0.9	1.4±0.7	49.3±23.7*	48.8±8.0*
TUNEL$^+$cells/ tubular field	0.65±0.68	0.23±0.14	1.75±1.12	1.30±0.77*

Mean±SD. *P<0.05: 2K vs. CKD.

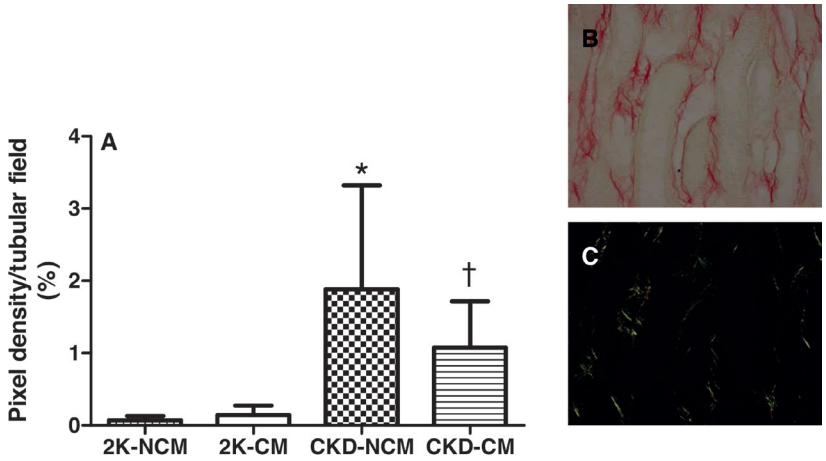

Figure 7 Tubular collagen I and III deposition was reduced after CM treatment in CKD rats shown by sirius red staining (A). Raw (B) and polarized (C) pictures are shown. 2K-NCM (n=6); 2K-CM (n=6); CKD-NCM (n=13); CKD-CM (n=13). * P<0.05: CKD vs. 2K, †P<0.05: CKD-CM vs. CKD-NCM

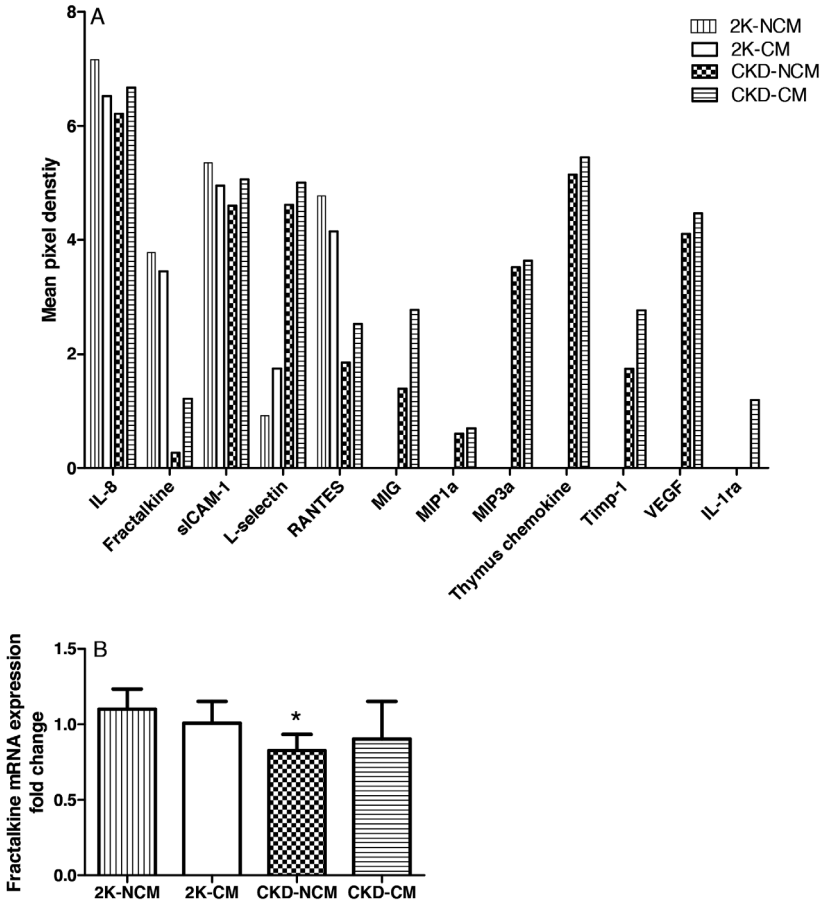

Figure 8 Inflammatory cytokine expression in healthy and CKD kidneys. A: Cytokine array. Striped bars = 2K-CM (n=6); dotted bars = 2K-NCM (n=6); black bars = CKD-NCM (n=7); white bars = CKD-CM (n=4). IL-8= interleukin 8; sICAM= soluble Inter-Cellular Adhesion Molecule; L-selectin= leucocyte cell-adhesion molecule; RANTES= Regulated upon Activation, Normal T-cell Expressed, and Secreted; MIG= Monokine Induced by Gamma-Interferon; MIP1α= Macrophage Inflammatory Protein-1 alpha; MIP3α= Macrophage Inflammatory Protein-3 alpha; Timp-1= Tissue Inhibitor of Metalloproteinase 1; VEGF= Vascular Endothelial Growth Factor; IL-1RA= Interleukin 1 Receptor Antagonist.

B. Fractalkine mRNA in healthy and CKD kidneys. Striped bars = 2K-CM (n=6); dotted bars = 2K-NCM (n=6); black bars = CKD-NCM (n=7); white bars = CKD-CM (n=4). * P<0.05: CKD vs. 2K

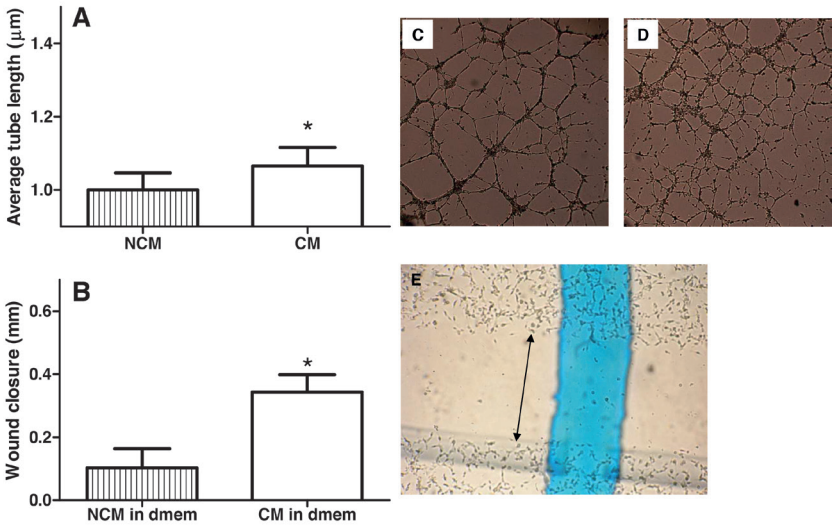

Figure 9 CM stimulates in vitro angiogenesis (A) and wound closure (B). Average tube length was increased after CM treatment compared to NCM (C+D). In a scratch wound assay, CM treatment increased wound (indicated by black arrow in E) closure compared to NCM treatment. * P<0.05 CM vs. NCM.

Discussion

Our study demonstrates for the first time that repeated IV administration of human embryonic MSC derived CM as a 'rescue intervention'– i.e. 6 weeks after CKD induction - can markedly attenuate the reduction of both GFR and ERPF as assessed by classical "gold standard" inulin and PAH clearance methodology and that this effect is detectable at 6 weeks after administration indicating long-term protection. Furthermore, histology showed a reduction in renal injury.

Previous studies showed beneficial effects of MSC administration in models of AKI (reviewed in[5,7]) and have even led to phase I clinical trials on allogenic MSC administration in AKI (clinicaltrial.gov Identifier: NCT00733876 and NCT01275612). However, the relevance of these observations in AKI to CKD is unclear and data on MSC administration in CKD are sparse. In a few studies, administration of MSC was shown to prevent development of CKD if administered directly after induction of the disease[6,25–28] or at early stages of CKD[29]. However, studies aiming at therapeutic 'rescue' in established CKD have not been reported. Furthermore, although most of the reports on beneficial effects suggest that the therapeutic effect is at least in part mediated by paracrine factors secreted by the cells[30], only

two studies have applied MSC-CM as therapeutic strategy, and both were performed in AKI models and report conflicting results[12,13]. More recently, two studies reported beneficial effects of microvesicles derived from human adult MSC-CM in experimental AKI[18,19].

We intravenously administered human embryonic MSC-CM that was harvested using a clinically compliant protocol. We used the 5/6th nephrectomy ablation model, a known experimental model of progressive renal disease, associated with systemic and glomerular hypertension, capillary loss, renal inflammation and gradual development of glomerulosclerosis, resembling human CKD[31,32]. Creatinine clearance tends to underestimate the decline in GFR due to extensive tubular creatinine secretion in rats[33], underlining the importance of the gold standard method to determine renal function by inulin and PAH clearance[34]. We previously showed a marked reduction of GFR and ERPF in this model using classic clearance technology, while this was less apparent from changes in plasma creatinine, plasma urea, or creatinine clearance[35]. Injection of CM IV at 6 weeks after induction of CKD, a time point at which kidney failure is established, resulted in a long-term beneficial effect on GFR and ERPF as well as a marked reduction in SBP of up to 27 mmHg, lasting up to at least six weeks post-injection between groups. Besides these functional effects, glomerulosclerosis was reduced and glomerular DNA damage repair increased. Our findings of a beneficial effect of human embryonic MSC secretions on progression of experimental established CKD may have relevance for treatment of human CKD. Clinical use of cell-free MSC secretions may have important advantages over MSC administration, for example with regard to risks of malignant[10,11] or non-malignant transdifferentiation [8,9].

Several mechanisms have been proposed for the beneficial effects of paracrine factors secreted by MSC on the injured kidney: immunosuppressive and inflammatory actions, proangiogenic, antifibrotic and anti-apoptotic effects. Our data points at enhanced glomerular endothelial regeneration and genome integrity preservation through active DNA damage signaling. Such enhancement of glomerular endothelial repair has previously been shown to provide protection against glomerulosclerosis progression[36]. We observed a favorable shift in glomerulosclerosis after CM as compared to NCM treatment, which was associated with higher glomerular endothelial cell numbers after CM, whereas glomerular size was not different. Approximately 10 % fewer glomeruli were totally sclerotic hence non-functional in CKD-CM rats which match the increase of GFR compared to CKD-NCM rats. The constant filtration fraction points at increased preglomerular and intraglomerular vascular capacity, possibly by preserved endothelial function. Furthermore, we show that human embryonic MSC CM enhanced endothelial cell migration and angiogenesis *in vitro*. These observations are in line with a report by Togel et al demonstrating in vitro vasculotropic effects of adult rat MSC CM[15].

Recently, our human embryonic MSC-CM was also shown to increase capillary density and improve cardiac function after acute myocardial infarction in a pig model[22]. In our CKD model, at 6 weeks after injection of MSC-CM or MSC-NCM we found no differences in the numbers of apoptotic and proliferating cells, nor in the presence of VEGF in the kidney, however, we cannot exclude that anti-apoptotic, mitogenic or VEGF effects have occurred in an earlier stage. We did observe a reduction in tubular inflammation and fibrosis as well as increased expression of fractalkine and Il-1RA, two cytokines that are involved in recruitment of inflammatory response[37,38] after CM as compared to NCM treatment, suggesting a role for paracrine anti-inflammatory and anti-fibrotic effects, consistent with findings in other disease models[39,40].

Recent studies on the effects of MSC-derived microvesicles in acute kidney injury models support a potential exosome-mediated renoprotective effect. Bruno et al. reported that human adult MSC-derived microvesicles, which include exosomes, mimicked the protection against AKI as provided by intravenously administered MSC[18]. Gatti et al showed that single administration of human MSC-derived microvesicles immediately after ischemia-reperfusion injury protected against the development of both acute and chronic kidney injury[19]. Furthermore, in a mouse myocardial infarction model it was recently shown that cardioprotection by human embryonic MSC was mediated by exosomes[21]. Based on the above reports we proposed exosomes to be the CM components that provide protection against CKD progression. However, repeated IV administration of human embryonic MSC derived exosomes in our model of established CKD did not affect progression of CKD (supplemental data).

We used exosome concentrations in CKD rats that were approximately fourfold the concentration of exosomes present in CM, similar to the exosome concentrations previously shown to improve cardiac function after myocardial infarction[21]. Moreover, *in vitro* both human embryonic MSC derived exosomes and CM effectively induced wound closure and angiogenesis. Lack of a significant therapeutic effect of exosomes in this model of chronic renal injury may be due to tissue specific requirements regarding exosome content and/or dose. Our results suggest that the beneficial effect in our model of CKD was mediated by soluble factors and cytokines. Whether rat exosomes would be more effective in the damaged kidney is unknown.

In line with an effect via soluble factors and cytokines, Togel at al. demonstrated that adult rat MSC-CM contains VEGF, HGF and IGF[15] which mediate renoprotection. Previous analysis on the secretory product of human embryonic MSC showed the presence of several gene products that play a role in angiogenesis; kinase insert domain receptor, VEGF, interleukin 8, angiopoietin and fibroblast growth factor[41]. Studies showing that MSC with knockdown of IGF-1 or VEGF failed to protect rats

from AKI[14,16] support a role for proangiogenic factors. Semedo et al. found higher levels of anti-inflammatory cytokines in kidney extracts of MSC-treated animals after ischemia reperfusion injury[29], which is consistent with our observations 6 weeks after CM administration in CKD.
A limitation of our study is that we did not administer CM depleted of exosomes in our CKD model. Therefore we cannot exclude that exosomes mediate the beneficial effect in CKD but need an immunomodulatory or anti-inflammatory factor that is present in the CM. In this respect a recent study may be of interest which reported that porcine MSC have limited immune-modulating activity which abolishes their protective efficacy in AKI[42].
In conclusion, our study demonstrates a marked renoprotective effect of human embryonic MSC derived CM in a rat model with established CKD, as shown by a higher GFR and considerably less glomerular damage after a CM administration. This is probably due to increased endothelial cell regeneration through active DNA damage repair, proliferation and angiogenesis. These findings provide a basis for further research towards potential clinical application of CM-based therapies in human CKD.

Materials and Methods

Animals

Ethics Statement
The protocol was approved by the Utrecht University committee of Animal Experiments (DEC nr 2007.II.050.131).

Animal model
Male inbred Lewis rats (Charles River, Sulzfeld, Germany) were housed under standard conditions in a light-, temperature- and humidity-controlled environment. CKD was induced in 8-week-old inbred male Lewis rats by two-stage subtotal nephrectomy (SNX) as described (t = 0)[43]. Briefly, the right kidney was removed (wk –1) and one week later (wk 0) the poles of the left kidney were cut off, equalling approximately 66 + /-4 % of the weight of the previously removed kidney. Progression of CKD was accelerated with L-N^G-Nitroarginine (L-NNA), a nitric oxide (NO)-synthase inhibitor (20 mg/L) in drinking water for 8 wk, (wk -4 to wk 4), and after wk 0, animals were fed standard powdered chow (CRM-FG; Special Diet Services Ltd., Witham, Essex, UK) supplemented with 6 % NaCl.

MSC-CM preparation

The protocols for MSC generation and CM preparation have been described previously[41]. In short, a chemically defined serum free culture medium (Dulbecco's modified eagle medium (DMEM), supplemented with insulin, transferrin, and selenoprotein, fibroblast growth factor 2, platelet derived growth factor AB, glutamine-penicillin-streptomycin, and ß-mercapto-ethanol) was conditioned by MSCs derived from human embryonic stem cells (hESCs) using a clinically compliant protocol. Three polyclonal, karyotypically stable and phenotypically MSC-like cultures that did not express pluripotency-associated markers but displayed MSC-like surface antigens ($CD29^+$, $CD44^+$, $CD49a^+/e^+$, $CD105^+$, $CD166^+$, $CD34^-$, $CD45^-$) and gene expression profile, were generated by trypsinization and propagation of hESCs from either HuES9 hESC line or H1 hESC line in feeder- and serum-free selection media[44]. One of these cultures, HuES9. E1 could be stably expanded for at least 80 population doublings. To harvest MSC secretions, hESC-derived MSC cultures were transferred to a chemically defined, serum free culture medium to condition the medium for three days before the media containing MSC secretions were collected, clarified by centrifugation, concentrated 25 times using 10 kDa MW cut-off ultra-filtration membranes and sterilized by filtration through a 220 nm filter. After these steps, the protein concentration was 0.50 mg/ml. As a negative control, the above-mentioned serum free culture medium was processed equally (non-conditioned medium, NCM). To study the effect of MSC-specific proteins, CM and NCM were diluted in sterile PBS in parallel before administration to reach a protein concentration of 50 µg/250 µl.

Effects of administration of MSC-derived conditioned medium in CKD rats

At week 5 rats with confirmed CKD were stratified based on plasma urea (> 9 mmol/L) and systolic blood pressure (SBP) to receive CM or NCM via tail vein injections (twice daily for 4 consecutive days) at week 6 when stable CKD has developed, as follows: healthy-NCM (n = 6), healthy rats received 250 µl NCM per injection; healthy-CM (n = 6), healthy rats received 250 µl CM per injection; CKD-NCM (n = 13), rats with CKD received 250 µl NCM per injection; CKD-CM (n = 13), rats with CKD received 250 µl NCM per injection.

At week 12 terminal kidney function was measured under barbiturate anesthesia (see below). Directly thereafter, rats were sacrificed and tissues were collected and either frozen in liquid nitrogen or fixed in 4% paraformaldehyde (PFA) for embedding in paraffin. For detailed time-line, see figure 10.

Longitudinal chronic kidney disease evaluation

Rats were weighed weekly. In week 5, 9 and 11, 24h urine, blood samples were collected and SBP was measured by tail cuff sphygmomanometry[45]. To collect 24h

urine, rats were placed in metabolism cages without food for 24h, but with free access to water with 2% glucose. Urine was collected on antibiotic/antimycotic solution (Sigma, St. Louis, MO; A5955) and stored at –80°C. Blood samples were collected from the tail vein. Urine protein was measured with Coomassie blue. Sodium and potassium were determined by flame photometry.

Terminal kidney function

Kidney function was assessed by inulin clearance to determine glomerular filtration rate (GFR) and para-ammino hippuric acid (PAH) clearance to determine the effective renal plasma flow (ERPF) as described[45]. Briefly, rats were anesthetized with intraperitoneal pentobarbital sodium (60 mg/kg) and placed on a servo-controlled surgical table that maintained body temperature at 37°C. The trachea was cannulated with a PE-10 cathether. A PE-50 catheter was placed in the left jugular vein for infusion of solutions and a PE-10 catheter was introduced in this PE-50 cathether for supplemental anesthetic. The left femoral artery was cannulated with PE-50 tubing for measurement of mean arterial pressure (MAP) and blood sampling. A PE-50 catheter was placed in the bladder for urine collection. During surgery, animals received an intravenous infusion of a 150 mM NaCl solution containing 6% bovine serum albumin (BSA). Following surgery, the infusion was switched to a 150 mM NaCl solution with 1% BSA at the same infusion rate. This infusion was maintained throughout the experiment. The solution also contained inulin and para-amino hippurate (PAH) for clearance measurements. A 60-min equilibration period was observed before the start of the 60-min clearance measurements. During this clearance measurement urine was sampled for 15 minute periods and before and after the clearance

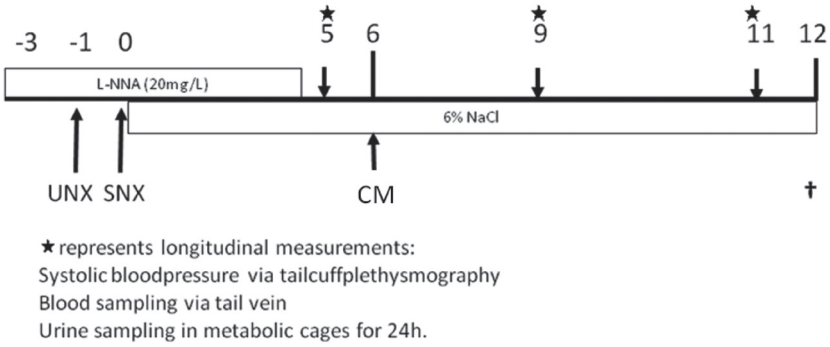

Figure 10 Representation of experimental set up. UNX= uninephrectomy; SNX= subtotal nephrectomy; CM= conditioned medium administration. Stars indicate longitudinal measurements.

measurement blood was sampled. Clearances and fractional excretions were calculated by standard formulae. Renal blood flow was calculated from ERPF and hematocrit.

Renal Morphology

Glomerulosclerosis and tubular interstitial damage were scored on 3 µm periodic acid Schiff (PAS)-stained paraffin-embedded slides[46]. Collagen I and III contents was stained with Sirius red, visualized with circular polarized light and digitally analyzed using ImageJ software[46]. The percentage of collagen area was calculated by dividing the Sirius red stained area by the total image area. Monocytes/macrophages (ED-1 stain) and leucocytes (CD3 stain) were counted in glomeruli and tubulo-interstitum[47]. Terminal deoxynucleotidyl transferase-mediated dUTP-biotin nick end labeling (TUNEL) staining (Apoptag Plus in situ Peroxidase kit, Millipore, Temecula, CA, USA) was performed according to manufacturer guidelines. The number of apoptotic cells was determined as the number of TUNEL-positive cells in the images of 50 randomly selected fields (x200 magnification) per section. Endothelial cells were stained with JG12 (Bender Medsystems GmbH, Vienne, Austria) after heat antigen retrieval in citrate buffer (pH 6.0)[48]. JG12 positive cells were determined in the glomeruli (calculated in at least 100 glomeruli per animal) and in peritubular areas (calculated in 20 peritubular fields per animals) using Adobe Photoshop software, version 8.0.1 (Adobe Systems; San Jose, CA) and ImageJ software, version 1.42q (National Institutes of Health; Bethesda, MD). To score nuclei repairing DNA damage, paraffin-embedded kidney sections were deparafinized and treated with PO block for 15 minutes and incubated at 100 °C in Citrate/HCL buffer for 20 minutes. The sections were stained with mouse anti-γH2AX (ser139) (Millipore, 1:200) overnight at 4°C. Polyclonal rabbit anti-mouse HRP (Dako, 1:100) was incubated 30 minutes at RT. Finally, BrightVision Poly HRP-Anti Rabbit IgG (Immunologic) was incubated for 1 hour RT. Nova RED substrate kit for Peroxidase (Vector, SK-4800) was used and counterstained with hematoxyline. Analysis was performed using the Aperio ImageScope software.

Cytokine array and gene expression in renal tissue

Kidney samples were collected at termination (6 weeks after CM or NCM administration) and quickly frozen in liquid nitrogen. A rat cytokine array (R&D systems) was performed on kidney homogenates according to manufacturer's instructions to screen whether CM treatment stimulated local secretion of specific inflammatory cytokines by the host kidney cells. Samples were pooled per treatment group and equal amounts of protein were loaded on the blots. From all pooled samples blots were performed in duplicate and averages of these two pixel densities were used to calculate the average density with Image J software.

Background staining and spot size were analysed as recommended by the manufacturer. Briefly, pictures were converted to 8-bit inverted jpeg files and spots were encircled. Per blot, equal spot sizes were analysed.
To determine whether a local production of cytokines could be confirmed on mRNA level, cDNA was isolated from frozen remnant kidney tissue and expression of fractalkine was determined using quantitative real-time RT-PCR (ABi PRiSM 790Sequence Detection SYStem, applied Biosystems, Foster City, CA). The following TaqMan® Gene Expression Assays (Applied Biosystems) were used: (fractalkine (CX3CL1): Rn00593186_m1), (ß-actin: Rn00667869_m1) and (calnexin: Rn00596877_m1). Reactions were carried out in duplicate. Cycle time (Ct) values for fractalkine were normalized for mean Ct-values of Calnexin and β-actin, which we previously determined to be the two most stable housekeeping genes across all groups using the geNorm-program (http://medgen.ugent.be/~jvdesomp/genorm/), and expressed relative to a calibrator (the sample with the lowest expression: the 2K controls), using the ΔΔCt-method. Hence, steady state mRNA levels were expressed as n-fold difference relative to the calibrator.

In vitro angiogenesis assay

The potential of CM to stimulate angiogenic tube formation was assessed *in vitro*. For this, 10 µl matrigel (Millipore, Temecula, CA, USA) was added in the inner compartment of an ibidi µ-angiogenesis slide (Ibidi, Munchen, Germany). After the matrigel had solidified, 50 µl of tests-suspension was added, containing respectively 10 µg CM or 10 µg NCM. Subsequently, 10 µl unsupplemented MCDB medium containing 10.000 trypsinized human microvascular endothelial cells (HMEC-1) cells (HMECs; Centers for Disease Control and Prevention, Atlanta, USA) was added. The angiogenesis area was photographed using light microscopy after 18 hours incubation at 37°C, 5% CO_2 and the mean tubule length, used as a measure of angiogenesis, was determined using Angioquant software[49]. Each sample was assayed in triplicate.

In vitro scratch wound assay

The potential of CM to stimulate endothelial cell migration was assessed by *in vitro* scratch wound assay. A mechanical scratch was created with a pipet tip in a confluent monolayer of HMECs. After washing with PBS, 200 µl DMEM medium containing respectively 40 µg CM or 40 µg NCM was placed on the cells. DMEM without supplementation served as control. Reference lines were made on the bottom of the wells to obtain exactly the same field during image acquisition. The scratched area was photographed using light microscopy at start and after 6 hours incubation (37˚). The extent of closure after 6 hours was determined relative to the starting width of the scratch (Image-Pro plus software, Media Cybernetics 3.0).

Each sample was measured in two wells and two picture-fields per well were examined. Results were averaged for analysis.

Statistical analyses

Data are presented as mean ± standard deviation and analyzed by analysis of variance (One-way ANOVA with a Newman-Keuls post-test, Two-way ANOVA with a Newman-Keuls post-test) or Student's T-test, where appropriate. $P < 0.05$ was considered significant.

Acknowledgements

We thank Krista den Ouden, Nel Willekes, Chantal Tilburgs, Frits Meeuwsen, Paula Martens and Nicole van Vliet for their expert technical assistance.

References

1. Vinhas J, Gardete-Correia L, Boavida JM, Raposo JF, Mesquita A, Fona MC, Carvalho R, Massano-Cardoso S (2011) Prevalence of Chronic Kidney Disease and Associated Risk Factors, and Risk of End-Stage Renal Disease: Data from the PREVADIAB Study. Nephron Clin Pract 119: c35-c40.
2. Zhang QL, Rothenbacher D (2008) Prevalence of chronic kidney disease in population-based studies: systematic review. BMC Public Health 8: 117.
3. Levin A, Stevens PE (2011) Early detection of CKD: the benefits, limitations and effects on prognosis. Nat Rev Nephrol 7: 446-457.
4. McDonald SP, Tong B (2011) Morbidity burden of end-stage kidney disease in Australia: Hospital separation rates among people receiving kidney replacement therapy. Nephrology (Carlton) 16: 758-766.
5. Imai N, Kaur T, Rosenberg ME, Gupta S (2009) Cellular therapy of kidney diseases. Semin Dial 22: 629-635.
6. Choi SJ, Kim JK, Hwang SD (2010) Mesenchymal stem cell therapy for chronic renal failure. Expert Opin Biol Ther 10: 1217-1226.
7. Humphreys BD, Bonventre JV (2008) Mesenchymal stem cells in acute kidney injury. Annu Rev Med 59: 311-325.
8. Kunter U, Rong S, Boor P, Eitner F, Muller-Newen G, Djuric Z, van Roeyen CR, Konieczny A, Ostendorf T, Villa L, Milovanceva-Popovska M, Kerjaschki D, Floege J (2007) Mesenchymal stem cells prevent progressive experimental renal failure but maldifferentiate into glomerular adipocytes. J Am Soc Nephrol 18: 1754-1764.
9. Breitbach M, Bostani T, Roell W, Xia Y, Dewald O, Nygren JM, Fries JW, Tiemann K, Bohlen H, Hescheler J, Welz A, Bloch W, Jacobsen SE, Fleischmann BK (2007) Potential risks of bone marrow cell transplantation into infarcted hearts. Blood 110: 1362-1369.
10. Foudah D, Redaelli S, Donzelli E, Bentivegna A, Miloso M, Dalpra L, Tredici G (2009) Monitoring the genomic stability of in vitro cultured rat bone-marrow-derived mesenchymal stem cells. Chromosome Res 17: 1025-1039.
11. Jeong JO, Han JW, Kim JM, Cho HJ, Park C, Lee N, Kim DW, Yoon YS (2011) Malignant tumor formation after transplantation of short-term cultured bone marrow mesenchymal stem cells in experimental myocardial infarction and diabetic neuropathy. Circ Res 108: 1340-1347.
12. Bi B, Schmitt R, Israilova M, Nishio H, Cantley LG (2007) Stromal cells protect against acute tubular injury via an endocrine effect. J Am Soc Nephrol 18: 2486-2496.
13. Gheisari Y, Ahmadbeigi N, Naderi M, Nassiri SM, Nadri S, Soleimani M (2011) Stem cell-conditioned medium does not protect against kidney failure. Cell Biol Int 35: 209-213.
14. Imberti B, Morigi M, Tomasoni S, Rota C, Corna D, Longaretti L, Rottoli D, Valsecchi F, Benigni A, Wang J, Abbate M, Zoja C, Remuzzi G (2007) Insulin-like growth factor-1 sustains stem cell mediated renal repair. J Am Soc Nephrol 18: 2921-2928.
15. Togel F, Weiss K, Yang Y, Hu Z, Zhang P, Westenfelder C (2007) Vasculotropic, paracrine actions of infused mesenchymal stem cells are important to the recovery from acute kidney injury. Am J Physiol Renal Physiol 292: F1626-F1635.
16. Togel F, Zhang P, Hu Z, Westenfelder C (2009) VEGF is a mediator of the renoprotective effects of multipotent marrow stromal cells in acute kidney injury. J Cell Mol Med 13: 2109-2114.
17. Zarjou A, Kim J, Traylor AM, Sanders PW, Balla J, Agarwal A, Curtis LM (2011) Paracrine effects of mesenchymal stem cells in cisplatin-induced renal injury require heme oxygenase-1. Am J Physiol Renal Physiol 300: F254-F262.
18. Bruno S, Grange C, Deregibus MC, Calogero RA, Saviozzi S, Collino F, Morando L, Busca A, Falda M, Bussolati B, Tetta C, Camussi G (2009) Mesenchymal stem cell-derived microvesicles protect against acute tubular injury. J Am Soc Nephrol 20: 1053-1067.
19. Gatti S, Bruno S, Deregibus MC, Sordi A, Cantaluppi V, Tetta C, Camussi G (2011) Microvesicles derived from human adult mesenchymal stem cells protect against ischaemia-reperfusion-induced acute and chronic kidney injury. Nephrol Dial Transplant 26: 1474-1483.
20. Camussi G, Deregibus MC, Bruno S, Cantaluppi V, Biancone L (2010) Exosomes/microvesicles as a mechanism of cell-to-cell communication. Kidney Int 78: 838-848.

21. Lai RC, Arslan F, Lee MM, Sze NS, Choo A, Chen TS, Salto-Tellez M, Timmers L, Lee CN, El Oakley RM, Pasterkamp G, de Kleijn DP, Lim SK (2010) Exosome secreted by MSC reduces myocardial ischemia/reperfusion injury. Stem Cell Res 4: 214-222.
22. Timmers L, Lim SK, Hoefer IE, Arslan F, Lai RC, van Oorschot AA, Goumans MJ, Strijder C, Sze SK, Choo A, Piek JJ, Doevendans PA, Pasterkamp G, de Kleijn DP (2011) Human mesenchymal stem cell-conditioned medium improves cardiac function following myocardial infarction. Stem Cell Res 6: 206-214.
23. MacPhail SH, Banath JP, Yu Y, Chu E, Olive PL (2003) Cell cycle-dependent expression of phosphorylated histone H2AX: reduced expression in unirradiated but not X-irradiated G1-phase cells. Radiat Res 159: 759-767.
24. MacPhail SH, Banath JP, Yu TY, Chu EH, Lambur H, Olive PL (2003) Expression of phosphorylated histone H2AX in cultured cell lines following exposure to X-rays. Int J Radiat Biol 79: 351-358.
25. Caldas HC, Fernandes IM, Gerbi F, Souza AC, Baptista MA, Ramalho HJ, Kawasaki-Oyama RS, Goloni-Bertollo EM, Pavarino-Bertelli EC, Braile DM, bbud-Filho M (2008) Effect of whole bone marrow cell infusion in the progression of experimental chronic renal failure. Transplant Proc 40: 853-855.
26. Cavaglieri RC, Martini D, Sogayar MC, Noronha IL (2009) Mesenchymal stem cells delivered at the subcapsule of the kidney ameliorate renal disease in the rat remnant kidney model. Transplant Proc 41: 947-951.
27. Lee SR, Lee SH, Moon JY, Park JY, Lee D, Lim SJ, Jeong KH, Park JK, Lee TW, Ihm CG (2010) Repeated administration of bone marrow-derived mesenchymal stem cells improved the protective effects on a remnant kidney model. Ren Fail 32: 840-848.
28. Villanueva S, Ewertz E, Carrion F, Tapia A, Vergara C, Cespedes C, Saez PJ, Luz P, Irarrazabal C, Carreno JE, Figueroa F, Vio CP (2011) Mesenchymal stem cell injection ameliorates chronic renal failure in a rat model. Clin Sci (Lond) 121: 489-499.
29. Semedo P, Correa-Costa M, Antonio CM, Maria Avancini Costa MD, Antonia dos RM, Shimizu MH, Seguro AC, Pacheco-Silva A, Saraiva Camara NO (2009) Mesenchymal stem cells attenuate renal fibrosis through immune modulation and remodeling properties in a rat remnant kidney model. Stem Cells 27: 3063-3073.
30. La Manna G, Bianchi F, Cappuccilli M, Cenacchi G, Tarantino L, Pasquinelli G, Valente S, Della BE, Cantoni S, Cavallini C, Neri F, Tsivian M, Nardo B, Ventura C, Stefoni S (2010) Mesenchymal stem cells in renal function recovery after acute kidney injury. Use of a differentiating agent in a rat model. Cell Transplant .
31. Fleck C, Appenroth D, Jonas P, Koch M, Kundt G, Nizze H, Stein G (2006) Suitability of 5/6 nephrectomy (5/6NX) for the induction of interstitial renal fibrosis in rats--influence of sex, strain, and surgical procedure. Exp Toxicol Pathol 57: 195-205.
32. Griffin KA, Picken MM, Churchill M, Churchill P, Bidani AK (2000) Functional and structural correlates of glomerulosclerosis after renal mass reduction in the rat. J Am Soc Nephrol 11: 497-506.
33. Darling IM, Morris ME (1991) Evaluation of "true" creatinine clearance in rats reveals extensive renal secretion. Pharm Res 8: 1318-1322.
34. Hostetter TH, Meyer TW (2004) The development of clearance methods for measurement of glomerular filtration and tubular reabsorption. Am J Physiol Renal Physiol 287: F868-F870.
35. van Koppen A, Joles JA, Bongartz LG, van den Brandt J, Reichardt HM, Goldschmeding R, Nguyen TQ, Verhaar MC (2012) Healthy bone marrow cells reduce progression of kidney failure better than CKD bone marrow cells in rats with established chronic kidney disease. Cell Transplant .
36. Rookmaaker MB, Smits AM, Tolboom H, Van 't WK, Martens AC, Goldschmeding R, Joles JA, van Zonneveld AJ, Grone HJ, Rabelink TJ, Verhaar MC (2003) Bone-marrow-derived cells contribute to glomerular endothelial repair in experimental glomerulonephritis. Am J Pathol 163: 553-562.
37. Mizutani N, Sakurai T, Shibata T, Uchida K, Fujita J, Kawashima R, Kawamura YI, Toyama-Sorimachi N, Imai T, Dohi T (2007) Dose-dependent differential regulation of cytokine secretion from macrophages by fractalkine. J Immunol 179: 7478-7487.
38. Arend WP, Malyak M, Guthridge CJ, Gabay C (1998) Interleukin-1 receptor antagonist: role in biology. Annu Rev Immunol 16: 27-55.
39. Katsha AM, Ohkouchi S, Xin H, Kanehira M, Sun R, Nukiwa T, Saijo Y (2011) Paracrine factors of multipotent stromal cells ameliorate lung injury in an elastase-induced emphysema model. Mol Ther 19: 196-203.

40. Yew TL, Hung YT, Li HY, Chen HW, Chen LL, Tsai KS, Chiou SH, Chao KC, Huang TF, Chen HL, Hung SC (2011) Enhancement of Wound Healing by Human Multipotent Stromal Cell Conditioned Medium: The Paracrine Factors and p38 MAPK Activation. Cell Transplant 20: 693-706.
41. Sze SK, de Kleijn DP, Lai RC, Khia Way TE, Zhao H, Yeo KS, Low TY, Lian Q, Lee CN, Mitchell W, El Oakley RM, Lim SK (2007) Elucidating the secretion proteome of human embryonic stem cell-derived mesenchymal stem cells. Mol Cell Proteomics 6: 1680-1689.
42. Brunswig-Spickenheier B, Boche J, Westenfelder C, Peimann F, Gruber AD, Jaquet K, Krause K, Zustin J, Zander AR, Lange C (2010) Limited immune-modulating activity of porcine mesenchymal stromal cells abolishes their protective efficacy in acute kidney injury. Stem Cells Dev 19: 719-729.
43. Tornig J, Amann K, Ritz E, Nichols C, Zeier M, Mall G (1996) Arteriolar wall thickening, capillary rarefaction and interstitial fibrosis in the heart of rats with renal failure:the effects of ramipril, nifedipine and moxonidine. J Am Soc Nephrol 7: 667-675.
44. Lian Q, Lye E, Suan YK, Khia Way TE, Salto-Tellez M, Liu TM, Palanisamy N, El Oakley RM, Lee EH, Lim B, Lim SK (2007) Derivation of clinically compliant MSCs from CD105+. Stem Cells 25: 425-436.
45. Koeners MP, Racasan S, Koomans HA, Joles JA, Braam B (2007) Nitric oxide, superoxide and renal blood flow autoregulation in SHR after perinatal L-arginine and antioxidants. Acta Physiol (Oxf) 190: 329-338.
46. Bongartz LG, Braam B, Verhaar MC, Cramer MJ, Goldschmeding R, Gaillard CA, Steendijk P, Doevendans PA, Joles JA (2010) The nitric oxide donor molsidomine rescues cardiac function in rats with chronic kidney disease and cardiac dysfunction. Am J Physiol Heart Circ Physiol 299: H2037-H2045.
47. Attia DM, Verhagen AM, Stroes ES, van Faassen EE, Grone HJ, De Kimpe SJ, Koomans HA, Braam B, Joles JA (2001) Vitamin E alleviates renal injury, but not hypertension, during chronic nitric oxide synthase inhibition in rats. J Am Soc Nephrol 12: 2585-2593.
48. Kunter U, Rong S, Djuric Z, Boor P, Muller-Newen G, Yu D, Floege J (2006) Transplanted mesenchymal stem cells accelerate glomerular healing in experimental glomerulonephritis. J Am Soc Nephrol 17: 2202-2212.
49. Niemisto A, Dunmire V, Yli-Harja O, Zhang W, Shmulevich I (2005) Robust quantification of in vitro angiogenesis through image analysis. IEEE Trans Med Imaging 24: 549-553.

Supplemental text

Materials and methods

MSC-CM derived exosome preparation

The protocols for MSC-CM derived exosome generation and preparation have been described by Lai et al[1]. Exosomes form approximately 3% of the CM by protein weight.

Effects of administration of MSC-derived exosomes in CKD rats

To investigate whether exosomes could be the renoprotective factor of MSC-derived CM, the effect of MSC-derived exosomes was studied in the same experimental setting as CM.

The dose of exosomes was extrapolated from a dose that was effective in reducing myocardial injury after coronary ligation in mice[1]. In this experiment at wk 6, rats received MSC-derived exosomes or PBS via tail vein injections, twice daily for 4 consecutive days: CKD-exosomes (n = 8), rats with CKD received 7 µg exosomes in 250 µl PBS per injection; CKD-PBS (n = 7), rats with CKD received 250 µl PBS per injection. Longitudinal follow-up and terminal measurements were performed as described before.

In vitro angiogenesis assay

The potential of CM and exosomes to stimulate angiogenic tube formation was assessed *in vitro*. For this, 10 µl matrigel (Millipore, Temecula, CA, USA) was added in the inner compartment of an ibidi µ-angiogenesis slide (Ibidi, Munchen, Germany). After the matrigel had solidified, 50 µl of tests-suspension was added, containing respectively 1.4 µg exosomes or PBS. Subsequently, 10 µl unsupplemented MCDB medium containing 10.000 trypsinized human microvascular endothelial cells (HMEC-1) cells (HMECs; Centers for Disease Control and Prevention, Atlanta, USA) was added. The angiogenesis area was photographed using light microscopy after 18 hours incubation at 37°C, 5% CO_2 and the mean tubule length, used as a measure of angiogenesis, was determined using Angioquant software[2]. Each sample was assayed in triplicate.

Results

Exosome treatment does not reduce CKD progression or renal damage

To investigate whether exosomes would be the CM component responsible for the renoprotective effects, exosomes derived from MSC-CM were administered in

rats with established CKD and compared with vehicle (PBS). Exosomes did not influence GFR, ERPF, hematocrit, or renal blood flow (supplemental table 1). No differences were observed in MAP, RVR, filtration fraction and fractional excretion of sodium and potassium between exosome- and PBS-treatment (supplemental table 1). SBP, proteinuria, urea, diuresis, creatinine clearance (supplemental table 2), glomerulosclerosis and tubular damage (supplemental figure 1) were also not different between CKD-exosomes or CKD-PBS rats.

CM and exosomes stimulate tube formation in vitro

To evaluate the effectiveness of exosomes and CM *in vitro*, an matrigel tube formation assay was performed. Both CM and exosomes were able to significantly induce tube formation compared to their respective controls, i.e. NCM and PBS (supplemental figure 2).

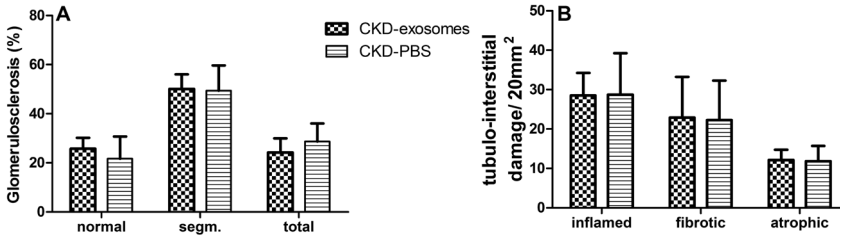

Figure S1 Glomerulosclerosis and tubulo-interstitial damage after exosome treatment. A: Segmental (segm) and total (tot) glomerulosclerosis (GS); B: Tubulo-interstitial damage. Exosomes (n=8); PBS (n=7). There were no significant differences.

Table S1

	CKD-exosomes n=8	CKD-PBS n=7
MAP (mm HG)	122±32	122±22
GFR (ml/min/100gr)	0.31±0.13	0.32±0.07
ERPF (ml/min/100gr)	1.12±0.39	0.99±0.33
RBF (ml/min/100gr)	1.93±0.76	1.71±0.59
RVR (mmHg/ml/min)	18±8	24±17
Hematocrit	43±5	46±4
FF	0.28±0.05	0.28±0.04
FeNa (%)	0.96±0.65	1.43±1.53
FeK (%)	44±9	38±8

MAP= mean arterial pressure. GFR=glomerular filtration rate. ERPF-effective renal plasma flow. RBF=renal blood flow. RVR=renal vascular resistance. FF=filtration fraction. FeNa=fractional excretion of sodium. FeK=fractional excretion of potassium.

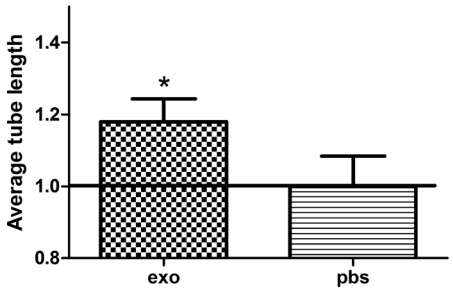

Figure S2 Exosomes stimulates *in vitro* angiogenesis. Average tube length was increased after exosome treatment compared to PBS. * P<0.05: exosomes vs. PBS.

Table S2

	CKD-exosomes n=8	**CKD-PBS n=7**
Systolic blood pressure (mm Hg)		
wk 5	146±15	150±10
wk 9	158±17	160±16
wk 11	162±16	172±15
Proteinuria (mg/24h)		
wk 5	13±3	12±4
wk 9	40±28	29±18
wk 11	44±12	39±11
Urea (mmol/L)		
wk 5	10.6±0.9	10.4±0.9
wk 9	10.7±1.4	10.5±0.8
wk 11	10.5±1.1	9.9±0.5
Creatinine clearance (ml/min)		
wk 5	1.16±0.14	1.20±0.16
wk 9	1.47±0.33	1.43±0.26
wk 11	1.19±0.17	1.22±0.23

Supplemental References

1. Lai RC, Arslan F, Lee MM, Sze NS, Choo A, et al. (2010) Exosome secreted by MSC reduces myocardial ischemia/reperfusion injury. Stem Cell Res 4: 214-222.
2. Niemisto A, Dunmire V, Yli-Harja O, Zhang W, Shmulevich I (2005) Robust quantification of in vitro angiogenesis through image analysis. IEEE Trans Med Imaging 24: 549-553.

Chapter Seven

A DOCA SALT INDUCED 2-KIDNEY MOUSE MODEL OF CARDIORENAL DISEASE

In preparation

Arianne van Koppen[1], Sanne de Jong[3], Magda S. C. Fontes[3], Lennart G. Bongartz[1,4], Jaap A. Joles[1], Tri Q. Nguyen[2], Harold van Rijen[3] and Marianne C. Verhaar[1].

[1]*Dept. of Nephrology and Hypertension, University Medical Center Utrecht, Utrecht, The Netherlands*
[2]*Dept. of Pathology, University Medical Center Utrecht, Utrecht, The Netherlands*
[3]*Dept. of Medical Physiology, University Medical Center Utrecht, Utrecht, The Netherlands*
[4]*Dept. of Cardiology, University Medical Center Utrecht, Utrecht, The Netherlands*

Abstract

The combination of renal failure and cardiovascular disease is associated with adverse prognosis. Insight in the pathogenesis of the cardiorenal syndrome (CRS) remains limited. Limitations of currently available CRS rat models are the small amount of remaining kidney tissue and lack of transgenic and knock-out rat models. To better understand the underlying mechanisms involved in development and progression of CRS, a 2-kidney mouse model is needed. We studied functional and structural effects of DOCA-salt administration in a two-kidney aging mouse model on development of kidney and heart failure.

129Sv mice of 30 weeks of age received DOCA and high salt diet for 8 weeks in combination with or without angiotensin II for 4 weeks (first hit). Three weeks later, high salt diet was continued (second hit) for a further 27 weeks. Untreated age-matched mice were used as controls. Effectiveness of first hit was shown by increased albuminuria (DOCA + ANGII: 117 ± 12; DOCA: 21 ± 10 mg/day) vs. controls (0.29 ± 0.18 mg/day) in wk 4 and hypertension in wk 5 (DOCA + ANG II:145 ± 17; DOCA: 128 ± 13mmHg) vs. controls (110 ± 14 mmHg). After withdrawal of DOCA and ANGII, albuminuria and blood pressure almost reversed to control levels. The second hit resulted in persistent hypertension in both DOCA groups (DOCA + ANGII: 134 ± 11; DOCA: 135 ± 13mmHg) vs. controls (88 ± 15mmHg) and albuminuria (DOCA: 7.5 ± 2.7 vs. both DOCA + ANGII: 2.2 ± 1.2 and controls: 0.1 ± 0.04 mg/day). Tubulo-interstitial damage and glomerulosclerosis were most pronounced in DOCA mice. Heart and lung weight were increased, cardiac fibrosis was increased and fractional shortening and Connexin43 were decreased in both DOCA and DOCA + ANGII mice vs. controls. All DOCA and 75% of DOCA + ANGII mice were susceptible to arrhythmias, but control hearts were not. Administration of high salt after discontinuation of either DOCA or DOCA + Ang II in 129Sv mice induces renal and cardiac injury.

Introduction

Renal failure contributes to the development of cardiovascular disease with 43.6 % of all deaths in end stage renal disease patients due to cardiac causes[1]. Although clinical studies hint at a specific bidirectional interaction between heart failure (HF) and chronic kidney disease (CKD), insight in the pathogenesis of the cardiorenal syndrome (CRS) remains limited. Bongartz et al developed a model for severe CRS in the rat which was based on combined CKD and myocardial infarction and allowed longitudinal follow-up of cardiorenal function combined with structural assessment[2]. Limitations of these models are the lack of transgenic and knock-out rat models and the small amount of remaining kidney tissue, indicating the need for a 2-kidney CRS mouse model. However, development of renal failure in the mouse is often only effective after removal of a large amount of renal tissue[3,4]. Interestingly, Kirchhoff et al reported that the combination of DOCA salt and angiotensin II (ANGII) infusion resulted in rapid development of renal and cardiac injury in uninephrectomized C57Bl6 mice[5]. Several studies suggested that 129Sv mice are more susceptible to develop kidney injury and proteinuria[6,7]. Aging increases vulnerability for development of hypertension and renal failure as well as cardiac failure[8]. The aim of this study was to develop a model of cardiac and renal failure in wild-type 129S mice to study the cardiorenal connection and to develop and evaluate therapeutic strategies. Subsequent studies in genetically modified mice would allow characterization of the specific impacts of defined genetic traits on the pathophysiology of the CRS. Here, we focussed on characterization of renal and cardiac function in aging 129SV mice subjected to DOCA salt with and without ANGII, hypothesizing that these mice would develop marked renal injury, loss of renal function and cardiac dysfunction.

Methods

Animal model

Thirty week old male 129Sv mice were used (Harlan laboratories, Horst, the Netherlands) and housed under standard conditions in a light-, temperature- and humidity-controlled environment. Hypertension was induced by a first hit (wk 0) in 30-week-old inbred male 129 SV mice by either the combination of a DOCA pellet (3.3 mg/day) and a high salt diet (3 % NaCl) for a period of 8 weeks (DOCA group; n = 4) or the combination of a DOCA pellet (3.3 mg/day), a high salt diet (3 % NaCl) for eight weeks and angiotensin II infusion (0.5 mg/kg BW/day) for 4 weeks (DOCA + ANGII group; n = 4). At wk 8, both DOCA pellet and ANGII pump

were removed and high salt diet was withdrawn. In wk 11, high salt diet (6% NaCl) was continued until termination at week 38. At week 38, mice were anesthetized by 4-5% isoflurane in oxygen and air. The heart was excised, prepared, and attached to a Langendorff perfusion setup (see below). After stimulation in Langendorff setup heart weight was determined and the heart was partly frozen and partly fixed. Kidney, liver, spleen and lungs were harvested and partly frozen and partly fixed in 4% paraformaldehyde (PFA) for embedding in paraffin. Untreated age-matched mice were used as controls (n = 4). The study protocol was approved by the Utrecht University committee of Animal Experiments.

Longitudinal renal function evaluation

Mice were weighed weekly and at regular intervals urine and blood were collected and systolic blood pressure was measured using tail cuff plethysmography (for detailed time line, see figure 1). To collect 24h urine, mice were placed in metabolism cages with food and water for 16h. Urine was collected on antibiotic/antimycotic solution (Sigma, St. Louis, MO; A5955) and stored at –80°C. Blood samples were collected by cheek puncture. Albumin was measured with a mouse albumin ELISA kit (Bethyl Laboratories Inc.). Sodium and potassium were determined by flame photometry. Plasma urea and urinary creatinine were determined by DiaSys Urea CT FS (DiaSys Diagnostic Systems, Holzheim, Germany).

Echocardiography

Trans-thoracic echocardiography was performed with a digital ultrasound machine (Vevo 2100) with probe MS550D for the following parameters:

Long axis

Cardiac output; (Stroke Volume*Heart rate (at the first frame drawn)/1000), ejection fraction; (100*Stroke Volume/Diastolic Volume), fractional shortening; (100*[Average LVID (diastole)-Average LVID (systole)]/Average LVID (diastole)), heart rate; (beat per minute), stroke volume; (diastolic Volume-systolic Volume), diastolic volume; ([7.0/(2.4 + Average diastolic Diameter)*(Average diastolic Diameter)^3]), systolic volume; ([7.0/(2.4 + Average systolic Diameter)*(Average systolic Diameter)^3]).

Short axis

Cardiac output; (Stroke Volume*Heart rate (at the first point drawn)/1000), ejection fraction; (100*Stroke Volume/Diastolic Volume), fractional shortening; (100*[Average Diameter (diastole)–Average Diameter (systole)]/Average Diameter (diastole)), heart rate; (beats per minute), left ventricle mass; (1.053*(Average diastolic Diameter at outer wall)3-(Average diastolic Diameter at inner wall)^3).

Mitral Valve
Early velocity, after velocity and early/after (MV E / MV A).

Ex vivo cardiac electrophysiological mapping
In week 38, mice were anesthetized by 4-5% isoflurane in oxygen and air. Afterward, the heart was excised, prepared, and connected to a Langendorff perfusion setup. The heart was continuously perfused with carbogen-gassed buffer of 37°C, composed of (in mmol/L): NaCl 116, KCl 5, MgSO4 1.1, NaH_2PO_4 0.35, $NaHCO_3$ 27, glucose 10, mannitol 16 and $CaCl_2$ 1.8. Extracellular electrograms were recorded using a 208-point multiterminal electrode (16 x 13 grid, 0.5-mm spacing) of both the left ventricle (LV) and right ventricle (RV) of the heart, as previously described[9]. Recordings were made during stimulation (1-ms pulse duration, 2 x diastolic stimulation threshold) from the center of the grid at a basic cycle length of 120 ms. The effective refractory period (ERP) was determined by premature stimulation, the longest coupling interval of the premature stimulus that failed to activate the entire heart, was determined for each ventricle separately. Every sixteenth stimulus was followed by 1 premature stimulus. Starting at 110 ms, the coupling interval of the premature stimulus was reduced in steps of 10 ms until the ERP. If spontaneous arrhythmias were absent, susceptibility for arrhythmias was provoked by programmed stimulation in the following sequence. First, 16 basic stimuli followed by 1 or 3 premature stimuli 5 ms longer than the locally determined ERP were applied. Next, if 1 or 3 premature stimuli failed to induce arrhythmias, 2-second burst pacing at the shortest possible cycle length was applied.

Renal Morphology
Glomerulosclerosis and tubulo-interstitial damage were scored on PAS-stained paraffin-embedded slides[10]. Inflammatory cells (CD45-stain) and proliferating cells (KI67-stain) were counted in 50 glomeruli and 20 randomly selected tubular fields (x200 magnification)[11,12].

Cardiac Morphology
Cardiac collagen content was stained on frozen transversal cardiac slides with Picrosirius red as described previously[9] visualized with light microscopy and digitally analyzed using ImageJ software[13]. The percentage of collagen area was calculated by dividing the Picrosirius red stained area by the total tissue area. Connexin43 (Cx43) was determined by immunohistochemistry on frozen slides as described previously[9]. The following antibodies were used: rabbit polyclonal antibodies against Cx43 (1:250, Zymed, Invitrogen) and FITC-conjugated anti rabbit whole IgG (1:250, Jackson Laboratories) as a secondary antibody.

The amount of fibrosis and Cx43 immuno-signals was determined using at least 6 randomly chosen pictures of each heart at 200x magnification. Blinded operators calculated Cx43 expression as percentage of the total tissue using Image J. Photomicrographs were transformed into RGB (i.e. Red Green Blue) stack, and true Cx43 pixels were defined in the 256-leveled green channel using a minimal cut-off level.

Statistical analyses

Data are presented as mean ± SD and analyzed by analysis of variance One-way ANOVA with a Dunnet post-test, Two-way RM ANOVA with a Bonferroni post-test, and Student's T-test or Mann Whitney test with Graphpad (Prism Software, La Jolla, Calif.) $p < 0.05$ was considered significant. Animals that did not complete the experiment were excluded from analysis.

Results

DOCA induced albuminuria and hypertension but did not affect plasma urea

First hit with DOCA and ANGII did not affect body weight, creatinine excretion, plasma urea and diuresis. DOCA increased albuminuria during ANGII infusion (117 ± 12 mg/24h) and to a lesser extent without ANGII (21 ± 10 mg/24h) vs. controls (0.3 ± 0.2 mg/24h). After withdrawal of DOCA and ANGII albumin excretion decreased in both DOCA + ANGII (4.3 ± 3.2) and DOCA (1.1 ± 0.3). Systolic blood pressure rose from 90 mmHg to 135 mmHg in DOCA and to 145 mmHg in DOCA + ANGII mice during the first period but declined after withdrawal of DOCA and ANGII to 80 mmHg.

Second hit with 6 % NaCl diet did not affect body weight or creatinine excretion. Plasma urea was significantly increased in week 37 in DOCA vs. healthy mice (13.9 ± 0.55 vs. 10.98 ± 1.72mM) whereas DOCA + ANGII mice had less uremia (8.95 ± 0.38 mM). Due to high salt diet, water intake and thereby diuresis was significantly increased in DOCA and DOCA + ANGII mice vs. control (figure 1a) which was confirmed by natriuresis (figure 1b). In wk 37, albumin excretion was significantly higher in DOCA vs. both DOCA + ANGII and controls ($p < 0.05$) (figure 2). During the 6 % NaCl diet, systolic blood pressure was significantly higher in both DOCA and DOCA + ANGII mice vs. controls (figure 3).

Echocardiography

Echocardiography data assessed in wk 34 are shown in table 1. Long axis fractional shortening was significantly decreased in both DOCA and DOCA + ANGII mice.

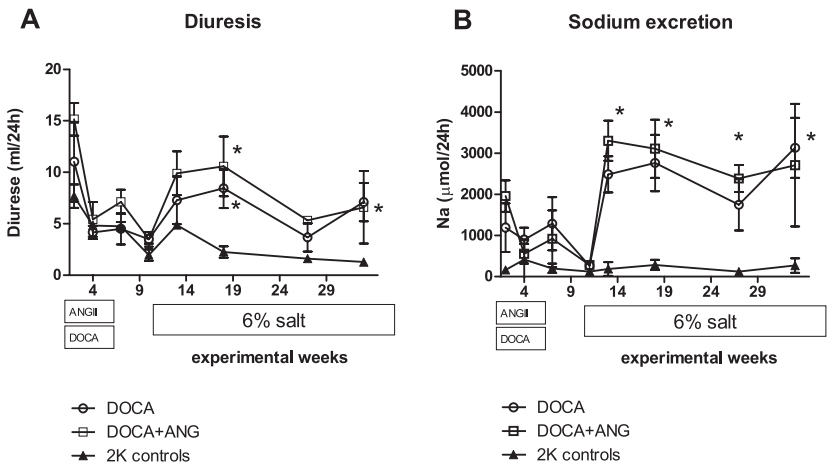

Figure 1 Diuresis (a) and natriuresis (b) were increased during 6% salt diet. * p<0.05 compared 2K controls

Table 1 Echocardiography data. Mean±SD. * p<0.05 compared 2K controls.

Long axis	**2K controls (n=4)**	**DOCA (n=4)**	**DOCA+ANGII (n=4)**
Cardiac output (ml/min)	11.9±2.6	10.9±1.7	12.3±4.5
Ejection fraction (%)	47.0±6.4	42.4±13.7	45.8±8.8
Fractional shortening (%)	13.4±2.6	7.4±1.1*	6.6±2.3*
Heart rate (bpm)	338±44	337±41	364±41
Stroke volume (uL)	35.9±9.3	32.8±7.3	34.7±15.0
Diastolic volume (uL)	76.7±16.4	79.3±12.9	73.7±25.6
Systolic volume (uL)	40.8±9.7	46.5±15.7	38.9±12.0
Short axis			
Cardiac output (mL/min)	12.3±4.5	9.6±2.2	13.5±1.6
Ejection fraction (%)	58.8±4.4	50.6±6.4	56.4±9.3
Fractional shortening (%)	27.5±2.4	25.3±4.1	29.7±6.0
Mitral Valve			
Velocity (early) (mm/s)	655±81	566±74	547±106
Velocity (after) (mm/s)	428±59	476±132	434±151
Early/After (mm)	1.55±0.25	1.22±0.17	1.35±0.46
VTI- peak gradient (mm/s)	1.52±0.75	1.26±0.39	0.68±0.50
VTI- peak velocity (mmHg)	582±190	556±83	465±86

Terminal data

Terminal body weight was not different between groups. Left and right kidney were heavier in DOCA + ANGII mice vs. healthy controls ($p < 0.05$). In DOCA mice, left ($p = 0.08$ and right ($p = 0.07$) kidney tended to be heavier then control kidneys. Liver and spleen weight were not different. Heart and lung weight were significantly higher in both DOCA and DOCA + ANGII compared to healthy mice (table 2).

Cardiac electrophysiological mapping

Ex vivo cardiac electrophysiological mapping in Langendorff set-up at 38 weeks showed susceptibility for arrhythmias in all DOCA and 3 out of 4 DOCA + ANGII mice whereas none of the age-matched control mice responded to electrical stimulation (table 3).

Table 2. Organ weights. * p<0.05 compared 2K controls.

Long axis	2K controls (n=4)	DOCA (n=4)	DOCA+ANGII (n=4)
Body weight (g)	33.3±1.4	32.8±0.9	33.1±2.6
Liver weight/g BW (mg)	37.7±2.8	36.5±3.6	40.1±2.7
Spleen weight/g BW (mg)	2.1±0.8	1.9±0.3	2.3±0.3
Left kidney/g BW (mg)	7.5±0.5	8.3±0.5	8.7±0.6*
Right kidney/g BW (mg)	7.5±0.5	8.5±0.5	9.3±0.7*
Heart weight/g BW (mg)	7.6±0.8	10.3±0.5*	11.2±0.8*
Lung weight/g BW (mg)	5.8±0.6	7.0±0.3*	8.0±1.1*

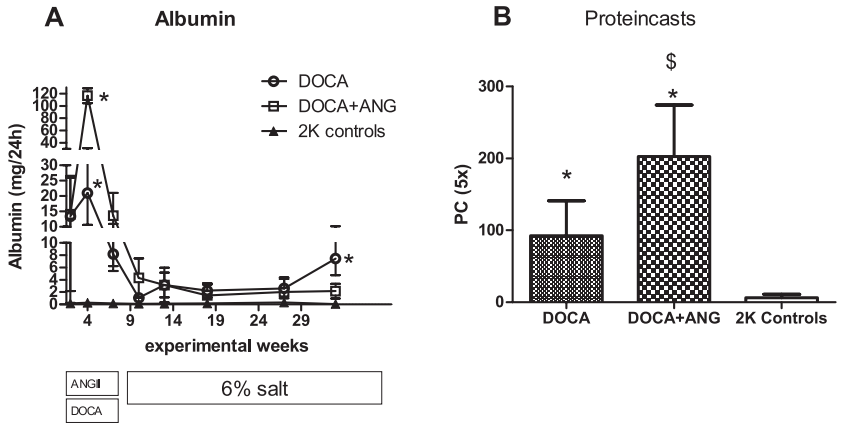

Figure 2 Albumin excretion was increased in DOCA and DOCA+ANGII mice in week 4. In week 37, albumin excretion was increased in DOCA mice (a). Proteincasts were detected in both DOCA and DOCA+ANGII mice (b). * p<0.05 compared 2K controls

Renal Morphology

In both DOCA and DOCA + ANGII mice more totally sclerotic glomeruli and more tubulo-interstitial damage were observed as compared to controls (figure 4a and b). Despite lower albuminuria in the second phase, DOCA + ANGII mice had more protein casts than DOCA mice. Protein casts were absent in healthy mice (figure 2b). No differences were found in tubular influx of $KI67^+$ cells in DOCA (3.8 ± 1.1), DOCA + ANGII (5.0 ± 1.6) and 2K controls (10.3 ± 7.8) and $CD45^+$ cells in DOCA (3.2 ± 0.1), DOCA + ANGII (5.2 ± 3.0) and 2K controls (2.9 ± 0.5).

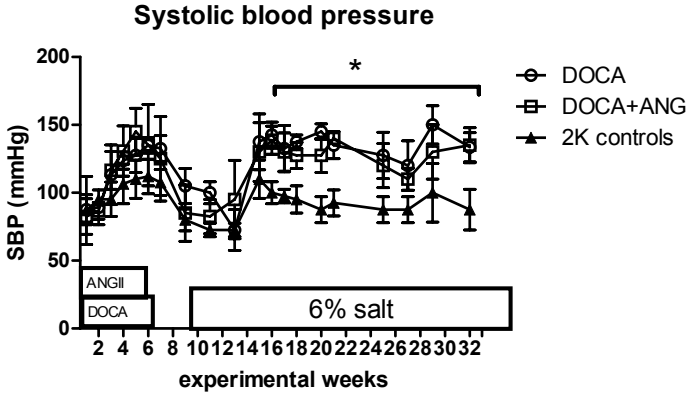

Figure 3 Systolic blood pressure was induced by high salt diet in both DOCA and DOCA+ANGII mice. * $p<0.05$ compared 2K controls.

Table 3. Susceptibility to arrhythmias.

Mouse nr	Group	Arrhythmia inducibility	Type
1	2K control	No	-
2	2K control	No	-
3	2K control	No	-
4	2K control	No	-
5	DOCA+ANGII	No	-
6	DOCA+ANGII	Yes	1 extra beat in burst pacing (RV)
7	DOCA+ANGII	Yes	2,6,9 or 16 extra beats in burst pacing and 3 times VT+ (RV)
8	DOCA+ANGII	Yes	1 or 2 extra beats in burst pacing (RV)
9	DOCA	Yes	1,2,4 or 5 extra beats in burst pacing (RV)
10	DOCA	Yes	1,3 or 4 extra beats in burst pacing, 1 extra beat in 3 extra stimuli (RV), 1 extra beat (LV)
11	DOCA	Yes	2,3,4,5 or 6 extra beats in burst pacing (RV)

RV: Right ventricle. VT: Ventricular tachycardia. LV: Left ventricle

Cardiac Morphology

Cardiac interstitial fibrosis was significantly more pronounced in DOCA mice vs. controls and tended to be increased in the DOCA + ANGII mice vs. controls (figure 5b-e). Cx43 expression was significantly lower in both DOCA and DOCA + ANGII mice (figure 5a and 5f-h). Cx43 also seems more lateralized in the DOCA and DOCA + ANGII group vs. controls (5g-h), but this was not quantified.

Discussion

Our experiments show that aging 129SV mice subjected to DOCA salt with and without ANGII develop renal injury with albuminuria, hypertension, glomerulosclerosis, tubulo-interstitial damage and protein casts as well as cardiac remodeling, assessed as increased heart and wet lung weight, decreased long axis fractional shortening, increased cardiac interstitial fibrosis, decreased Cx43 expression, and increased susceptibility to arrhythmias.

Mouse models have large value for dissecting mechanisms and testing interventions in complex diseases such as the cardiorenal disease as mice provide the possibility to study the effects of single gene knockout or overexpression. However, mice are known to be very resistant to induction of renal failure[6,7], requiring removal of large parts of the kidneys, leaving little renal tissue for analyses. Kirchhoff et al showed that the combination of DOCA and salt diet with Angiotensin II infusion and uninephrectomy in C57Bl6 mice, a mouse strain regarded most resistant to induction of renal injury of all common mouse strains, caused significant hypertension, proteinuria and both renal and cardiac injury[5].

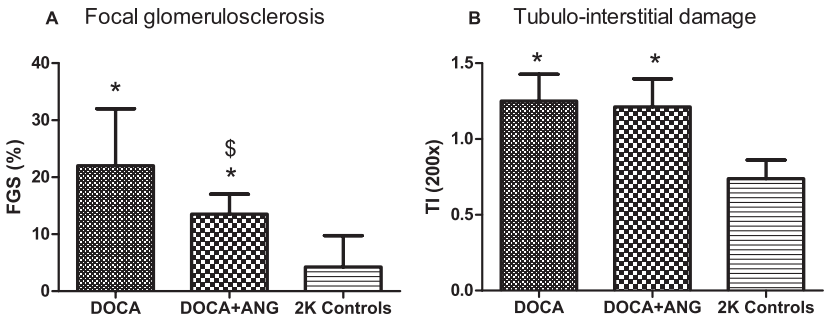

Figure 4 Focal glomerulosclerosis (a) and tubulo-intestitial damage (b) were increased in DOCA and DOCA+ANGII mice. * $p<0.05$ compared 2K controls, $ $p<0.05$ vs. DOCA.

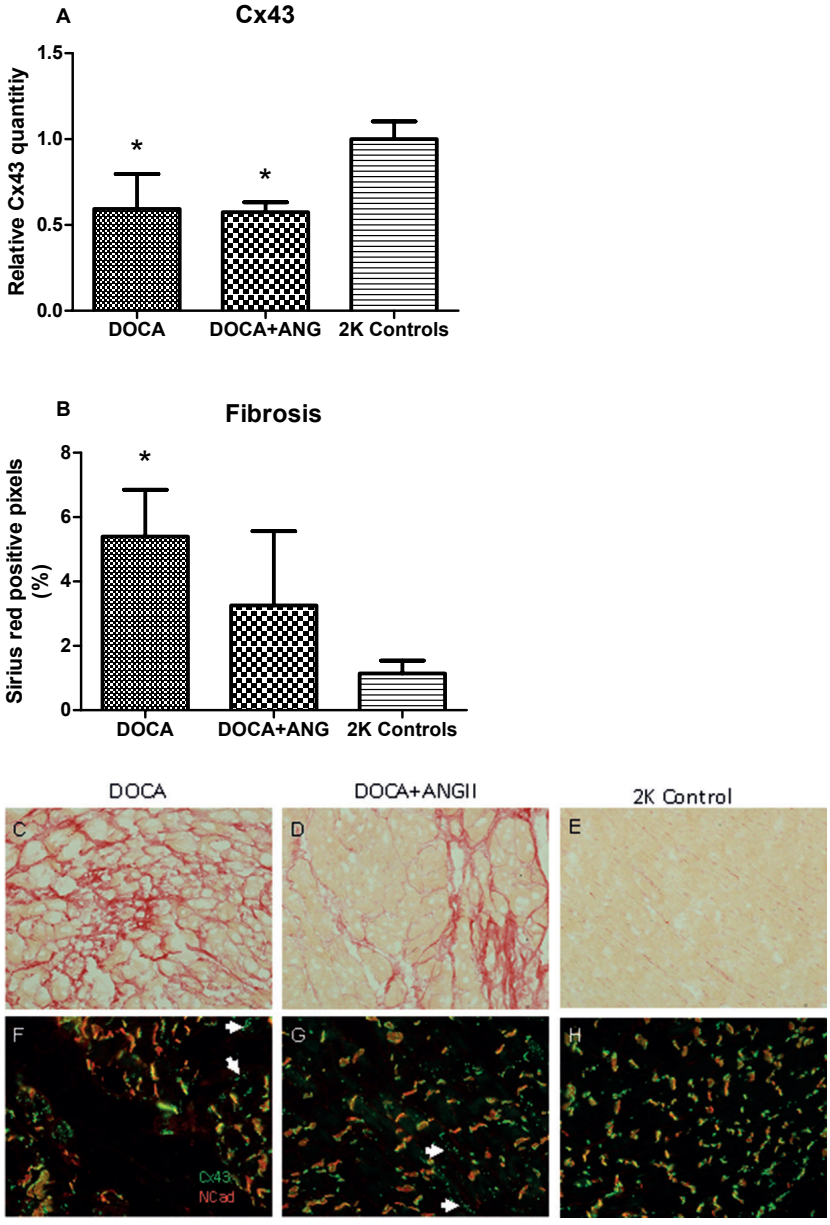

Figure 5 Cx43 was decreased in both DOCA and DOCA+ANGII mice vs. controls (a,f-h). White arrowheads in g and h indicate lateralization of Cx43. Interstitial fibrosis was increased in DOCA mice vs. DOCA+ANGII and controls (b-e). * $p<0.05$ compared to 2K controls.

We aimed to develop a 2-kidney mouse model of cardiorenal disease and used 30 wk old 129Sv mice, a strain that has previously been shown to be more susceptible to develop kidney injury and proteinuria. We used aging mice as aging increases the susceptibility for development of hypertension and renal as well as cardiac failure[14,15]. In our model the 'first hit' with DOCA for 8 weeks with or without ANGII for 4 weeks, caused hypertension and albuminuria. However, this was almost completely reversible after withdrawal of treatment. A subsequent 'second hit' with high salt diet for 27 weeks induced long term hypertension. Although DOCA and ANGII were removed long time before the mice were sacrificed, protein casts were more abundant in DOCA + ANGII mice, possibly due to the history of high albuminuria. Studies on the role of angiotensin II and aldosterone in the pathogenesis of hypertension have shown that both agents initiate a program of vascular and tissue inflammation[16]. Influx of $CD45^+$ cells was not different between healthy and DOCA or DOCA + ANGII mice. Both in DOCA and DOCA + ANGII mice we observed glomerulosclerosis and tubulo-interstitial damage as well as protein casts. Glomerulosclerosis was more abundant in DOCA mice whereas protein casts occurred more often in the DOCA + ANGII mice. Overall, our data show that in an ageing, 129Sv 2-kidney mouse model administration of DOCA, followed by a high salt diet induces renal injury, without the need of removing renal tissue. Additional 4 weeks ANGII administration did not seem to significantly influence the induction of kidney injury in this model.

Besides renal injury, administration of DOCA followed by high salt diet in an ageing 129Sv mouse model induces significant cardiac hypertrophy, decreased fractional shortening and cardiac fibrosis. With echocardiography, long axis fractional shortening was significantly decreased. Other variables of systolic function were not affected, indicating that at least stroke volume and cardiac output were maintained. The increased lung weight suggests some degree of pulmonary edema existed in DOCA and DOCA + ANGII mice, as evidence of fluid congestion. Long-standing hypertension, LV hypertrophy, and cardiac fibrosis can lead to diastolic dysfunction (defective cardiac filling). The decrease in early filling velocity (and secondary the E/A ratio) as well as the reduced peak gradient of mitral inflow suggests impaired diastolic function. Additional 4 weeks ANGII also did not seem to enhance cardiac injury, we observed no enhanced effect on cardiac hypertrophy or fractional shortening and cardiac fibrosis seemed even a little less. Several previous studies suggested that the development of cardiac hypertrophy and fibrosis in the DOCA model is at least partly independent of the extent of hypertension[17-20]. Our current data do not allow mechanistic dissection of the influences of hypertension, direct DOCA effects or the influence of renal injury on the development of cardiac injury. However, our model with cardiac as well as renal injury provides an interesting and relevant model for

future studies on the pathophysiology of the cardiorenal syndrome and potential interventions.

Moreover, our mouse model of cardiorenal disease was prone to develop arrhythmias. Arrhythmias were detected in all DOCA and 75% of DOCA + ANGII mouse hearts but were absent in controls. This may have large relevance for clinical translation. Arrhythmias and sudden cardiac death are a major cause of death in patients with renal and cardiac failure[21] but models of spontaneous and experimental arrhythmic development in mice are sparse. Our previous studies have shown a spectrum of tissue alterations in the aging myocardium, including increased interstitial fibrosis and reduced and redistributed Cx43[22]. These alterations may result in conduction slowing perpendicular to fiber orientation, whereas patchy replacement fibrosis may increase arrhythmia susceptibility. However, in our ageing 129Sv mice without renal or cardiac injury this did not result in the development of arrhythmias or fibrosis. In contrast, the aging mice 129Sv with cardiorenal disease displayed arrhythmias in all 75-100%.

Our study has some limitations. First, we did not include an ANGII without DOCA group as control. However, Kirchhoff showed that, although administration of ANGII did increase systolic blood pressure, this was only associated with mild injury[5]. Furthermore, we were not able to perform a final golden standard renal function measurement to determine GFR by FITC-inulin clearance due to animal facility related logistical problems.

In conclusion, our data provide first evidence that the combination of a first hit with DOCA and salt followed by a second hit of high salt diet in aging 129Sv mice induces renal injury and pronounced cardiac remodeling as well as a markedly enhanced susceptibility to arrhythmias, without the need of removing large amounts of kidney tissue. This 2-kidney cardiorenal disease mouse model will facilitate further mechanistic studies on cardiorenal disease, the impact of specific genes on its pathophysiology and the development and evaluation of novel therapeutic interventions.

Acknowledgements

We thank Krista den Ouden, Paula Martens and Myrthe den Toom for their excellent technical assistance.

References

1. Bongartz L.G., Cramer M.J. et al. The severe cardiorenal syndrome: 'Guyton revisited'. Eur. Heart J. 2005; 26:11-17.
2. Bongartz L.G., Joles J.A. et al. Subtotal nephrectomy plus coronary ligation leads to more pronounced damage in both organs than either nephrectomy or coronary ligation. Am. J. Physiol Heart Circ. Physiol 2012; 302:H845-H854.
3. Gava A.L., Freitas F.P. et al. Effects of 5/6 nephrectomy on renal function and blood pressure in mice. Int. J. Physiol Pathophysiol. Pharmacol. 2012; 4:167-173.
4. Mendoza M.G., Castillo-Henkel C. et al. Kidney damage after renal ablation is worsened in endothelial nitric oxide synthase -/- mice and improved by combined administration of L-arginine and antioxidants. Nephrology. (Carlton.) 2008; 13:218-227.
5. Kirchhoff F., Krebs C. et al. Rapid development of severe end-organ damage in C57BL/6 mice by combining DOCA salt and angiotensin II. Kidney Int. 2008; 73:643-650.
6. Ishola D.A., Jr., van der Giezen D.M. et al. In mice, proteinuria and renal inflammatory responses to albumin overload are strain-dependent. Nephrol. Dial. Transplant. 2006; 21:591-597.
7. Ma L.J., Fogo A.B. Model of robust induction of glomerulosclerosis in mice: importance of genetic background. Kidney Int. 2003; 64:350-355.
8. Franczyk-Skora B., Gluba A. et al. Prevention of sudden cardiac death in patients with chronic kidney disease. BMC. Nephrol. 2012; 13:162.
9. Jansen J.A., Noorman M. et al. Reduced heterogeneous expression of Cx43 results in decreased Nav1.5 expression and reduced sodium current that accounts for arrhythmia vulnerability in conditional Cx43 knockout mice. Heart Rhythm. 2012; 9:600-607.
10. Koeners M.P., Braam B. et al. A perinatal nitric oxide donor increases renal vascular resistance and ameliorates hypertension and glomerular injury in adult fawn-hooded hypertensive rats. Am. J. Physiol Regul. Integr. Comp Physiol 2008; 294:R1847-R1855.
11. Dendooven A., van O.O. et al. Loss of endogenous bone morphogenetic protein-6 aggravates renal fibrosis. Am. J. Pathol. 2011; 178:1069-1079.
12. van Koppen A., Joles J.A. et al. Healthy Bone Marrow Cells Reduce Progression of Kidney Failure Better Than CKD Bone Marrow Cells in Rats With Established Chronic Kidney Disease. Cell Transplant. 2012; 21:2299-2312.
13. Bongartz L.G., Braam B. et al. The nitric oxide donor molsidomine rescues cardiac function in rats with chronic kidney disease and cardiac dysfunction. Am. J. Physiol Heart Circ. Physiol 2010; 299:H2037-H2045.
14. Esposito C., Dal C.A. Functional changes in the aging kidney. J. Nephrol. 2010; 23 Suppl 15:S41-S45.
15. Shiba N., Shimokawa H. Chronic kidney disease and heart failure--Bidirectional close link and common therapeutic goal. J. Cardiol. 2011; 57:8-17.
16. Guzik T.J., Hoch N.E. et al. Role of the T cell in the genesis of angiotensin II induced hypertension and vascular dysfunction. J. Exp. Med. 2007; 204:2449-2460.
17. Loch D., Hoey A. et al. Prevention of hypertension in DOCA-salt rats by an inhibitor of soluble epoxide hydrolase. Cell Biochem. Biophys. 2007; 47:87-98.
18. Peng H., Carretero O.A. et al. Effects of angiotensin-converting enzyme inhibitor and angiotensin type 1 receptor antagonist in deoxycorticosterone acetate-salt hypertensive mice lacking Ren-2 gene. Hypertension 2001; 37:974-980.
19. Rothermund L., Vetter R. et al. Endothelin-A receptor blockade prevents left ventricular hypertrophy and dysfunction in salt-sensitive experimental hypertension. Circulation 2002; 106:2305-2308.
20. Young M., Head G., Funder J. Determinants of cardiac fibrosis in experimental hypermineralocorticoid states. Am. J. Physiol 1995; 269:E657-E662.
21. Lisowska A., Tycinska A. et al. The incidence and prognostic significance of cardiac arrhythmias and conduction abnormalities in patients with acute coronary syndromes and renal dysfunction. Kardiol. Pol. 2011; 69:1242-1247.
22. Stein M., Noorman M. et al. Dominant arrhythmia vulnerability of the right ventricle in senescent mice. Heart Rhythm. 2008; 5:438-448.

Chapter Eight

SUMMARIZING DISCUSSION

The burden of chronic kidney disease (CKD) is not limited to its potential progression to end-stage renal failure, requiring renal replacement strategies, but also contributes importantly to the global burden of death due to cardiovascular diseases. Development of new therapies to reduce progression of CKD is therefore a major global public health target. The aim of this thesis was to investigate whether cell-based therapies have the potential to reduce progression of CKD.

To study cell-based therapies for CKD, we used the 5/6th nephrectomy ablation model, a well known experimental model of progressive renal disease, resembling human CKD[1,2]. For our experiments we used the Lewis rat, a rat strain that is relatively resistant to development of CKD, because of the availability of eGFP^{+} Lewis rats that allow tracking of donor BMC. In **Chapter 2**, we provide a detailed description of this technique.

In **Chapter 3** we studied the effect of BMC therapy on the progression of CKD in our rat model of established CKD. We showed that administration of a single renal artery injection of 50*10^{6} healthy BMC in established CKD effectively reduced progression of renal injury and that this effect was durable. We found that therapy with healthy BMC decreased hypertension, uremia, proteinuria and anemia. Six weeks after administration of BMCs, renal function was measured using gold standard inulin and PAH clearance methodology. GFR and ERPF were significantly better in BMC treated CKD rats as compared to CKD controls and focal glomerulosclerosis, tubulo-interstitial damage and endothelial damage were reduced. These findings suggest that therapy with healthy BMCs can be used to reduce renal disease progression and has long-lasting effects. However, for clinical application, use of autologous BMC would be preferable to prevent rejection. Therefore, we studied the effect of CKD-derived BMCs in our model of established CKD. We found that CKD-BMCs were less effective compared to healthy BMC, implying that this approach may not be suitable for clinical application in this form. Therefore, dysfunction of CKD BMCs needs to be reversed.

NO-availability, an important determinant of endothelial function, is crucial for normal BMC function and appropriate differentiation of BMCs. In CKD NO-availability is reduced and such reduced NO-availability may also play a role in BMC dysfunction in CKD. NO-enhancing strategies in BM-cells may improve safety and efficacy of BM-cell therapy. Pravastatin, a lipid-lowering drug, is known to exert pleiotropic effects including improved NO-availability, anti-inflammatory and anti-oxidant effects and improved migration towards damaged cells. In **Chapter 4** we studied the effect of *ex vivo* pre-treatment of CKD BMC with pravastatin on their subsequent *in vivo* therapeutic effect on the progression of

renal failure in established CKD. We also evaluated the effects of systemic *in vivo* treatment of CKD rats with pravastatin. We decided to use pravastatin as it can be dissolved in water which makes oral *in vivo* supplementation possible and allows us to add it to cell cultures without first dissolving it in low pH buffers which is not desirable for cell cultures. Previous experiments showed that myopathy occurred after high oral dose of simvastatin and lovastatin, but not after pravastatin[3]. Our study demonstrated for the first time that CKD BMC dysfunction could be reversed by short-term (2h) *in vitro* pre-treatment with pravastatin outside the CKD environment and that this short-term pre-treatment effect persisted when the cells were returned to the CKD environment. This was reflected by better renal function and less glomerulosclerosis and tubulo-interstitial damage of CKD rats treated with healthy or pravastatin-treated CKD BMC, who had comparable GFR, ERPF and histology, whereas rats treated with CKD BMC had a lower GFR and ERPF and more glomerulosclerosis and tubulo-interstitial damage. In contrast, 2 weeks of exposure to systemic oral pravastatin within the uremic environment had no beneficial effects on renal function or renal injury. As also described in chapter 3, the number of traced BMCs in the kidney was very low. There was no difference in the influx of BMCs after pravastatin pretreatment. The beneficial effects of pravastatin may be explained by enhanced excretion of effective paracrine factors. Indeed, pravastatin treatment of CKD BMC significantly decreased expression of the pro-inflammatory and pro-apoptotic cytokine LIX (CXCL5) and increased expression of promigratory thymus chemokine (CXCL7). In conclusion, although kidney function in rats with established CKD was not affected by systemic *in vivo* pravastatin treatment, *ex vivo* pretreatment of BMC enhanced their therapeutic efficacy.

Activation of BMC in disease states such as hypertension or CKD may contribute to enhanced myocardial fibrosis. In **Chapter 5**, we studied whether BMCs that are administered to reduce CKD progression in rats with CKD and hypertension - as described in Chapters 3 and 4 – may contribute to the development of cardiac fibrosis. BMCs – either obtained from healthy or CKD rats - did not contribute to cardiac fibrosis by trans-differentiation and durable incorporation. However, we observed a trend towards more cardiac fibrosis in rats that received CKD BMC as compared to rats that received either vehicle or healthy BMC. This may be due to differences in paracrine effects between CKD BMC and healthy BMC, with activated CKD BMC releasing cytokines and growth factors that favor local profibrotic processes in resident cells. Our data suggest that autologous BMC therapy in CKD may not only be less effective in reducing renal disease progression compared to healthy BMC therapy but may even induce unwanted side effects by enhancing cardiac fibrosis, underscoring the need for further research to restore this dysfunction.

Although mechanisms of tissue repair by stem cells were previously thought to occur mainly through incorporation and trans-differentiation into the desired cell-type, more recent literature suggests that paracrine factors may be largely responsible for the observed effects. Similarly, in our studies the number of cells that we could trace after six weeks but also at earlier time points was very low and we did not see incorporation in epithelial or endothelial structures. In **Chapter 6** we had the opportunity to study the effects of clinical grade mesenchymal stem cell (MSC) derived conditioned medium (CM) containing paracrine factors of human embryonic MSCs in our model of established CKD. We injected the conditioned medium intravenously twice daily with an interval of six hours for four consecutive days to mimic a continuous production of paracrine factors as may occur after stem or progenitor cell administration in the kidney. The dose we used was extrapolated from a dose that effectively reduced development of myocardial infarction in mice[4]. Our study showed that indeed administration of MSC-derived CM effectively decreased progression of renal disease. Recent reports suggest a central role for microvesicles[5,6] or exosomes[7] in MSC-mediated tissue repair. In experimental myocardial infarction the cardio-protective effects of human embryonic MSC conditioned medium were attributed to exosomes[8,9]. To get more insight in the effective renoprotective component of the conditioned medium we also studied the effect of human embryonic MSC derived exosomes on the progression of renal failure. However, repeated intravenous administration of human embryonic MSC derived exosomes in our model of established CKD did not affect progression of CKD. We used exosome concentrations in CKD rats that were approximately fourfold the concentration of exosomes present in the dose of conditioned medium we used, similar to the exosome concentrations previously shown to improve cardiac function after myocardial infarction[8], indicating that the amount we supplied was not the limiting factor. Moreover, *in vitro* both human embryonic MSC derived exosomes and CM effectively induced wound closure and angiogenesis. Lack of a significant therapeutic effect of exosomes in this model of chronic renal injury may be due to tissue specific requirements regarding exosome content and/or dose in this model and requires further research.

Mouse models would have large value for dissecting (regenerative) mechanisms and testing interventions in complex diseases such CKD or cardiorenal disease as mice provide the possibility to study the effects of defined genetic traits. However, mice are known to be very resistant to induction of renal failure requiring removal of large parts of the kidneys, leaving little renal tissue for analyses. In **Chapter 7** we report our data on the development of a mouse model of cardiorenal disease. We used DOCA-salt administration in a two-kidney aging mouse model to induce

kidney and heart injury. Although further research is needed, our results thus far suggest that this approach can provide a relevant experimental 2-kidney cardiorenal disease model.

In conclusion, our results show that cell-based therapies can decrease the progression of chronic kidney disease and that dysfunction of CKD BMC can be reversed. If confirmed for human CKD BMC, these results may be used to design a clinical trial to investigate safety and efficacy of BMC therapy in patients with CKD.

References

1. Fleck C., Appenroth D. et al. Suitability of 5/6 nephrectomy (5/6NX) for the induction of interstitial renal fibrosis in rats--influence of sex, strain, and surgical procedure. Exp. Toxicol. Pathol. 2006; 57:195-205.
2. Griffin K.A., Picken M.M. et al. Functional and structural correlates of glomerulosclerosis after renal mass reduction in the rat. J. Am. Soc. Nephrol. 2000; 11:497-506.
3. Reijneveld J.C., Koot R.W. et al. Differential effects of 3-hydroxy-3-methylglutaryl-coenzyme A reductase inhibitors on the development of myopathy in young rats. Pediatr. Res. 1996; 39:1028-1035.
4. Timmers L., Lim S.K. et al. Human mesenchymal stem cell-conditioned medium improves cardiac function following myocardial infarction. Stem Cell Res. 2011; 6:206-214.
5. Bruno S., Grange C. et al. Mesenchymal stem cell-derived microvesicles protect against acute tubular injury. J. Am. Soc. Nephrol. 2009; 20:1053-1067.
6. Gatti S., Bruno S. et al. Microvesicles derived from human adult mesenchymal stem cells protect against ischaemia-reperfusion-induced acute and chronic kidney injury. Nephrol. Dial. Transplant. 2011; 26:1474-1483.
7. Camussi G., Deregibus M.C. et al. Exosomes/microvesicles as a mechanism of cell-to-cell communication. Kidney Int. 2010; 78:838-848.
8. Lai R.C., Arslan F. et al. Exosome secreted by MSC reduces myocardial ischemia/reperfusion injury. Stem Cell Res. 2010; 4:214-222.
9. Timmers L., Lim S.K. et al. Human mesenchymal stem cell-conditioned medium improves cardiac function following myocardial infarction. Stem Cell Res. 2011; 6:206-214.

NEDERLANDSE SAMENVATTING

DANKWOORD

CURRICULUM VITAE

LIST OF PUBLICATIONS

Nederlandse samenvatting

Chronische nierinsufficiëntie (onvoldoende nierwerking) is wereldwijd een groeiend probleem. Het aantal patiënten dat een niervervangende behandeling (niertransplantatie of dialyse) nodig heeft neemt toe. In 2011 waren er in Nederland 60.000 nierpatiënten en dit aantal blijft stijgen. Daarnaast hebben patiënten met chronische nierinsufficiëntie een sterk verhoogd risico op hart- en vaatziekten. Het is daarom van groot belang om nieuwe methoden te ontwikkelen om voortschrijden van nierinsufficiëntie te vertragen, te voorkomen of zelfs herstel van nierfunctie te bewerkstelligen. Stamceltherapie lijkt hiervoor een veelbelovende optie.

Uit eerdere dierstudies is gebleken dat stamcellen uit het beenmerg het herstel van verschillende vormen van acute nierinsufficiëntie kunnen bevorderen. In dit proefschrift hebben wij in een rattenmodel waar reeds ernstige chronische nierschade aanwezig is, aangetoond dat behandeling met beenmergafkomstige cellen de progressie van chronisch nierfalen vertraagt. Als deze therapie in de kliniek zou worden toegepast zou men het liefst gebruik maken van de eigen beenmergcellen van de patiënt om afstoting te voorkomen. Omdat chronisch nierfalen niet alleen invloed heeft op de nier maar ook op andere organen zoals onder andere het hart en het beenmerg moet eerst onderzocht worden of het patiënteigen beenmerg wel geschikt is voor therapie. Dit hebben we ook bestudeerd in ons ratten model met ernstig chronisch nierfalen. Hieruit bleek dat wanneer we behandeling gaven met zieke beenmergcellen (afkomstig van een donor rat met chronische nierinsufficiëntie) deze behandeling aanzienlijk minder effectief was. Zelfs vonden we aanwijzingen dat deze zieke cellen mogelijk bij konden dragen aan schadelijke processen in het hartweefsel. Daarom hebben we onderzocht of het mogelijk is om beenmergcellen van ratten met chronisch nierfalen voor te behandelen voordat ze aan de ontvanger worden gegeven om de verminderde effectiviteit van deze cellen te verbeteren. We hebben aangetoond dat wanneer wij zieke beenmergcellen gedurende een korte periode behandelen met pravastatine, (een cholesterolverlagend middel dat ook effect heeft op celfunctie), deze een verbeterde functie hebben gekregen en, net als gezonde beenmergcellen de progressie van chronisch nierfalen kunnen remmen. Verder onderzoek zal moeten uitwijzen of het op deze manier ook mogelijk zal zijn om beenmergcellen afkomstig van patiënten met chronische nierschade zodanig te verbeteren dat deze geschikt zijn voor therapeutische toepassing in patiënten.

Op welke manier zorgen beenmergcellen nu voor vermindering van nierschade in ons model? Enkele jaren geleden was de algemeen heersende gedachte dat stam- en beenmergcellen, die de mogelijkheid hebben om zich te differentiëren

in een groot aantal verschillende celtypen, bijdragen aan herstel door zich naar het beschadigde orgaan te begeven en daar te differentiëren tot het vereiste celtype. De beenmergcellen die we in onze dierstudies hebben gebruikt waren afkomstig van donorratten die in al hun lichaamscellen, behalve huid en haar, een groen fluorescerend eiwit tot expressie brengen. Dit gaf ons de mogelijkheid om de geïnjecteerde cellen op te sporen in de met beenmerg behandelde ratten, die dat eiwit niet bezaten. In alle studies die we hebben gedaan hebben we echter maar heel weinig cellen terug gevonden. Het differentiëren van toegediende beenmergcellen tot celtypen die in de nier voorkomen bleek dus niet het belangrijkste mechanisme te zijn. Ook in de literatuur werd steeds meer gespeculeerd dat de producten die de beenmergcellen maken zoals groeifactoren en moleculen die een rol spelen bij afweer, die cytokines worden genoemd, mogelijk een belangrijke rol spelen in het herstellen van weefsels en orgaanfunctie. Inderdaad vonden wij verschillen tussen de groeifactoren die geproduceerd worden door gezonde cellen en die van zieke cellen wat ook het verminderde therapeutische effect van deze cellen kan verklaren. We denken nu dat de beenmergcellen in de zieke nier als een soort groeifactorfabrieken functioneren en op deze manier de schade in de zieke nier verminderen. In een aparte studie hebben wij onderzocht of een cocktail van stoffen die geproduceerd worden door een bepaald type stamcel, namelijk de mesenchymale stamcel, een gunstig effect hebben op het voortschrijden van nierinsufficiëntie. We hebben deze cocktail toegediend aan ratten met ernstig chronisch nierfalen en hieruit bleek dat ook deze cocktail zorgde voor minder progressie van nierfalen.

Recentelijk is in patiënten met hartziekten of vaatlijden in de benen het toedienen van beenmerg stamcellen veilig en uitvoerbaar gebleken waarbij veelbelovende effecten op het klinisch beloop werden gezien. Wanneer onze vervolgstudies inderdaad een gunstig effect van beenmergceltherapie laten zien, ook wanneer we voorbehandelde beenmergcellen van patiënten met chronisch nierfalen gebruiken, zullen deze bevindingen relatief snel kunnen worden vertaald naar een klinische toepassing. Wij verwachten dat dit proefschrift zal bijdragen aan een juist ontwerp van klinische studies waarin de effectiviteit van stamceltherapie in patiënten met chronische nierinsufficiëntie onderzocht zal worden.

Dankwoord

Met veel plezier heb ik tijdens mijn promotieonderzoek geopereerd, geïnjecteerd en gepipetteerd, mede doordat ik daarbij bijgestaan werd door gedreven, vaardige en behulpzame collega's. Er zijn dan ook veel mensen die direct of indirect hebben bijgedragen aan mijn boekje. Daarom wil ik graag iedereen bedanken die me tijdens mijn promotieonderzoek heeft gesteund, geholpen, opgevrolijkt, geadviseerd, becommentarieerd of op een andere manier heeft bijgedragen.

Beste Marianne, wat ben ik blij dat je me zo snel na mijn sollicitatiegesprek de baan aanbood. Ik had geen betere begeleider kunnen treffen! Je enthousiasme, enorme wetenschappelijke drive, kundige en zeer nuttige adviezen en sociale meevoelbaarheid tijdens het dinsdagmiddag overleg hebben er voor gezorgd dat ik daarna weer vol goede moed aan de slag ging. Heel veel dank voor alles!

Beste Jaap, wandelende encyclopedie met een enorme superhandige voorraad papieren manuscripten uit de oertijd in je GDL systeem en enthousiaste reisverhalen. Zeer veel dank voor alle ondersteuning, hulp en adviezen. Pas als jij de proefopzet of data goed vond wist ik zeker dat er iets van te maken viel. De komst van de iPhone resulteerde in telefoontjes en mailtjes vanaf de fiets (levensgevaarlijk) of op onchristelijke tijdstippen. Je wilt altijd het onderste uit de kan halen en wetenschap is voor jou een eerste levensbehoefte waarvoor ik grote bewondering heb.

Rachel, jouw kennis op moleculair biologisch gebied is gigantisch en je bent een enorme aanwinst voor ons lab. Ik kijk er naar uit om samen het zebravismodel op te gaan zetten.

Roel, bedankt voor alle hulp met kleuringen en andere pathologische vraagstukken. Tri, fijn dat je altijd wel even tijd kon maken om naar een coupe te kijken als ik langs kwam lopen met een vraag.

GDL collega's: Maarten K., ook al hebben we niet veel tijd samen in het lab doorgebracht, toch was je altijd bereikbaar voor adviezen met betrekking tot de terminale experimenten. Dank hiervoor. Wie weet komen we elkaar tegen in Auckland. Sebas, ik heb bewondering voor jouw positieve levensinstelling waarmee je altijd vrolijk de dag begint en grapjes maakt met iedereen. Manolo, good luck with your scientific career. Maarten W., succes met de kunstnier en de geit. Paula, zonder jouw hulp waren de experimenten in dit boekje lang zo mooi niet geworden. Je werkt altijd heel netjes en betrouwbaar, ook al waren het niet altijd

de leukste karweitjes. Ik bewonder hoe kalm en rustig je altijd bij het tailcuffapparaat zat met mijn ratten en muizen en ben je heel dankbaar voor alle werkzaamheden.

Dames Nefro, Nel en Adele. Dank voor het meten van alle urines, plasma's en klaringen die ik de afgelopen jaren bij jullie heb ingeleverd. Als er iets af moest kon er altijd in overleg wel iets geschoven worden. Nel, geniet van je welverdiende pensioen en bedankt dat je mijn laatste metingen nog bent komen doen ook al was je eigenlijk al weg. Adele, nu komen alle samples bij jou op je bordje, wel veel werk maar ook altijd weer een uitdaging, succes!
Kamergenootjes, dank voor alle gezelligheid afgelopen jaren. Martin, je bent er altijd als eerste en gaat als laatste naar huis, wat geleid heeft tot vele publicaties, respect! Komende tijd is voor jou een hele spannende maar ook hele leuke tijd; baby, boekje en opleiding! Geniet ervan! Diana, dankjewel voor de gezelligheid, de chocolaatjes die altijd wel in één of ander laatje te vinden waren en de vele uurtjes die we gezamenlijk op het GDL, AZU of congres hebben doorgebracht, je doet moeilijke experimenten in nieuwe modellen en ik weet zeker dat jouw boekje en promotie erg mooi gaan worden, hou vol! Petra, dankjewel voor de supergezellige tijd! Je was er altijd voor in om even over nieuwe jurkjes, nieuwtjes en andere niet-werk gerelateerde dingen te kletsen. Je bent in het lab onmisbaar, bestellingen doen, problemen oplossen en helpen met niet altijd leuke bepalingen, zonder jou was menig boekje lang niet zo mooi geworden, en daarom ben ik ook heel blij dat je mijn paranimf wil zijn. Dries, je bent een rustpunt in onze af en toe drukke kamer, succes met je proeven en boekje.

Buurmannen, Bas, Alain en Krijn. Dank jullie wel voor de gezelligheid en de mogelijkheid om af en toe een domme vraag te stellen over een celkweek-iets, een computer-iets of een ander-iets. Hendrik: perfecte voorbeeld van de homo imbibens. Ook jij krijgt onder invloed van enige spiritualiën vaak geniale ingevingen die tot de ontwikkeling van gecompliceerde proefopzetten of statistische weergaven van de gemiddelde alcoholconsumptie van collega's leidden. Ik ben heel blij dat je altijd bereid was om me te helpen met computergerelateerde dingen zoals facsen, gates zetten, figuren maken en rare instellingen op mijn computer corrigeren, dankjewel!

Krista, mijn hulp en bijstand tijdens experimenten. Samen zijn we begonnen aan de vele dierexperimenten en samen hebben we ook de laatste experimenten uitgevoerd. Zonder jouw hulp was ik nooit zover gekomen en waren de intrarenale beenmerginjecties onuitvoerbaar geweest. We hebben de GFP kleuring aan de praat gekregen en je hebt ook nog veel andere kleuringen voor me gedaan, hiervoor heel veel dank. Af en toe een spelletjesavond en pannenkoeken eten of

een mozaïekworkshop zorgden ervoor dat ik je ook wat beter heb leren kennen. Ik ben heel erg blij dat het goed met je gaat en wens je dan ook heel veel geluk in de toekomst!

Joost F, dankjewel dat ik af en toe even langs kon lopen met een vraag over een pathway of cytokine. Mede dankzij jouw ideeën en suggesties is het prava hoofdstuk zo mooi geworden.

Verre Oosten OIO's, Dimitri, Olivier, Gisela. Veel succes met jullie projecten. Nynke, ik hoop dat de rattenexperimenten uiteindelijk gaan lukken, nog even volhouden. Tim, thanks for answering all my stupid questions in the Hubrecht fish lab about the most simple procedures, I'm a complete fish nitwit, so I appreciate all your help very much. I'm looking forward to continue the fish work together.

Studenten: Nienke, Adrian, Lu, Myrthe, Frank, Ronne en Sumeyye, bedankt voor jullie hulp. Nicole; door je enthousiasme en inzet is het conditioned medium verhaal er gekomen, heel veel succes in het Erasmus. Maaike, dankjewel voor je flexibele werkhouding, je doorzettingsvermogen en je vaardigheid met het opzetten van allerlei cel-assays, ik ben blij dat ik wat heb kunnen bijdragen aan je verminderde afkeer van roze en rokjes en hoop dat we nog vaak samen op het fietsje zitten in de sportschool, ik hoop dat je snel een leuke baan vind en ben er van overtuigd dat je een supergoede analiste gaat worden.

Arjan, altijd vroeg op het lab en in voor een praatje, fijn dat we af en toe antilichaampjes mochten lenen. Wendy, bedankt voor het lay-outen, je begreep precies was ik bedoelde met omschrijvingen als "kringeltjes" enzo en het is helemaal naar mijn zin geworden.

Patho(ex)AIO's Jan-Willem, Stefan en Lucas, succes met jullie onderzoek en opleiding. Dionne, dank voor het lenen van antilichamen en protocollen en het beantwoorden van al mijn vragen over kleuringen en de gezelligheid op het GDL.

Aio's Cardio, teveel om op te noemen, succes met jullie promotie.

Medische Fysiologie: Harold, superfijn dat je ons de mogelijkheid geboden hebt om ritmestoornissen te meten in jullie opstelling. Ik heb nog nooit een hoogleraar zelf en met zoveel enthousiasme in het lab metingen zien doen, zeer veel dank hiervoor. Sanne en Magda, zonder jullie hulp waren de analyses voor het muizenstuk niet gelukt, bedankt!

Zonder ondersteuning van het GDL waren de dierproeven niet mogelijk geweest. Kees, Helma, Sabine, Paul en Anja, dank voor alle hulp.

Evalueren onder het genot van een hapje en drankje en een spelletje was ook af en toe even nodig. Karin en Frans, Amelie en Yannick en Lennart en Mayke, dankjullie wel hiervoor.

Katie en Erik, wekelijks bellen om bij te kletsen lukte niet altijd, maar dat wordt vast komende tijd wat beter. Martijn en Marloes, Chantal en Sebas, jullie maken het spreekwoord: 'gezelligheid kent geen tijd' tot waarheid. Chantal, jij hebt superveel bijgedragen aan dit boekje en ik ben er ook trots dat je mijn paranimf wilt zijn. Hoewel ik je heel erg heb gemist op het lab zit je helemaal op je plek in Leiden en wens ik je dan ook samen met Sebas alle goeds. Marloes, carrièrevrouw! Dank voor de handjes bij experimenten, beenmergisolaties en dierexperimenten. Ook jouw vertrek heb ik met lede ogen aangezien maar was ook heel begrijpelijk, CRA in de dop, zet 'm op!

Tante H, heel erg bedankt voor het schilderen van de cover, tis net wak wou. Oma van Koppen en Oma Buskop, ik ben heel blij dat jullie allebei nog in zo'n goede gezondheid in het leven staan en dat jullie bij mijn promotie aanwezig kunnen zijn.

Ouders Sloots, bedankt voor de relaxweekendjes in het rusthuis in Veendam. Jerryt en Ineke, we hebben nu weer tijd om de spelletjes uit de kast te halen, ik ga voor minstens 1x revanche met Munchkin.

Broertje, (hoewel dat allang niet meer geldt sinds je me hebt ingehaald in de lengte, wat nou ook weer niet heel moeilijk was), beiden zijn we in een lab beland, noem dat maar eens toevallig. Jij bent wat meer chemisch ingesteld dan ik en ik voorzie dan ook een mooie carrière al dan niet bij Nedlad in het verschiet liggen.

Pa en ma, ook al vonden jullie het heel eng dat ik naar Rotterdam wilde om te gaan studeren, en daarna op stage naar Nijmegen ging, vervolgens niet gewoon wilde gaan werken maar nog een studie wilde doen waarvoor ik naar Den Haag moest verhuizen en toen naar Utrecht ging om daar aan een promotie te beginnen, uiteindelijk is toch allemaal goed gekomen. Dankzij jullie opvoeding en levensinstelling die gekenmerkt door "niet van dat benauwde" en "eerst je werk afmaken" ben ik in staat geweest mijn promotie tot een goed einde te brengen. Dank jullie wel!

Arjen, dankjewel voor alles. Doordat je als post-doc een heel goed idee hebt van wat onderzoek doen inhoudt begreep je het ook als ik het weekend naar het lab moest en ‘s avonds nog dingen moest afronden terwijl jij eigenlijk andere plannen had. Ik ben heel blij dat ik je heb gevonden en heb dan ook superveel zin in 16 augustus!

Curriculum Vitae

Arianne van Koppen was born on August 10, 1984 in Dirksland, the Netherlands. After completing her secondary education in 2001, she obtained her bachelor's degree in Biology and Medical Laboratory Research at the Rotterdam University of Applied Sciences in 2005. During her bachelor, she performed two internships. The first internship was conducted at the department of General Internal Medicine at the Radboud University Nijmegen Medical Centre where she worked on detection of single nucleotide polymorphisms in a Dutch cohort of familial combined hyperlipidemia patients. She did her second internship at the department of Pharmacology and Toxicology at the Nijmegen Center for Molecular Life Sciences where she studied the effect of aminoguanidine on inducible nitric oxide synthase formation in response to endotoxemia-induced renal damage, which resulted in a second-author paper. During this internship, she became interested in the pathophysiology of kidney diseases and decided to obtain a Masters degree. In 2005, she started the masters program Animal Biology at Leiden University. During her Master, she performed two internships. One was conducted at the department of Behavioural Biology at Leiden University, where she studied the sounds of male Lake Victoria cichlids in territorial and courtship context. For her second master internship, she returned to the department of Pharmacology and Toxicology in Nijmegen and studied the influence of the pregnancy hormone relaxin on the vascular response in overweight rats which resulted in a second-author paper. After graduating in 2007, she started her PhD on the effect of bone marrow derived cell therapy on the progression of renal failure in rats under supervision of Prof. Marianne Verhaar and Dr. Jaap Joles, which resulted in this thesis. After her PhD she will continue her research on renal regeneration using zebrafish models of renal disease. She is planning to visit specialized laboratories abroad to gain knowledge and techniques on zebrafish related research.

List of publications

Heemskerk S, **van Koppen A**, van den Broek L, Poelen GJ, Wouterse AC, Dijkman HB, Russel FG, Masereeuw R. Nitric oxide differentially regulates renal ATP-binding cassette transporters during endotoxemia. *Pflugers Arch. 2007 May;454(2):321-34*

van Drongelen J, **van Koppen A**, Pertijs J, Gooi JH, Parry LJ, Sweep FC, Lotgering FK, Smits P, Spaanderman ME. Impaired vascular responses to relaxin in diet-induced overweight female rats. *J Appl Physiol. 2012 Mar;112(6):962-9*

van Koppen A, Joles JA, Bongartz LG, van den Brandt J, Reichardt HM, Goldschmeding R, Nguyen TQ, Verhaar MC. Healthy bone marrow cells reduce progression of kidney failure better than CKD bone marrow cells in rats with established chronic kidney disease. *Cell Transplant. 2012;21(10):299-312*

van Koppen A, Joles JA, van Balkom BW, Lim SK, de Kleijn D, Giles RH, Verhaar MC. Human embryonic mesenchymal stem cell-derived conditioned medium rescues kidney function in rats with established chronic kidney disease. *PLoS One. 2012;7(6):e38746*

van Koppen A, Verhaar MC, Bongartz LG, Joles JA. 5/6th nephrectomy in combination with high salt diet and NO synthase inhibition to induce chronic kidney disease in the Lewis rat. *JOVE in press*

van Koppen A, Papazova DA, Oosterhuis NR, Gremmels H, Fledderus JO, Joles JA, Verhaar MC. Exposing CKD rat bone marrow cells to pravastatin ex vivo improves their subsequent in vivo therapeutic efficacy in rats with established CKD. *Submitted*

van Koppen A, Joles JA, Verhaar MC. Comment on 'Elevated circulating fibrocyte levels in patients with hypertensive heart disease'. *Journal of Hypertension, in press*

van Koppen A, de Jong S, Fontes M, Bongartz LG, Joles JA, Nguyen TQ, van Rijen H, Verhaar MC. A DOCA salt induced 2-kidney mouse model of cardiorenal disease. *In preparation*